Radio detection of extensive air showers

Precision measurements of the properties of cosmic rays

«ETTORE MAJORANA» FOUNDATION AND CENTRE FOR SCIENTIFIC CULTURE

INTERNATIONAL SCHOOL OF COSMIC-RAY ASTROPHYSICS
«MAURICE M. SHAPIRO»

23rd Course: "Multi-Messenger Astroparticle Physics" 20 – 28 July 2024

PRESIDENT AND DIRECTOR OF THE CENTRE: PROFESSOR A. ZICHICHI

DIRECTORS OF THE COURSE: PROFESSORS J.R. HÖRANDEL, T. STANEV, R. SPARVOLI - J.P. WEFEL (director emeritus)

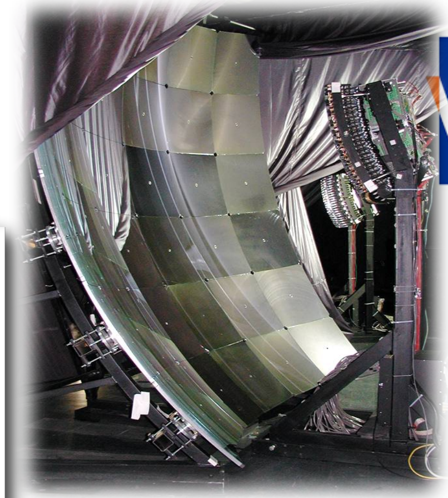

characterize cosmic rays:
-direction
-energy
-mass
@100% duty cycle

Jörg R. Hörandel **RU Nijmegen, Nikhef, VU Brussel** **http://particle.astro.ru.nl**

Radio detection of extensive air showers

Precision measurements of the properties of cosmic rays

«ETTORE MAJORANA» FOUNDATION AND CENTRE FOR SCIENTIFIC CULTURE

INTERNATIONAL SCHOOL OF COSMIC-RAY ASTROPHYSICS
«MAURICE M. SHAPIRO»

23rd Course: "Multi-Messenger Astroparticle Physics" 20 – 28 July 2024

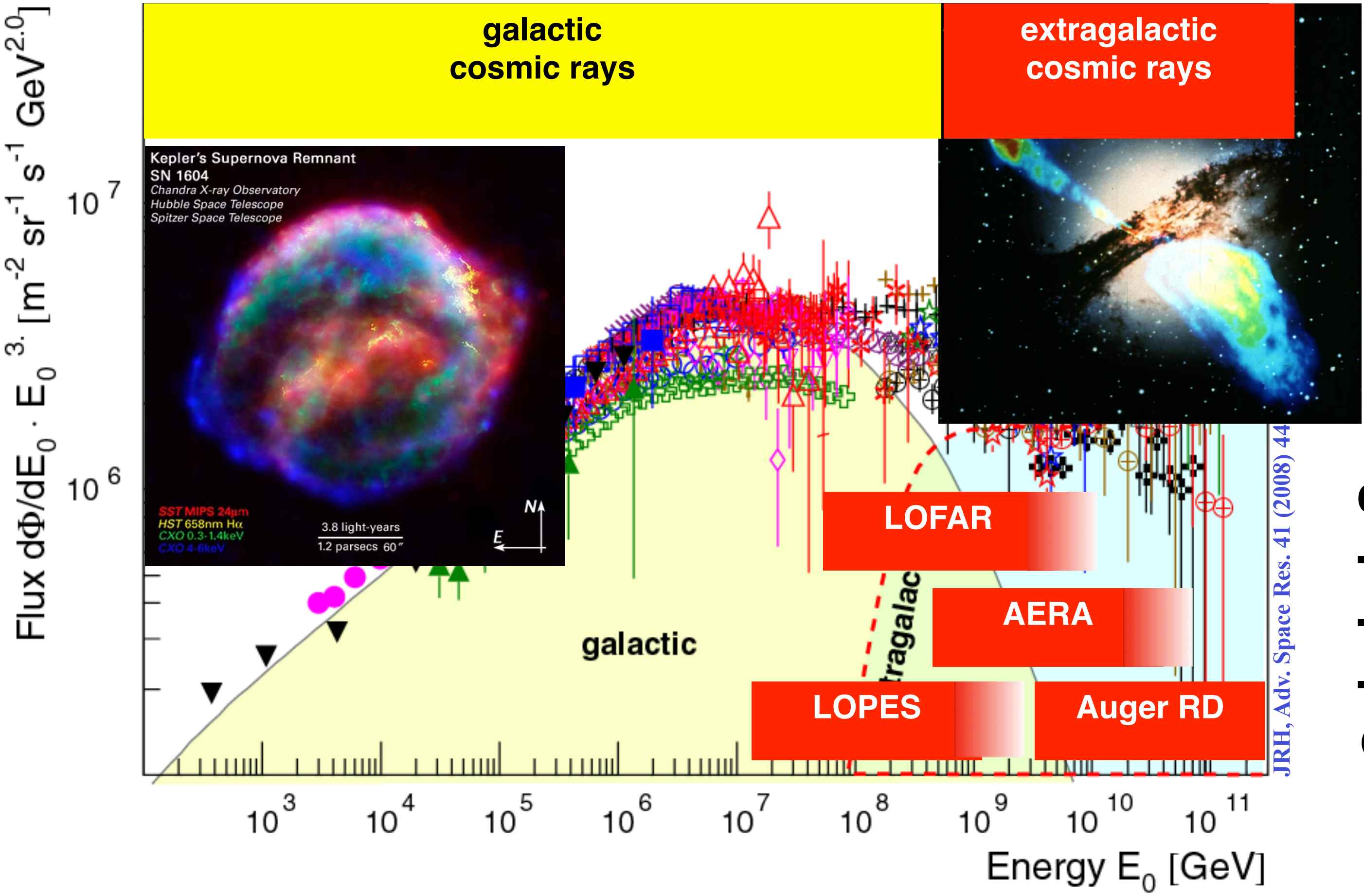

characterize cosmic rays:
-direction
-energy
-mass
@100% duty cycle

Jörg R. Hörandel **RU Nijmegen, Nikhef, VU Brussel** **http://particle.astro.ru.nl**

First radio detection of air showers 1965

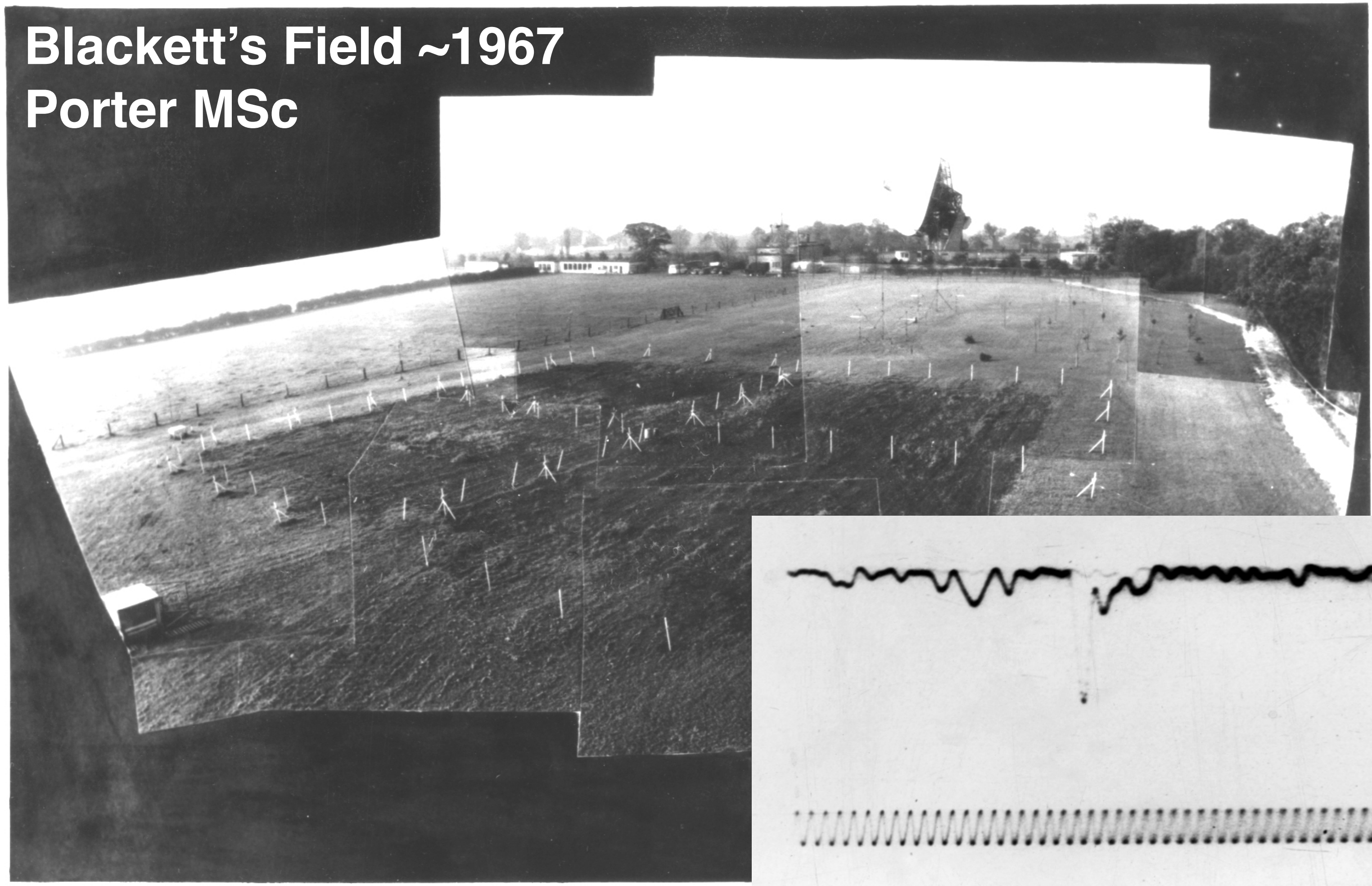

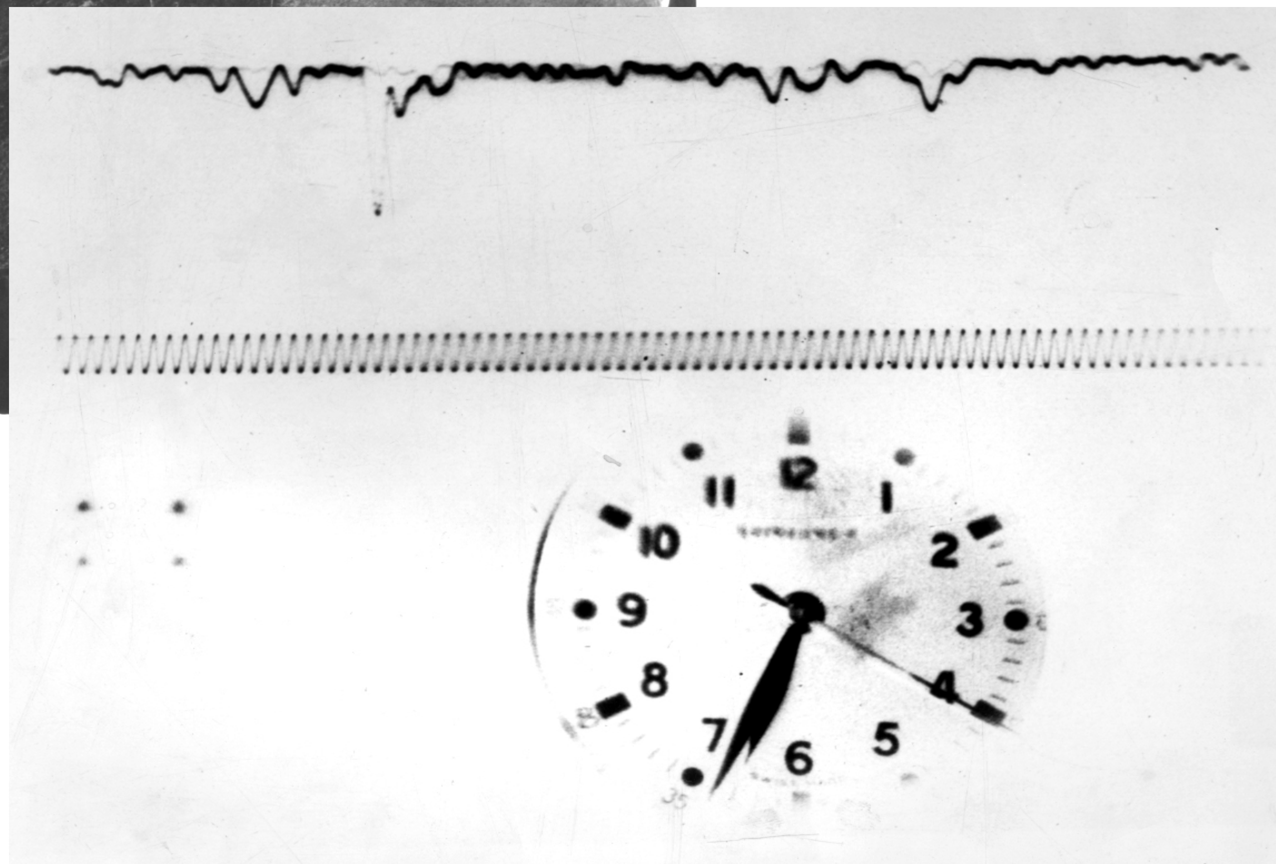

Jelley et al Nature 1965
R. A. Porter MSc Thesis 1967

The renaissance of radio detection of cosmic rays

TIM HUEGE[1]

2018: beyond capabilities of standard installations

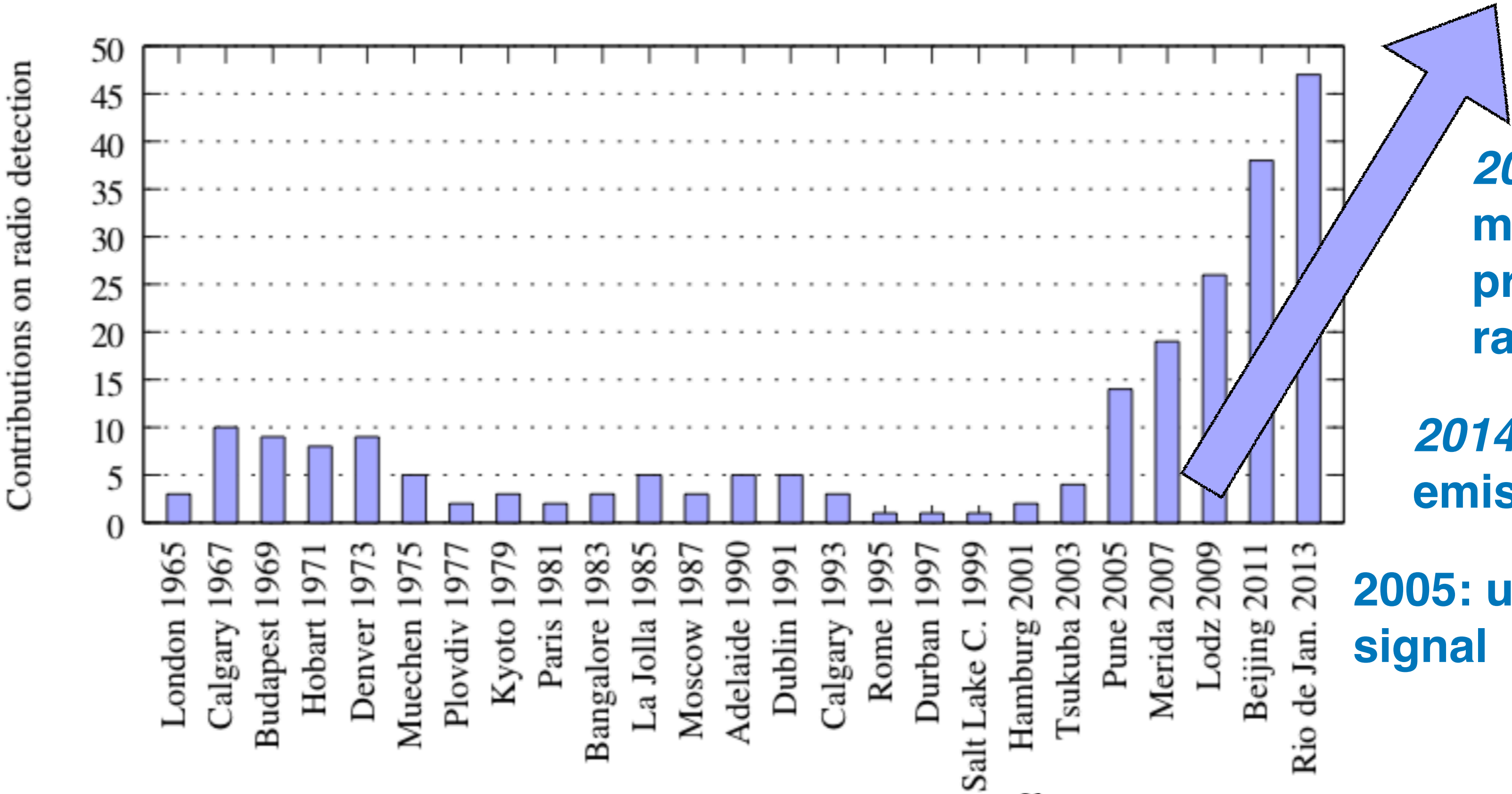

2016: radio technique mature: properties of cosmic rays

2014: understanding the emission processes

2005: understanding the signal

Figure 1: Number of contributions related to radio detection of cosmic rays or neutrinos to the ICRCs since 1965. The field has grown very impressively since the modern activities started around 2003. Data up to 2007 were taken from [11].

Radio Detectors

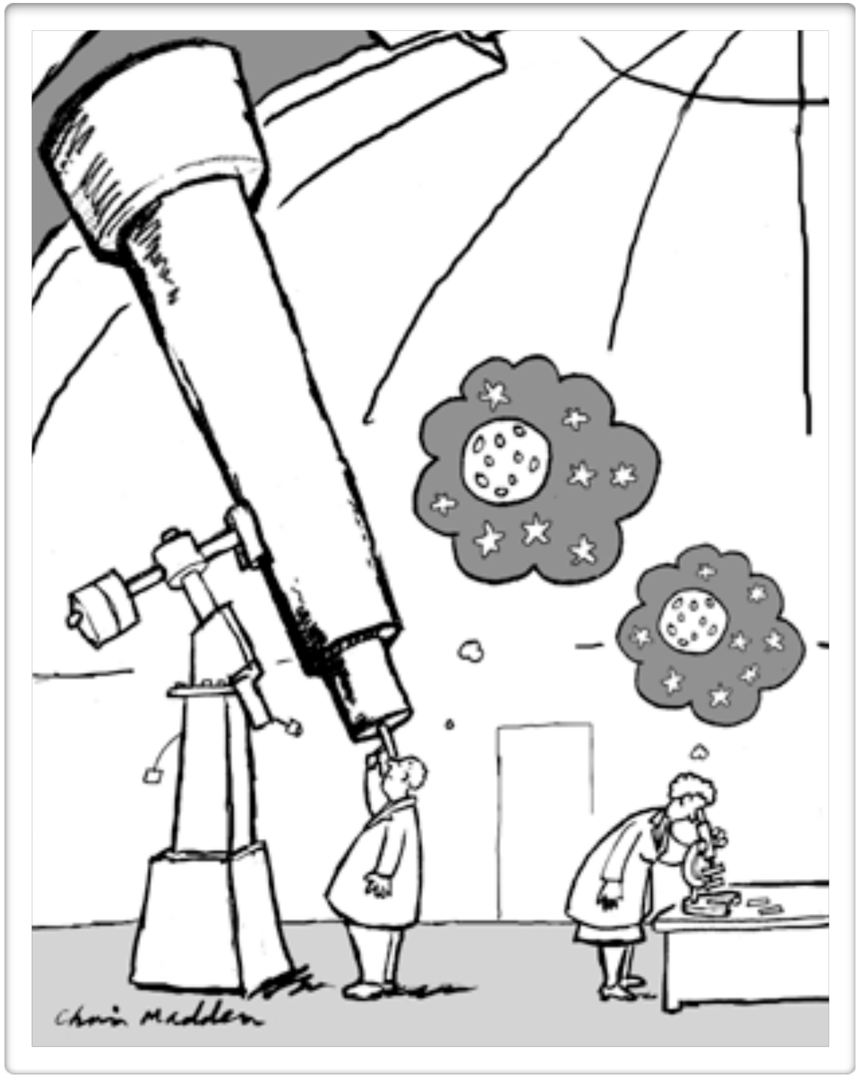

Radio detection of extensive air showers around the world

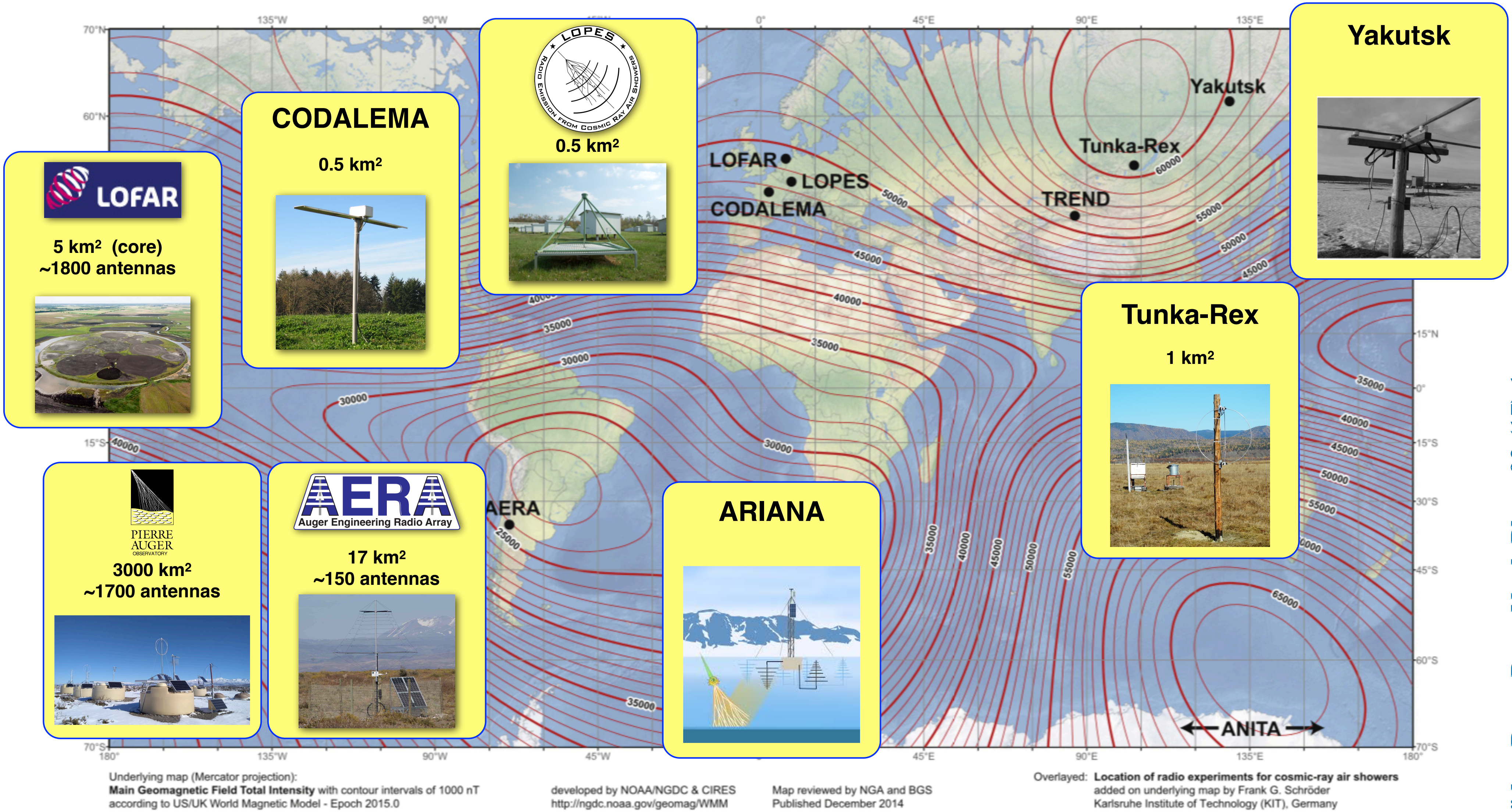

Fig. 21. Map of the total geomagnetic field strengths (world magnetic model [207]) and the location of various radio experiments detecting cosmic-ray air showers.

F.G. Schröder, Prog. Part. Nucl. Phys. 92 (17) 1

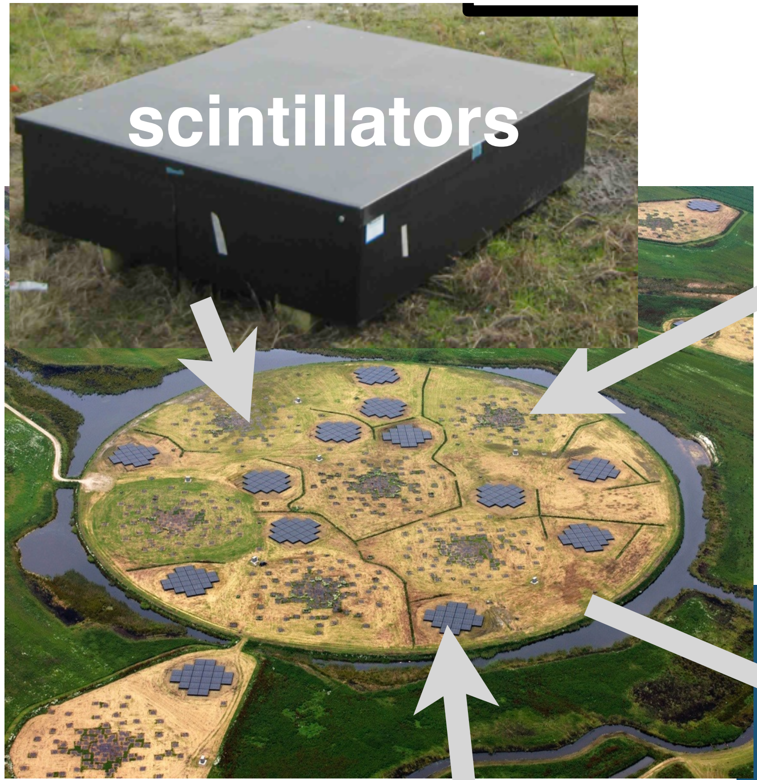

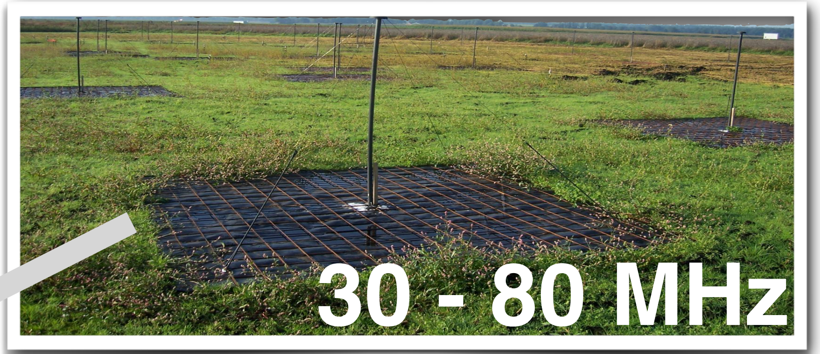

LOFAR

core
23 stations ~5 km^2

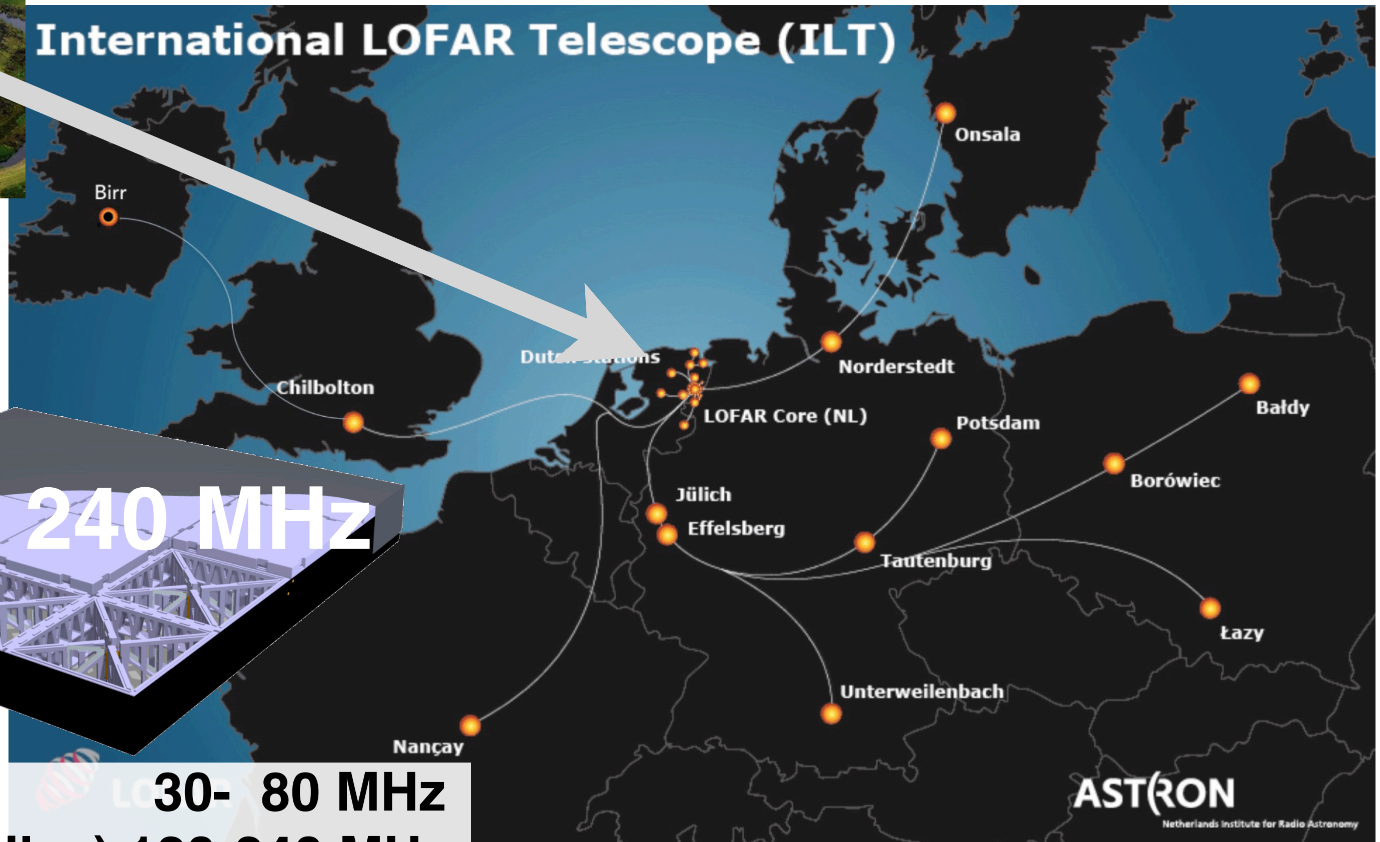

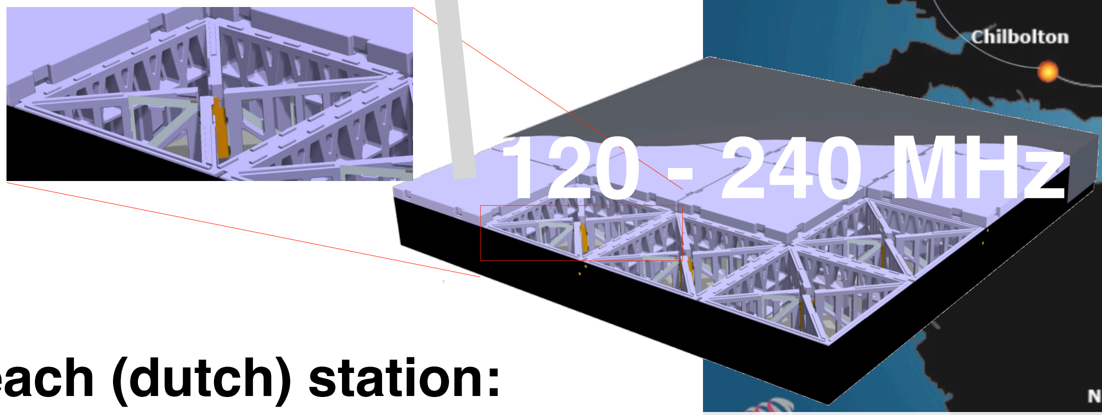

each (dutch) station:
- 96 low-band antennas 30- 80 MHz
- high-band antennas (2x24 tiles) 120-240 MHz

M. van Haarlem et al., A&A 556 (2013) A2

S. Thoudam et al., Nucl. Instr. Meth. A 767 (2014) 339

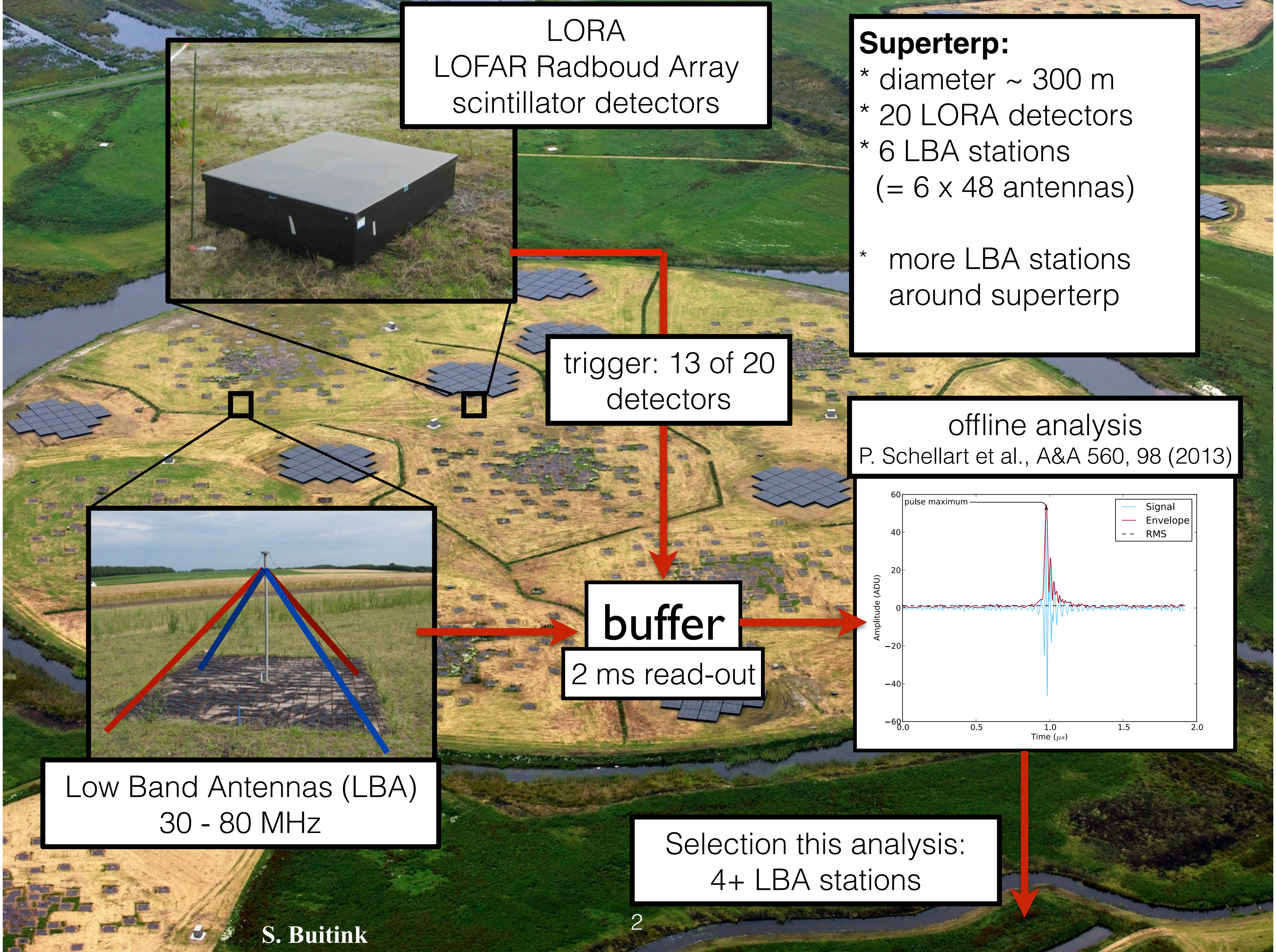
LORA
LOFAR Radboud Array
scintillator detectors
Superterp:
* diameter ~ 300 m
* 20 LORA detectors
* 6 LBA stations
(= 6 x 48 antennas)
* more LBA stations
around superterp
trigger: 13 of 20
detectors
offline analysis
P. Schellart et al., A&A 560, 98 (2013)
pulse maximum
Signal
Envelope
RMS
Amplitude (ADU)
Time (μs)
buffer
2 ms read-out
Low Band Antennas (LBA)
30 - 80 MHz
Selection this analysis:
4+ LBA stations
S. Buitink

A measured air shower

angular difference particles - radio

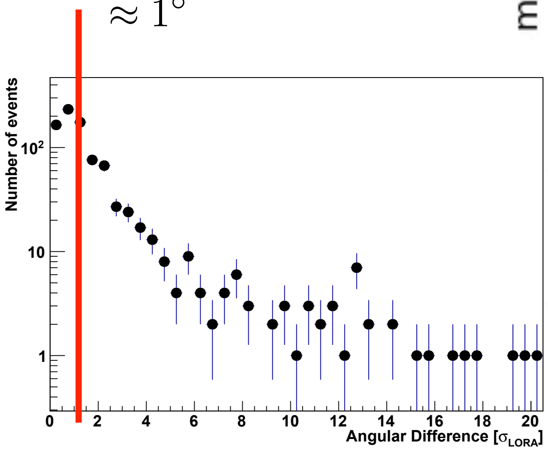

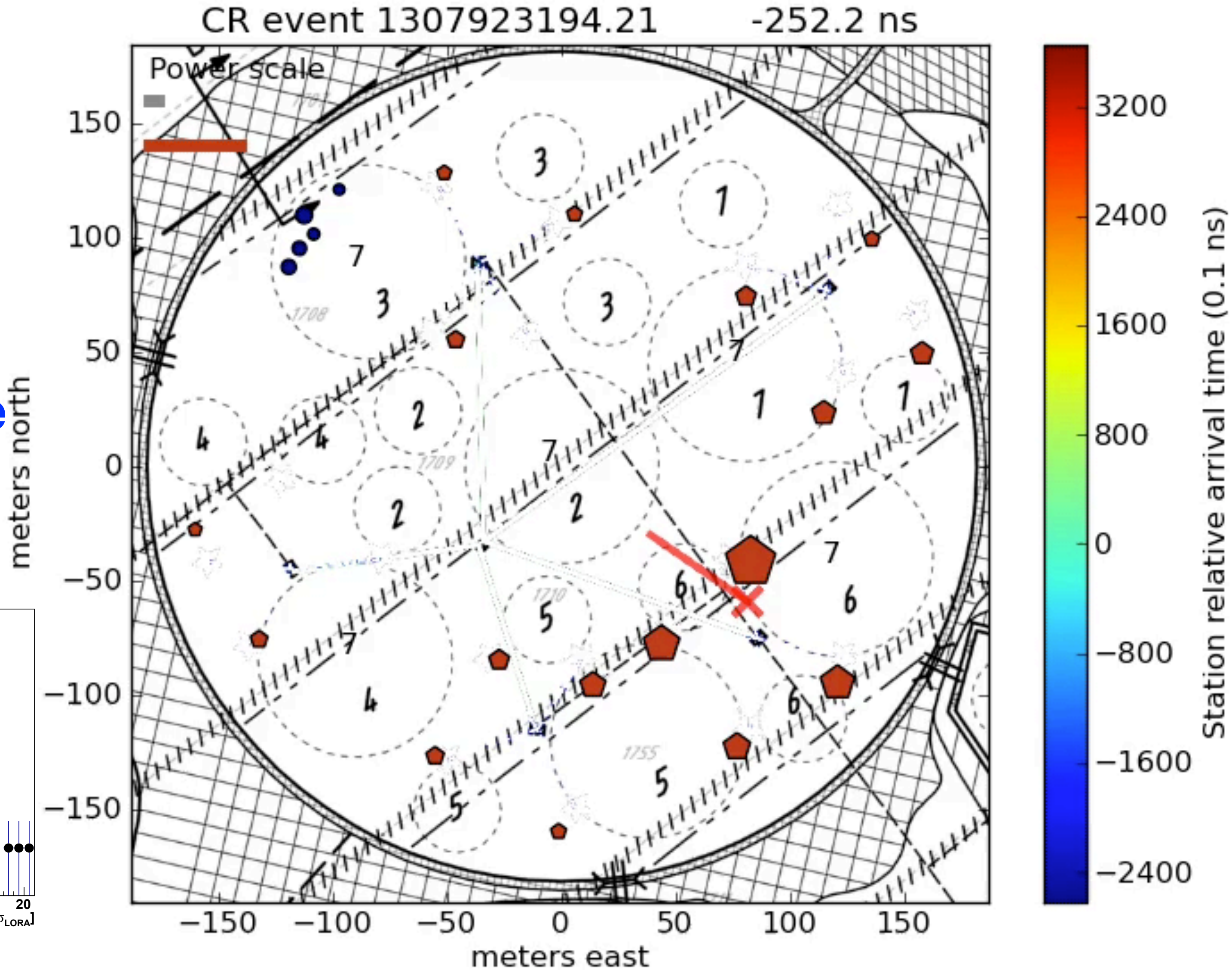

Circles: LOFAR antennas, Pentagons: LORA particle detectors, size denotes signal strength

LOFAR

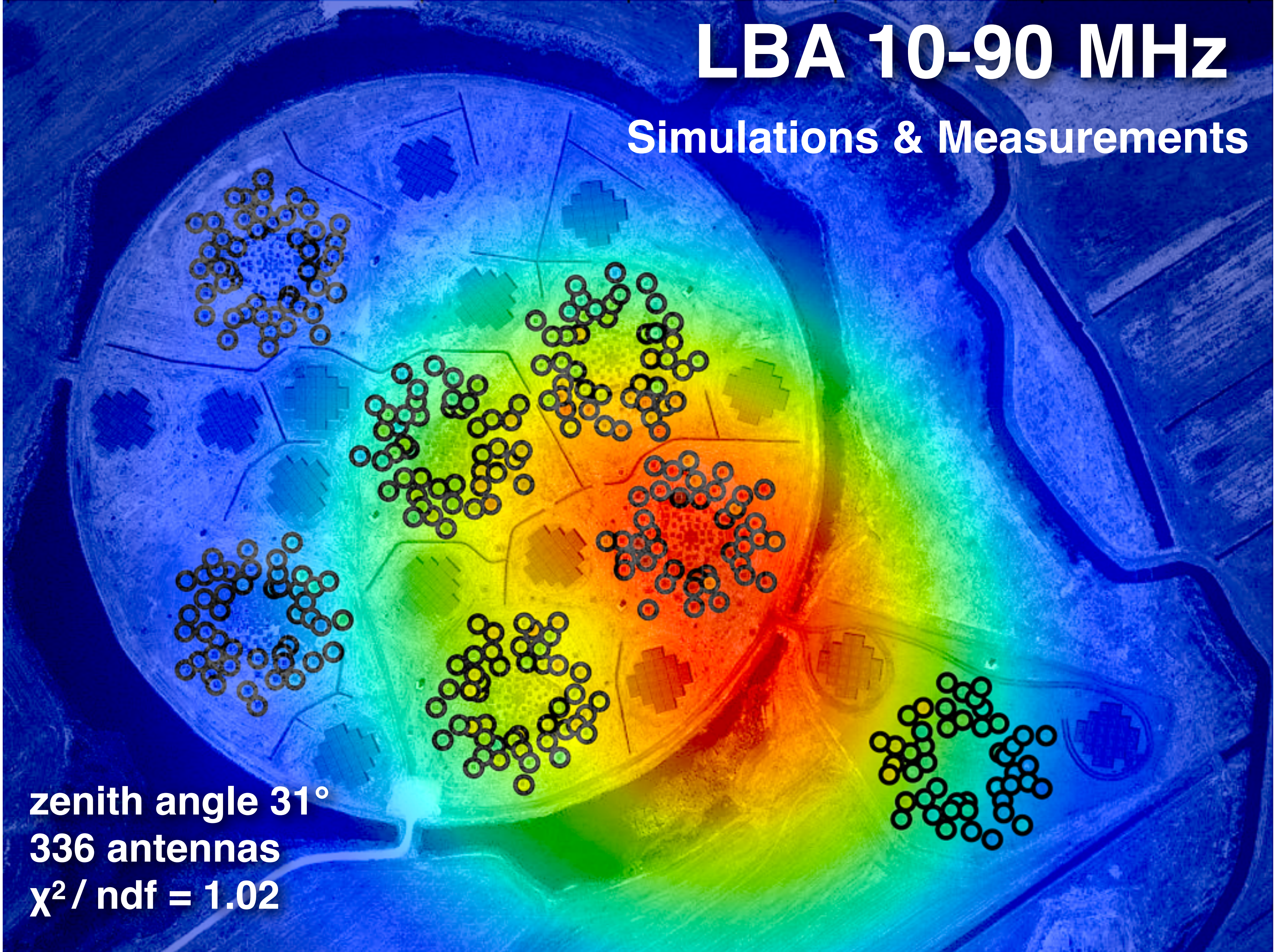

LBA 10-90 MHz
Simulations & Measurements
zenith angle 31°
336 antennas
χ² / ndf = 1.02

PIERRE AUGER OBSERVATORY

AERA
Auger Engineering Radio Array

~150 antennas
~17 km²
30-80 MHz

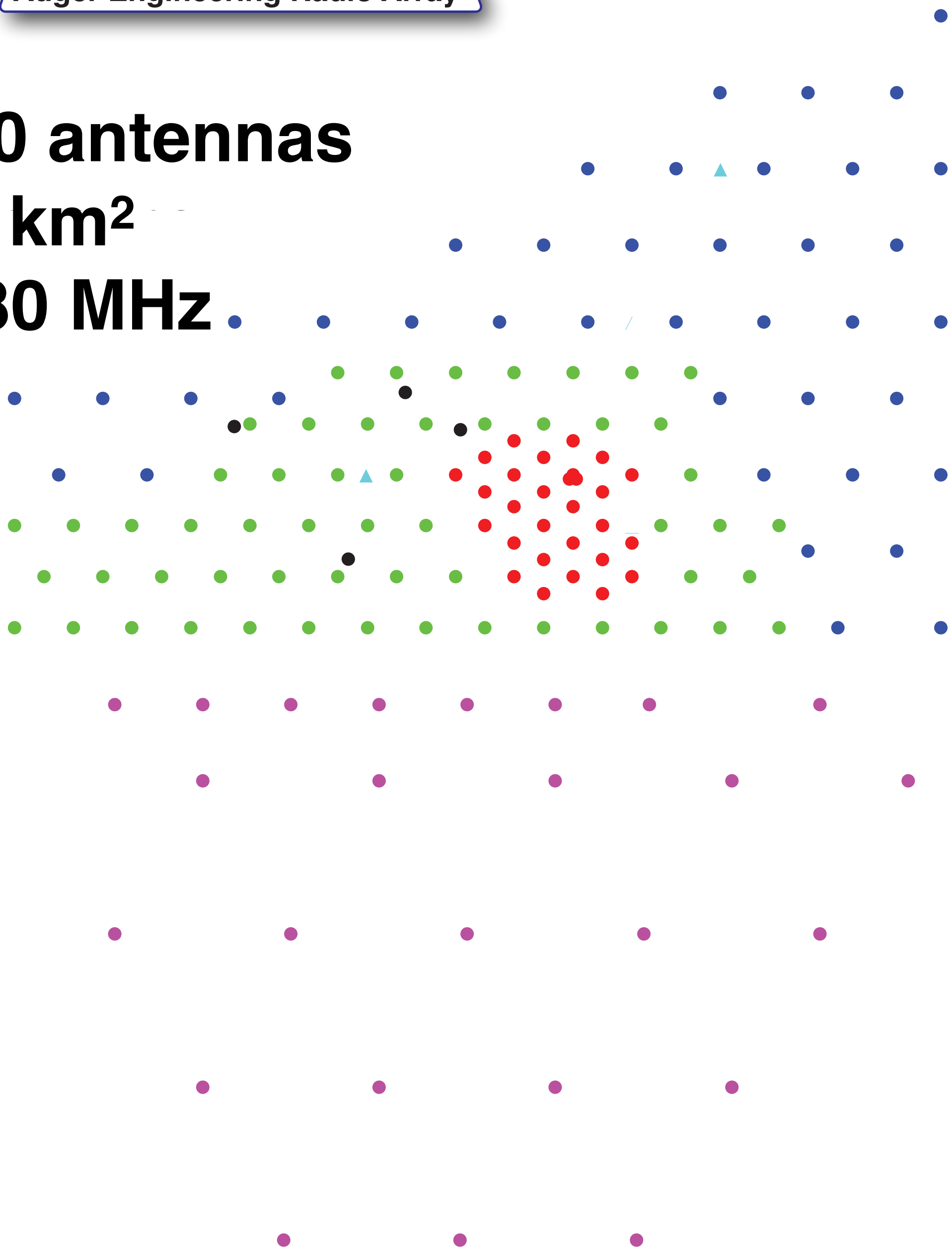

LOFAR core
23 stations ~5 km²

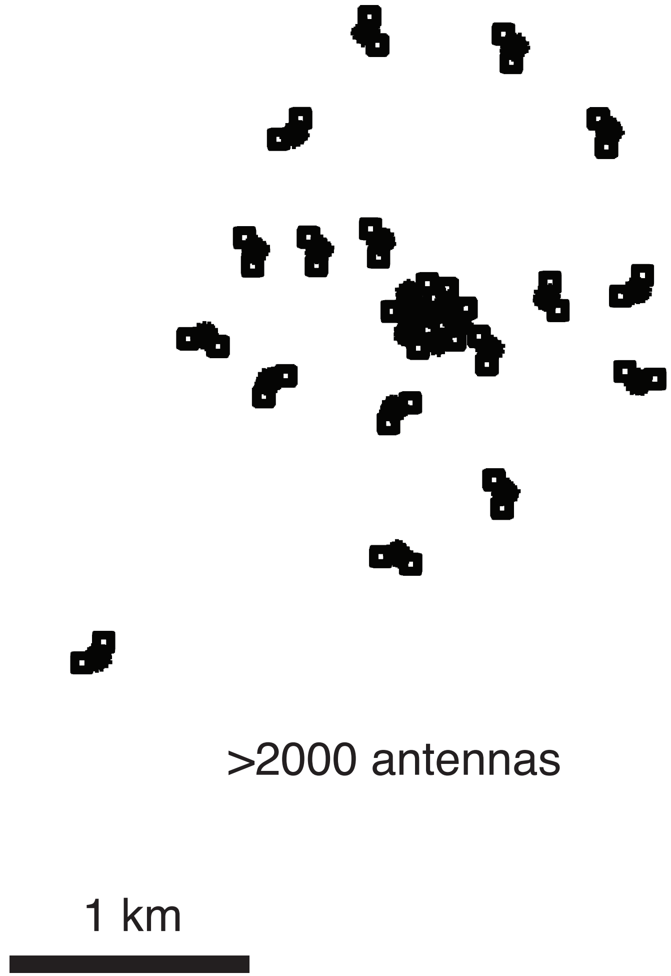

PIERRE AUGER OBSERVATORY

AERA
Auger Engineering Radio Array

~150 antennas
~17 km²
30-80 MHz

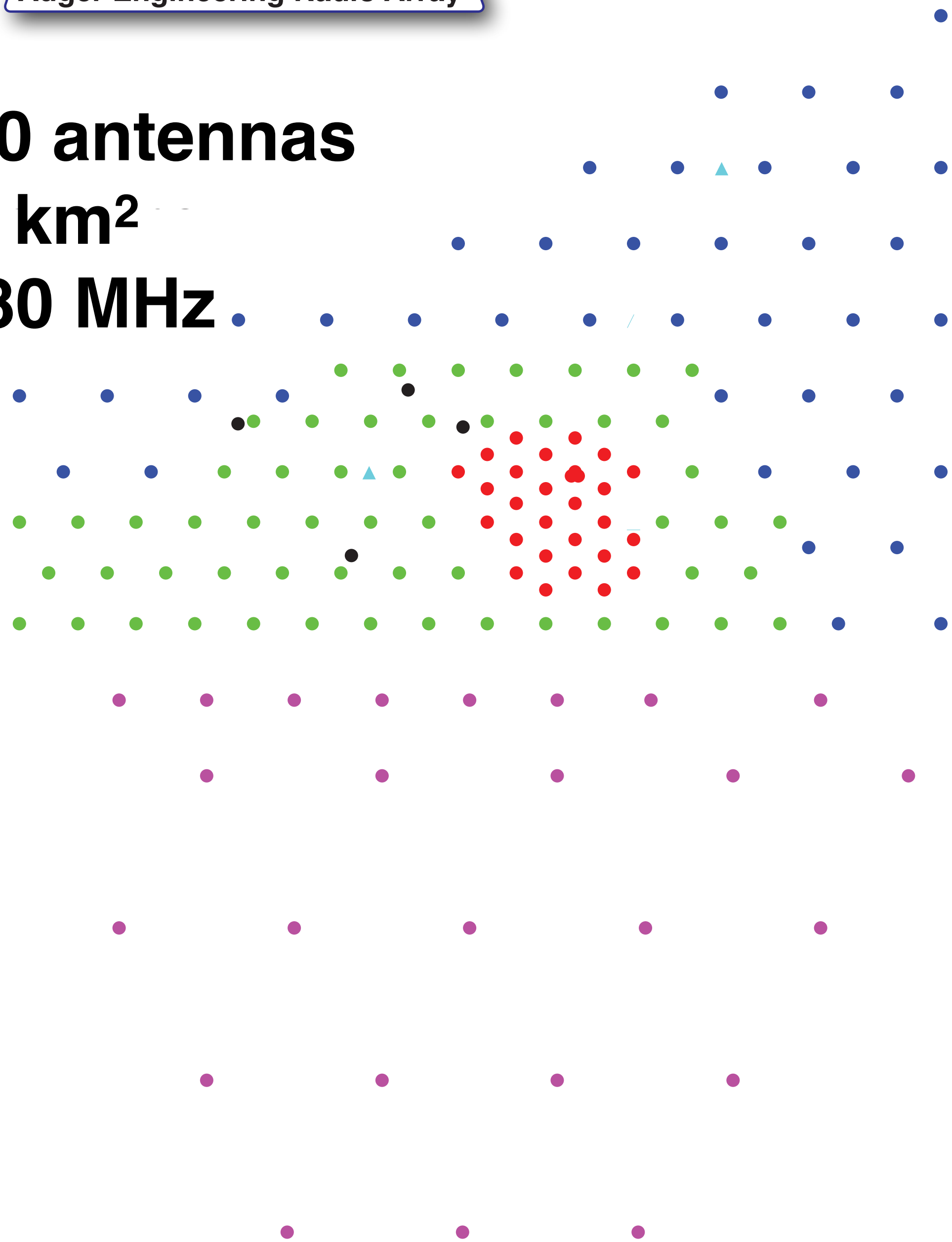

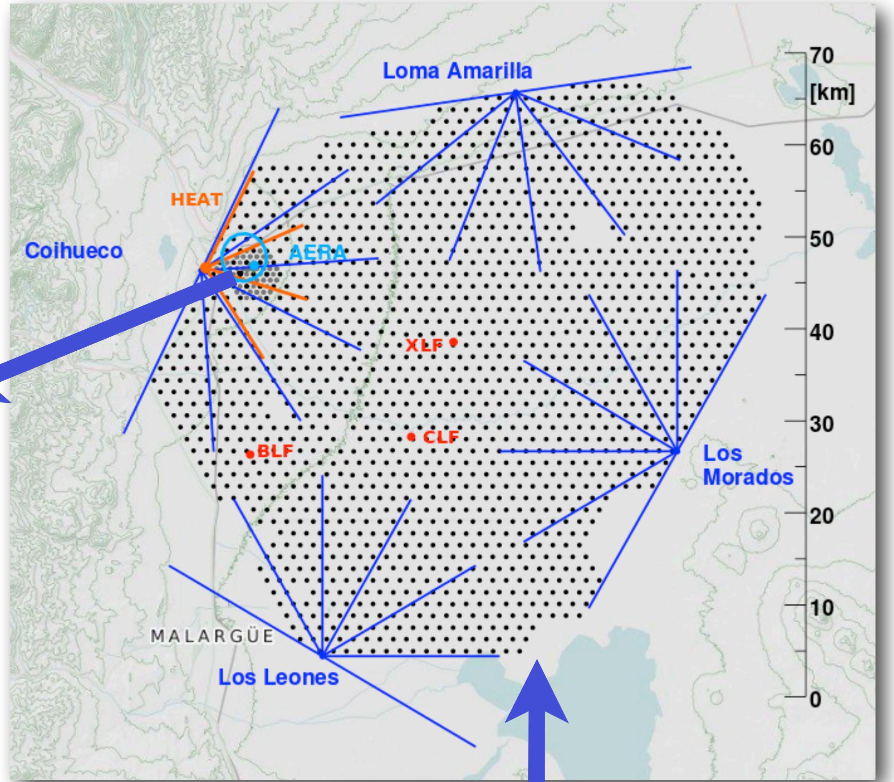

AERA
Auger Engineering Radio Array

~150 antennas
~17 km^2
30-80 MHz

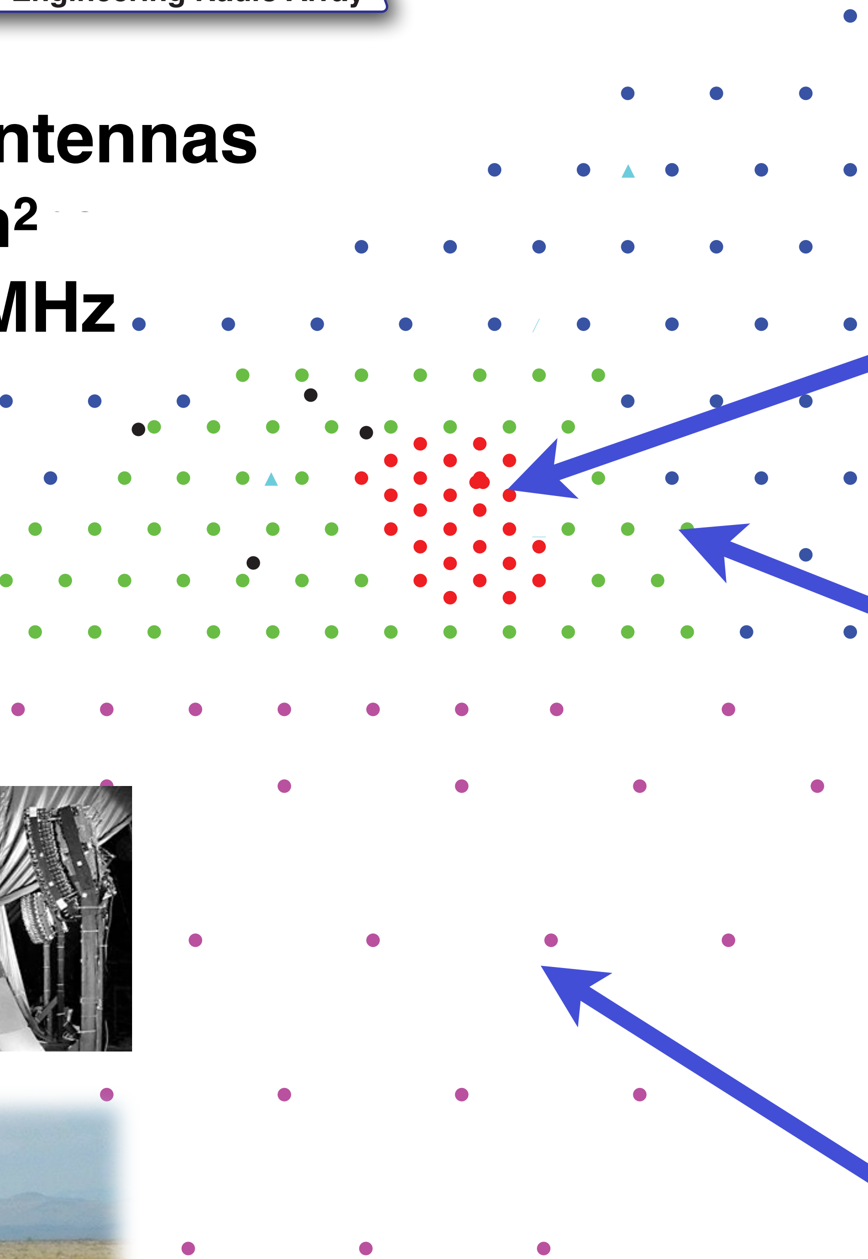

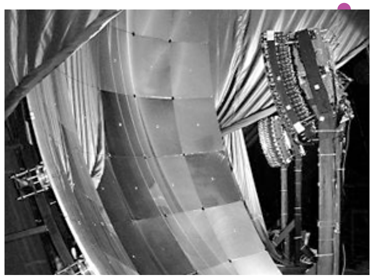

Calibration

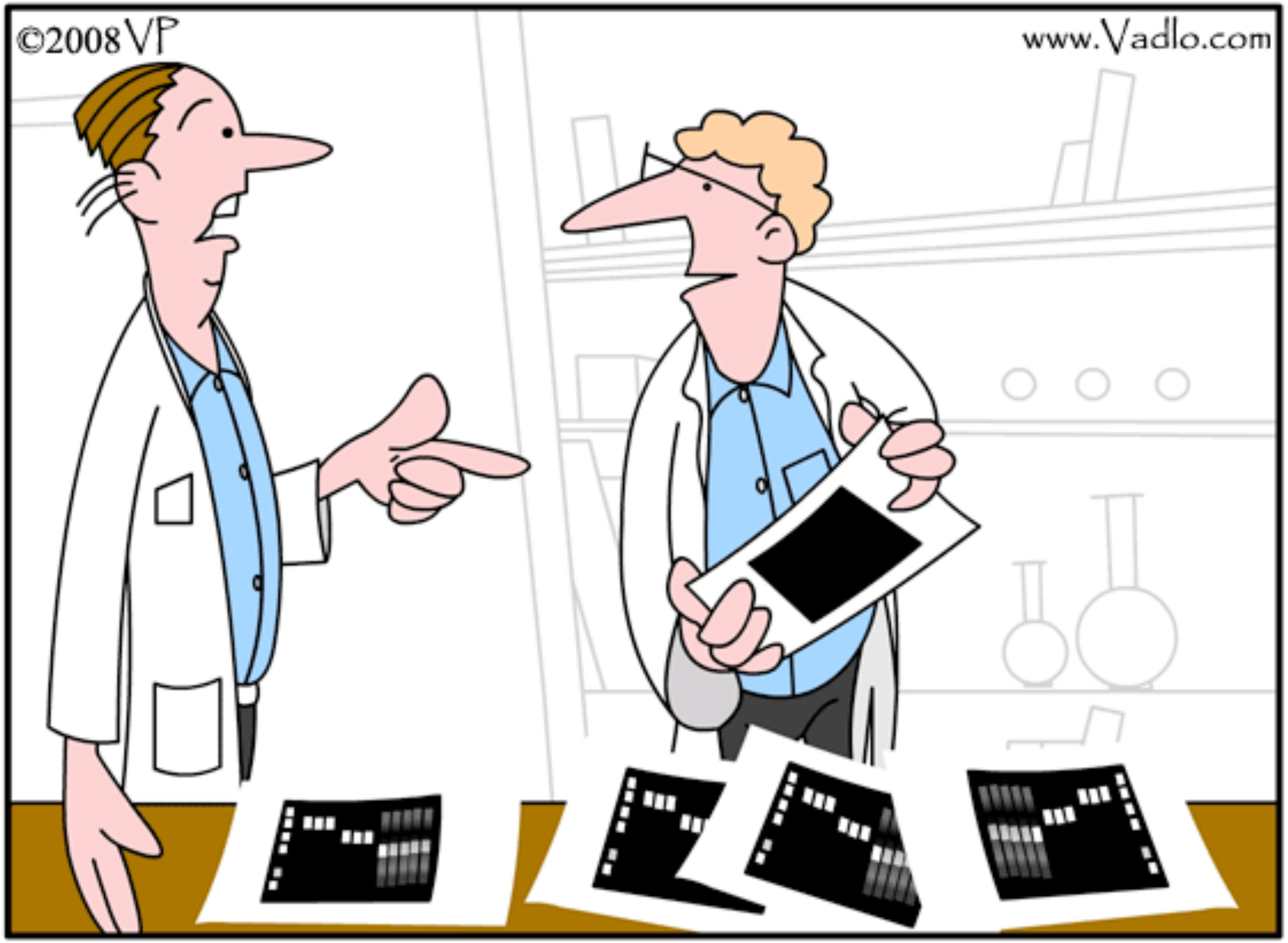

*Data don't make any sense, we will have to resort to **statistics**.*

Simulating Galaxy Noise

Visible galaxy at 00.00,6:00,12:00,18:00 Local Sidereal Time

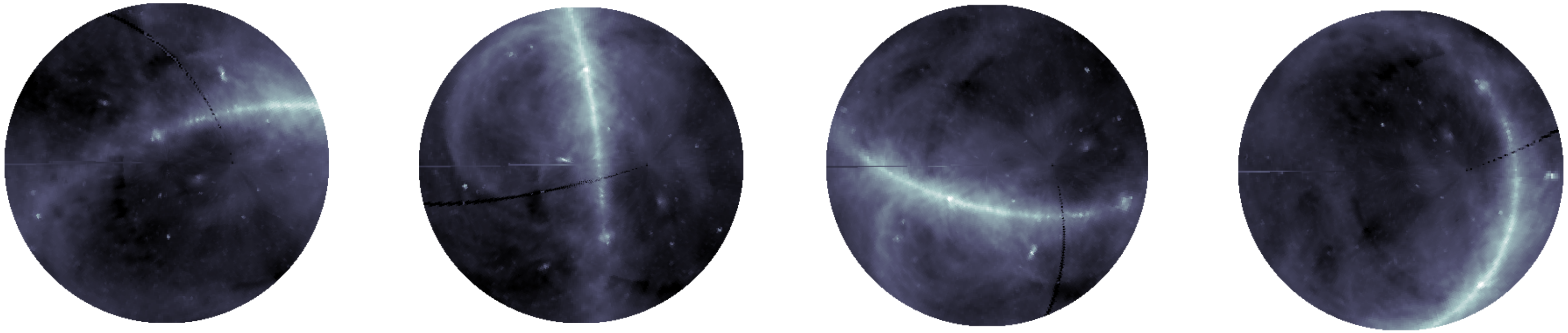

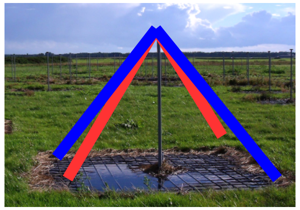

$$\mathbf{P}(\nu) = \frac{2\mathbf{k_B}}{\mathbf{c^2}}\nu^2 \int \mathbf{T_{sky}}(\nu,\theta,\phi)\frac{|\vec{\mathbf{H}}(\nu,\theta,\phi)|^2\mathbf{Z_0}}{2\mathbf{Z_a}}\mathbf{d}\Omega \quad \mathbf{WHz^{-1}}$$

Average antenna response at 55 MHz

$$< |\vec{\mathbf{H}}(\nu,\theta,\phi)|^2 >$$

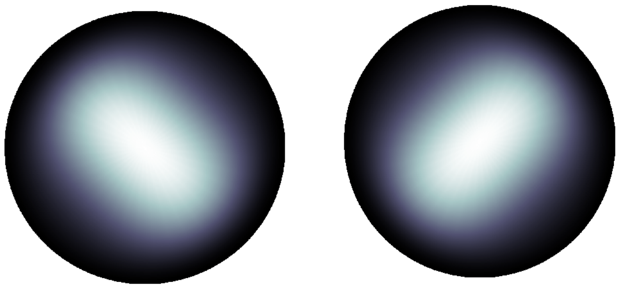

pol 0 pol 1

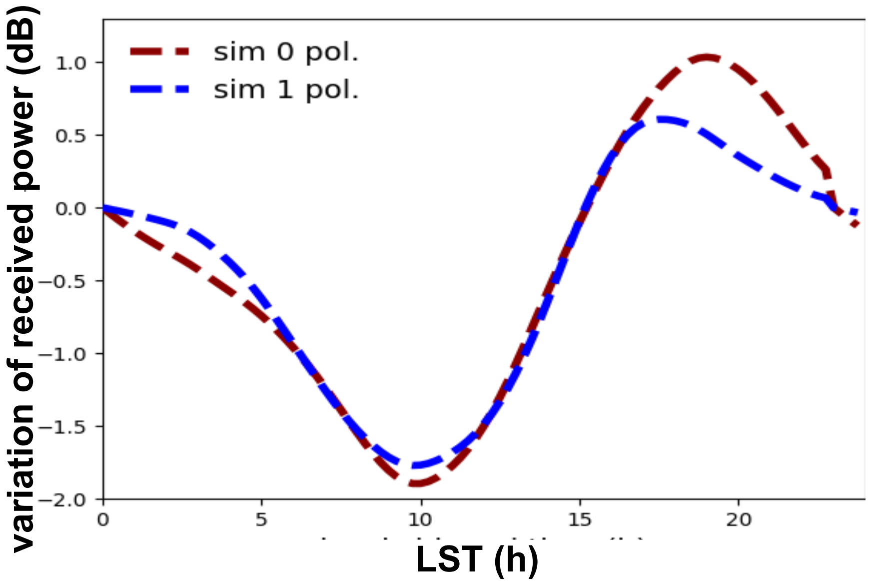

4

K. Mulrey et al., Astropart. Phys., 111 (2019) 1

A&A, 679, A50 (2023)
https://doi.org/10.1051/0004-6361/202245382
© The Authors 2023

Astronomy & Astrophysics

Uncertainties of the 30–408 MHz Galactic emission as a calibration source for radio detectors in astroparticle physics

M. Büsken[1,2], T. Fodran[3], and T. Huege[4,5]

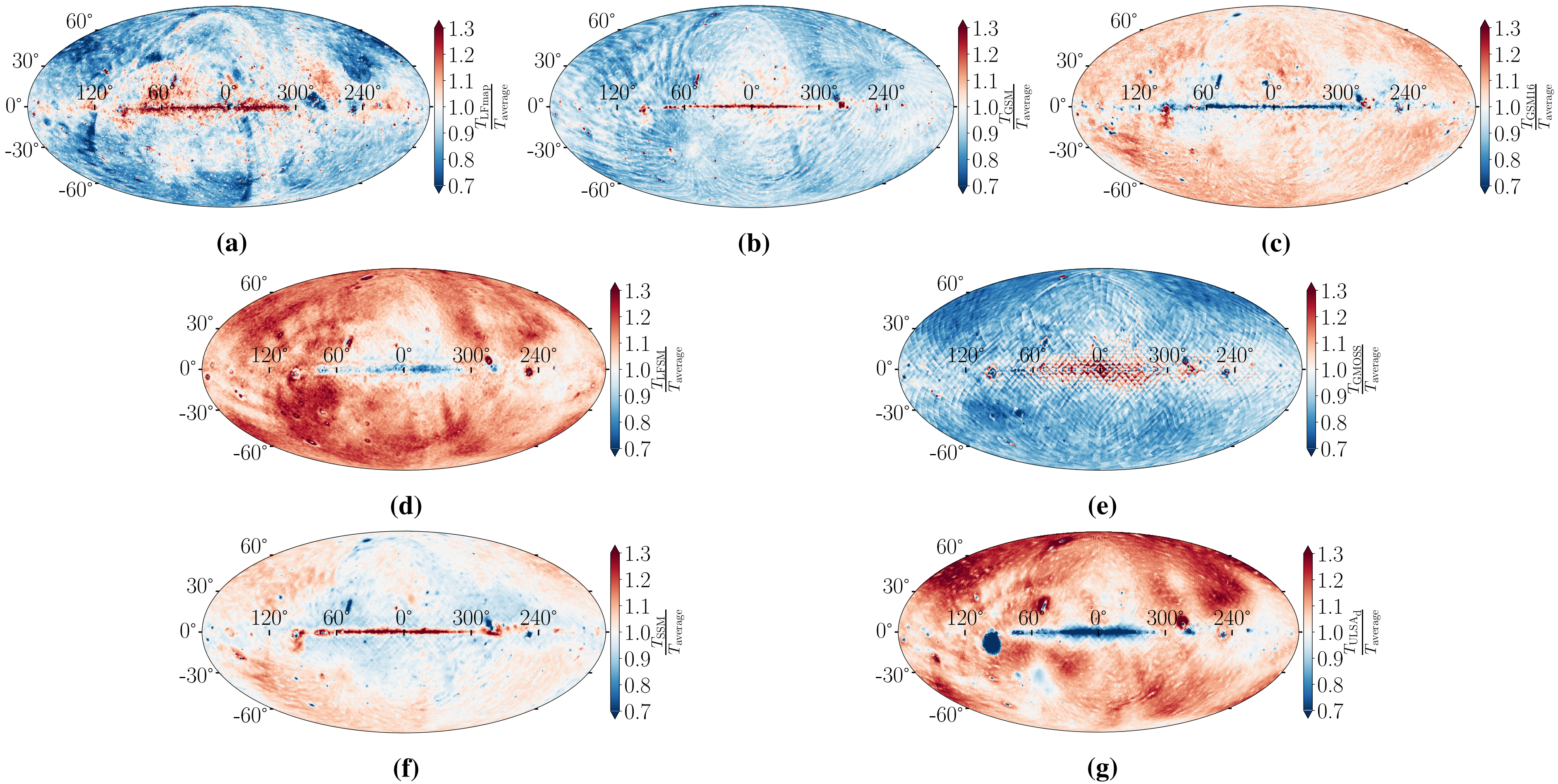

Fig. 2. Sky maps showing the temperature ratio of each model to the average from all seven models at 50 MHz in Galactic coordinates. The models are denoted as (a) LFmap, (b) GSM, (c) GSM16, (d) LFSM, (e) GMOSS, (f) SSM, (g) ULSA.

LOFAR Signal Chain

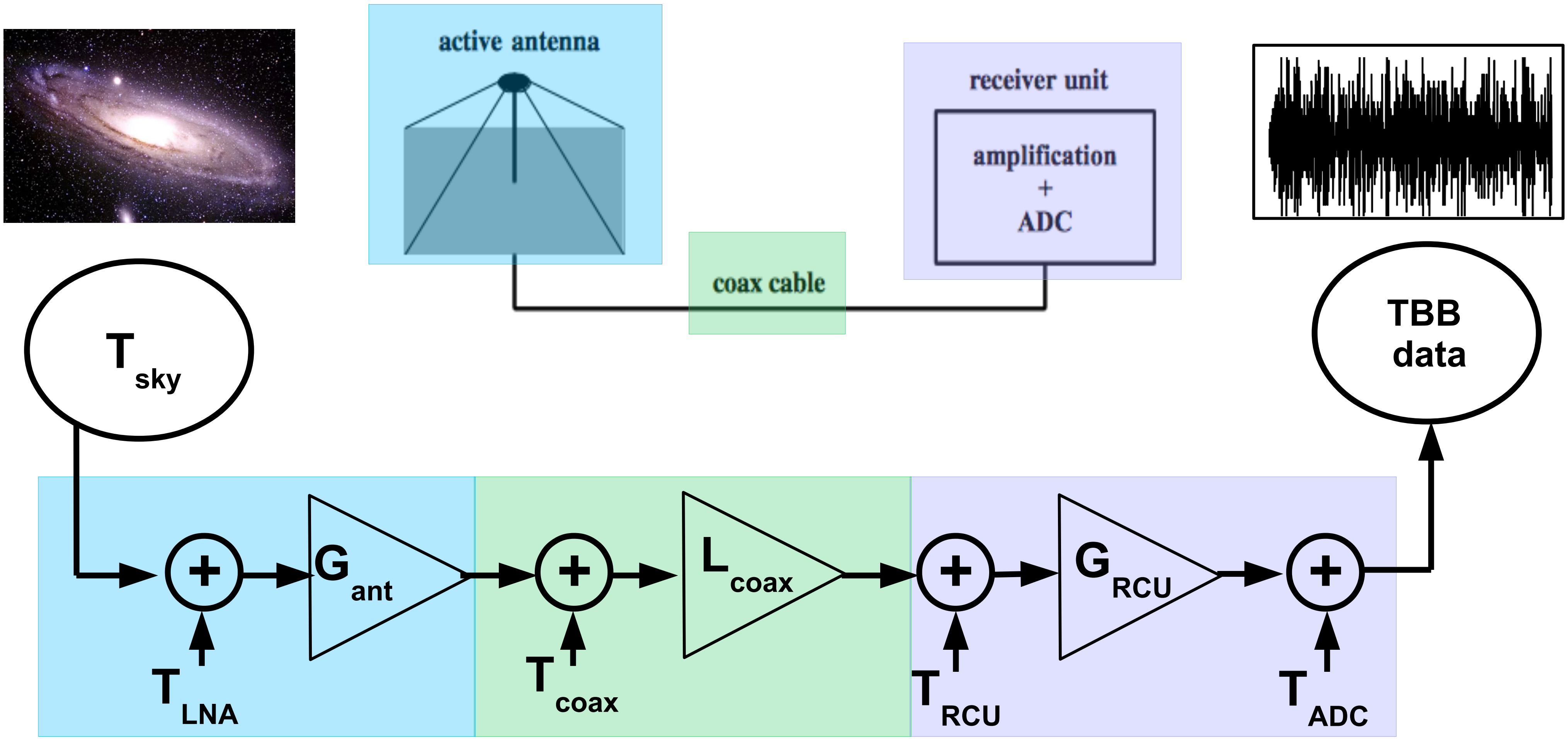

G_{ant} , L_{coax} , G_{RCU} → Freq. Dependent losses and gains

T_{LNA} , T_{coax} , T_{RCU} , T_{ADC} → Constant noise values

7

K. Mulrey et al., Astropart. Phys., 111 (2019) 1

LOFAR Signal Chain

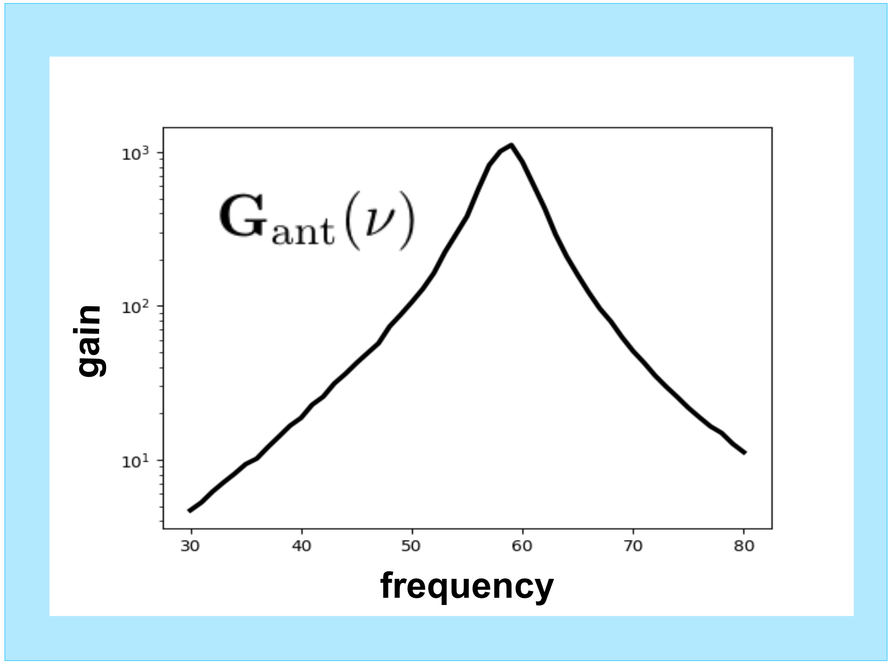

$$\left(\mathbf{P}_{\mathrm{sky}}(\nu, \mathbf{t}) + \mathbf{T}_{\mathrm{LNA}}\right)\mathbf{G}_{\mathrm{ant}}(\nu)\mathbf{A}(\nu)$$

$\mathbf{G}_{\mathrm{ant}}(\nu)$ Antenna gain, simulated with WIPL-D software, with known misaligned resonance frequency

$\mathbf{A}(\nu)$ correction to antenna model

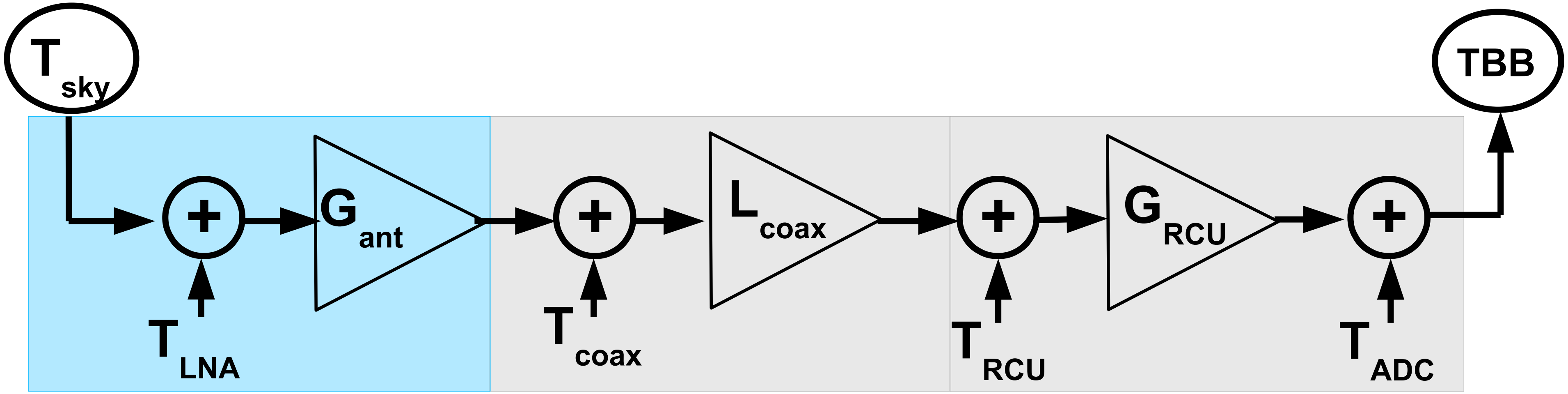

8

K. Mulrey et al., Astropart. Phys., 111 (2019) 1

LOFAR Signal Chain

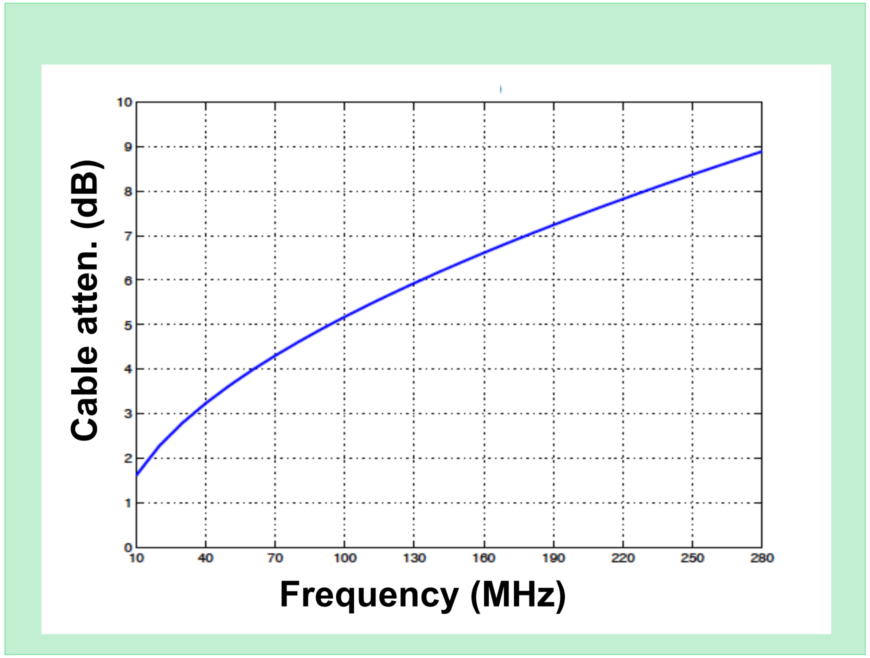

$$\left(\mathbf{P}_{\rm sky}(\nu,\mathbf{t}) + \mathbf{T}_{\rm LNA}\right)\mathbf{G}_{\rm ant}(\nu)\mathbf{A}(\nu)\mathbf{L}_{\rm coax}(\nu)$$

$\mathbf{L}_{\rm coax}(\nu)$ Cable attenuation (50m, 80m ,115m)

$$\mathbf{T}_{\rm coax} << \mathbf{T}_{\rm LNA}, \mathbf{T}_{\rm RCU}, \mathbf{T}_{\rm ADC}$$

(not included in model)

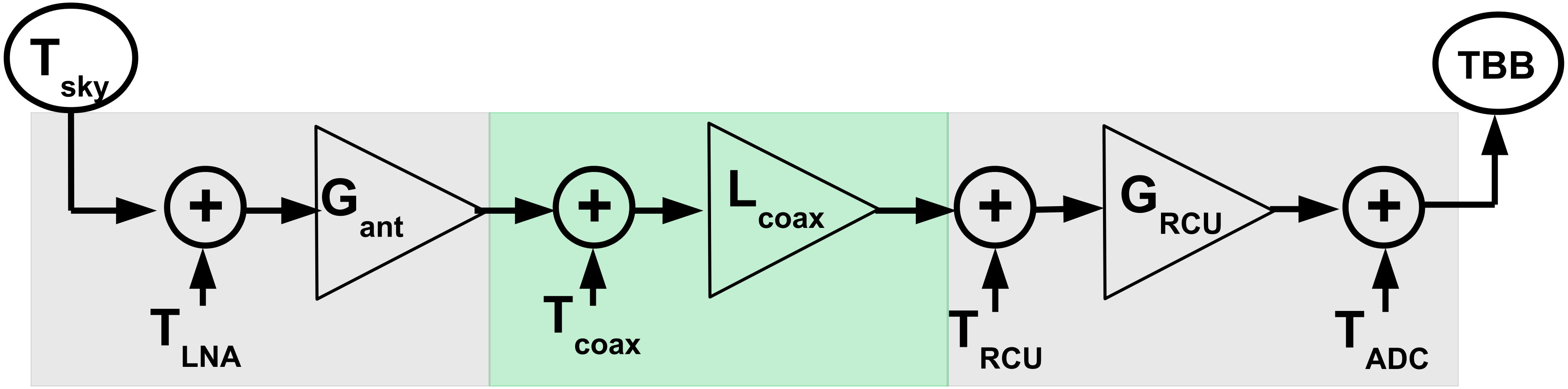

9

LOFAR Signal Chain

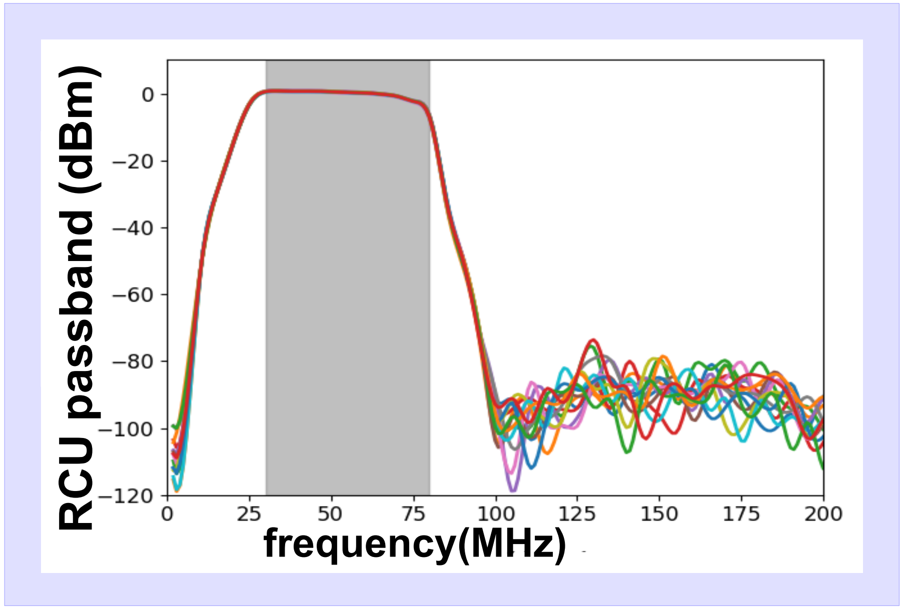

$\mathbf{T}_{\mathrm{RCU}}$ Noise from amplification in RCU

$\mathbf{G}_{\mathrm{RCU}}(\nu)$ RCU passband filter

$\mathbf{S}$ scale factor between voltage and ADC units

$\mathbf{T}_{\mathrm{ADC}}$ time jitter noise from digitization

$$\left(\left(\mathbf{P}_{\mathrm{sky}}(\nu,\mathbf{t})+\mathbf{T}_{\mathrm{LNA}}\right)\mathbf{G}_{\mathrm{ant}}(\nu)\mathbf{A}(\nu)\mathbf{L}_{\mathrm{coax}}(\nu)+\mathbf{T}_{\mathrm{RCU}}\right)\mathbf{G}_{\mathrm{RCU}}(\nu)\mathbf{S}+\mathbf{T}_{\mathrm{ADC}}=\mathbf{P}_{\mathrm{sim}}(\nu,\mathbf{t})$$

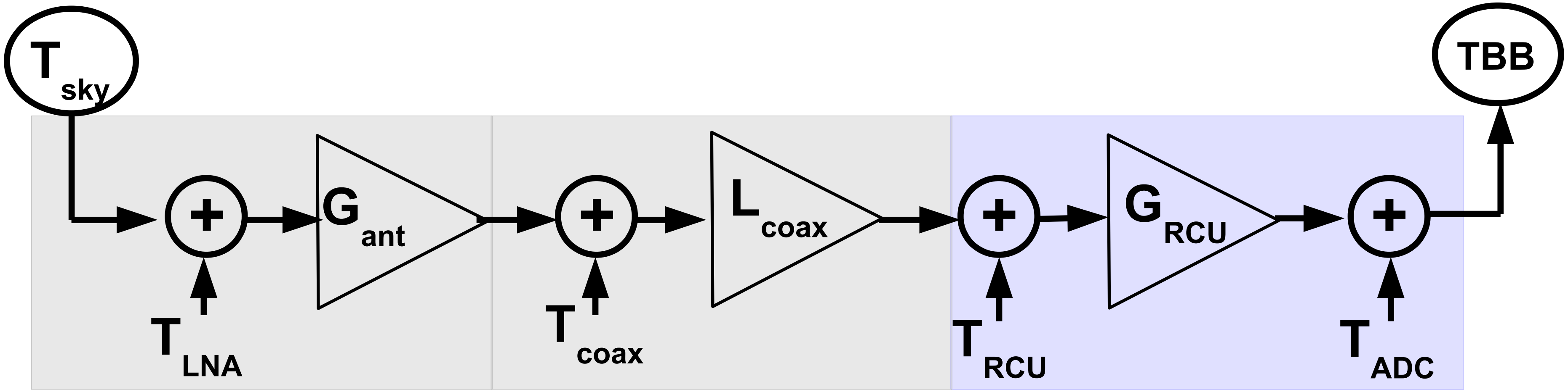

10

K. Mulrey et al., Astropart. Phys., 111 (2019) 1

LOFAR Signal Chain

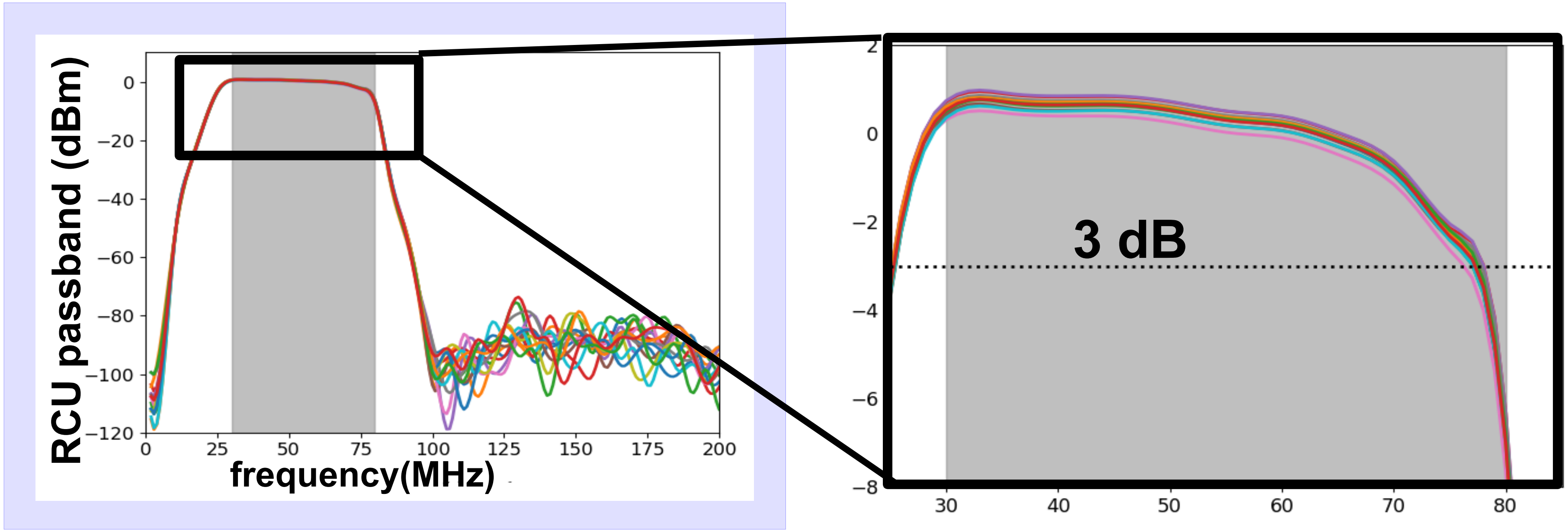

$$\left(\left(\mathbf{P}_{\text{sky}}(\nu,\mathbf{t})+\mathbf{T}_{\text{LNA}}\right)\mathbf{G}_{\text{ant}}(\nu)\mathbf{A}(\nu)\mathbf{L}_{\text{coax}}(\nu)+\mathbf{T}_{\mathbf{RCU}}\right)\mathbf{G}_{\text{RCU}}(\nu)\mathbf{S}+\mathbf{T}_{\text{ADC}}=\mathbf{P}_{\text{sim}}(\nu,\mathbf{t})$$

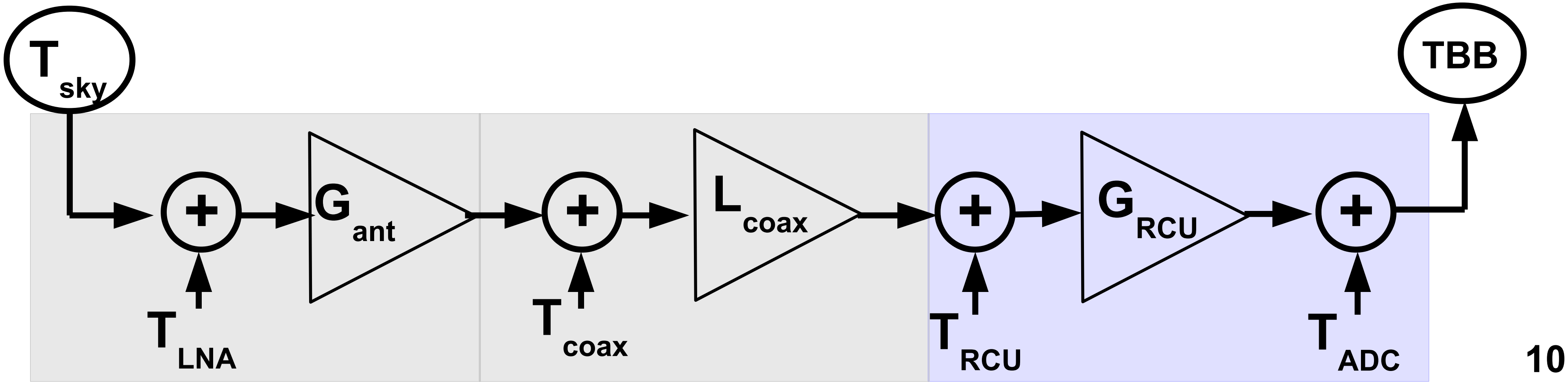

K. Mulrey et al., Astropart. Phys., 111 (2019) 1

Fitting for Electronic Noise

$$\left(\left(\mathbf{P}_{\mathrm{sky}}(\nu,\mathbf{t})+\mathbf{T}_{\mathrm{LNA}}\right)\mathbf{G}_{\mathrm{ant}}(\nu)\mathbf{A}(\nu)\mathbf{L}_{\mathrm{coax}}(\nu)+\mathbf{T}_{\mathrm{RCU}}\right)\mathbf{G}_{\mathrm{RCU}}(\nu)\mathbf{S}+\mathbf{T}_{\mathrm{ADC}}=\mathbf{P}_{\mathrm{sim}}(\nu,\mathbf{t})$$

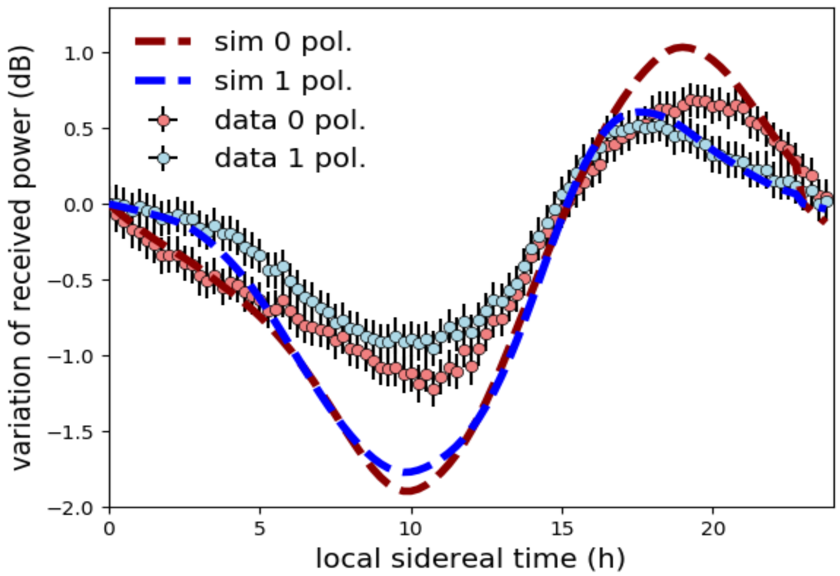

known, frequency dependent quantity

unknown, constant quantity

Fitted noise values at ADC

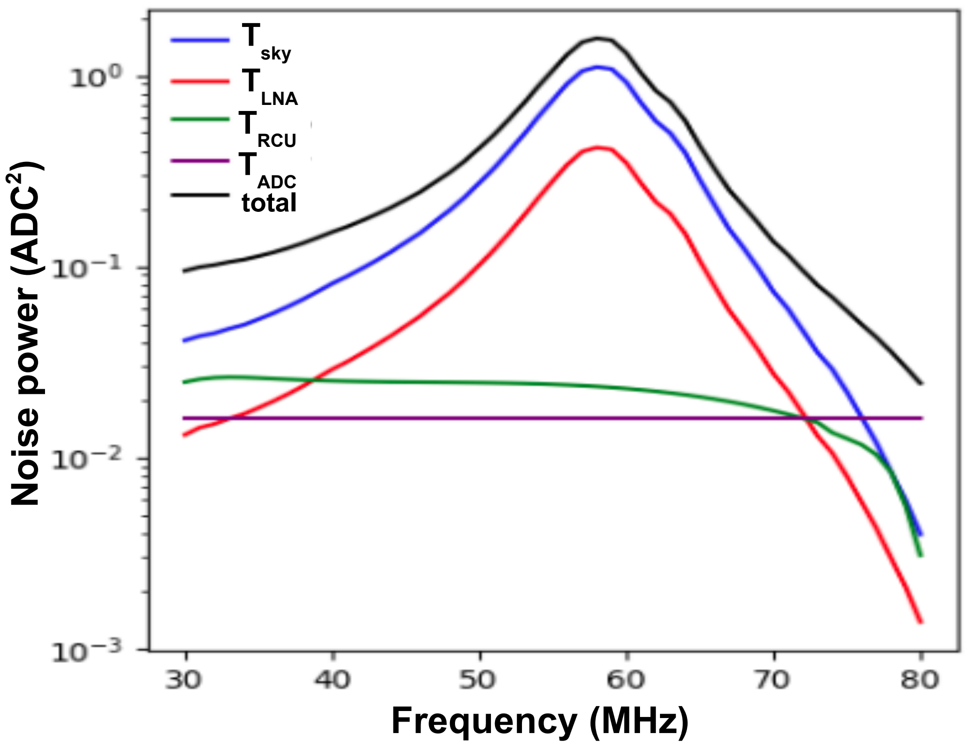

$$X^2=\sum\frac{(\mathrm{P}(\nu,\mathrm{t})_{\mathrm{data}}-\mathrm{P}(\nu,\mathrm{t})_{\mathrm{sim}})^2}{\sigma(\nu,\mathrm{t})_{\mathrm{data}}}$$

★ All noise contributions are required to fit simulation to data at all frequencies

11

K. Mulrey et al., Astropart. Phys., 111 (2019) 1

Calibration Results

$$\mathbf{C^2}(\nu) = \mathbf{A}(\nu)\mathbf{L}_{\mathrm{coax}}(\nu)\mathbf{G}_{\mathrm{RCU}}(\nu)\mathbf{S}$$

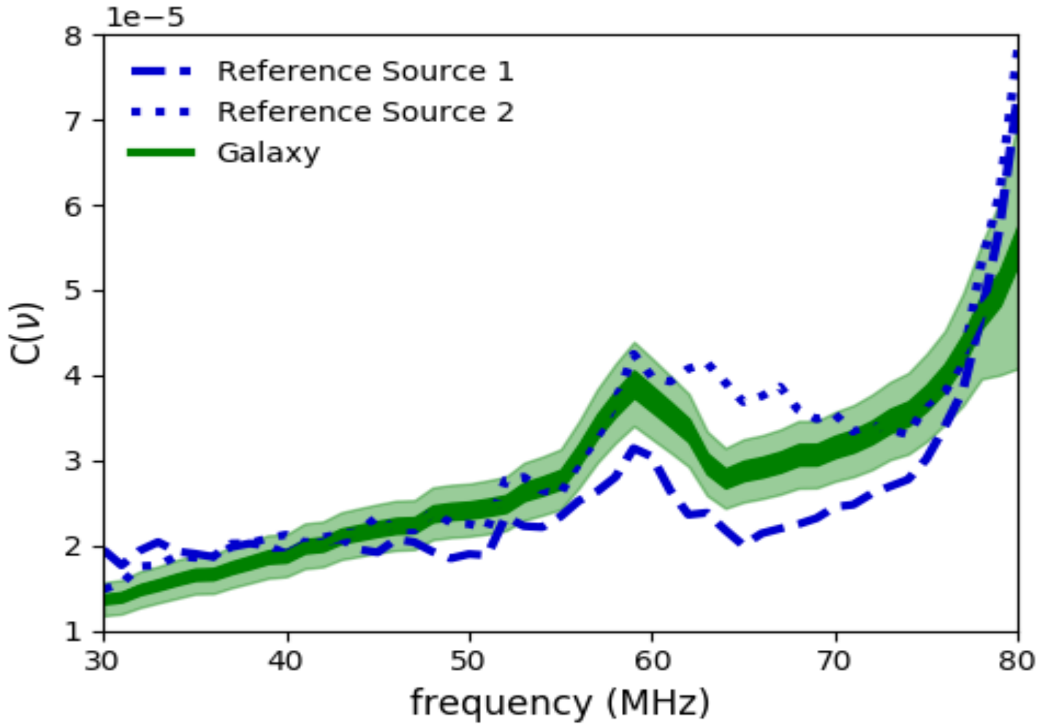

Uncertainty	Percentage
event-to-event fluctuation	4
galaxy model	12
electronic noise < 77 MHz	5-6
electronic noise > 77 MHz	10-20
total < 77 MHz	**14**

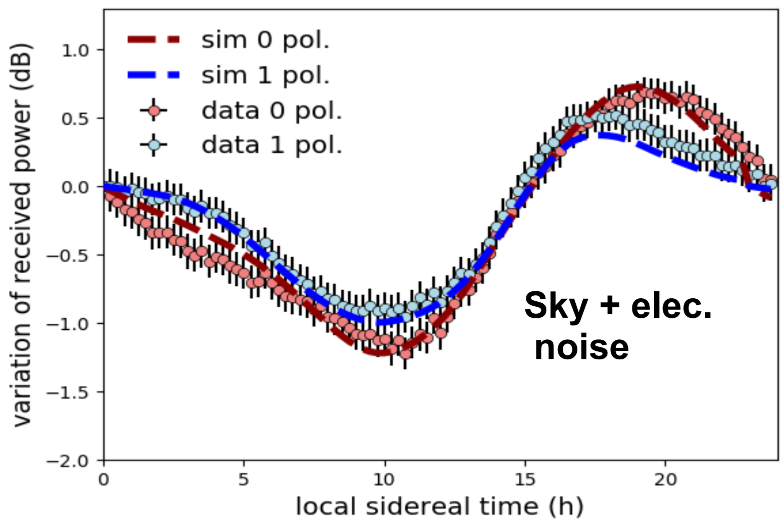

- Galaxy model now limits systematic uncertainties
- Uncertainties from electronic noise are found by comparing resulting calibration constants for different antennas

12

K. Mulrey, ARENA 2018

Timing calibration

A. Aab et al., JINST 11 (2016) no.01, P01018

Use beacon broadcasting at 4 different frequencies to measure relative time shifts

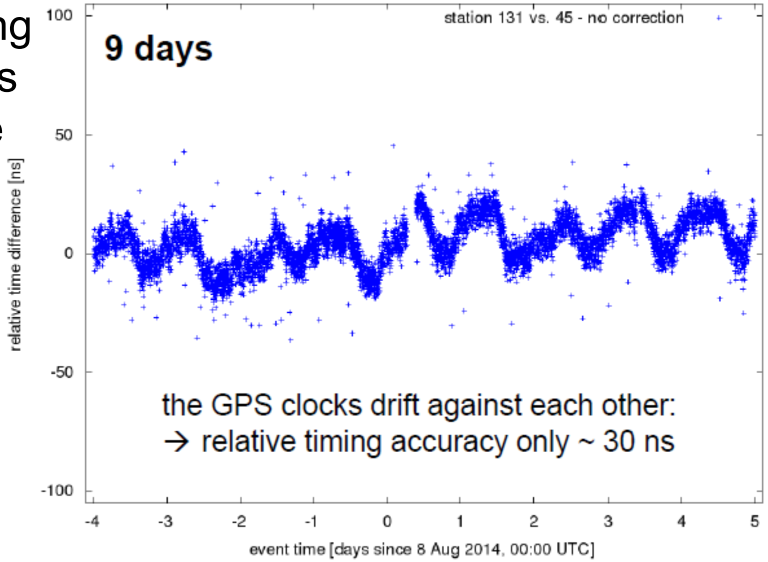

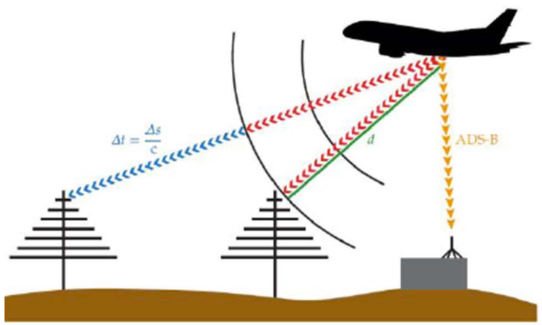

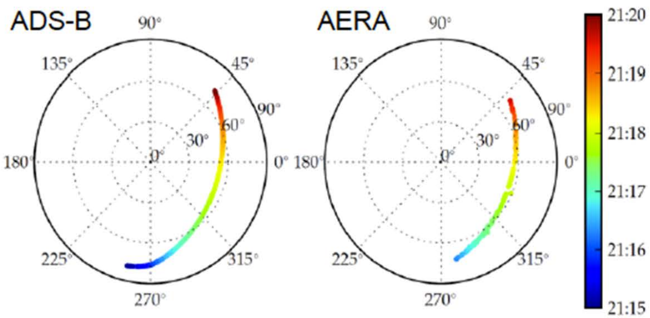

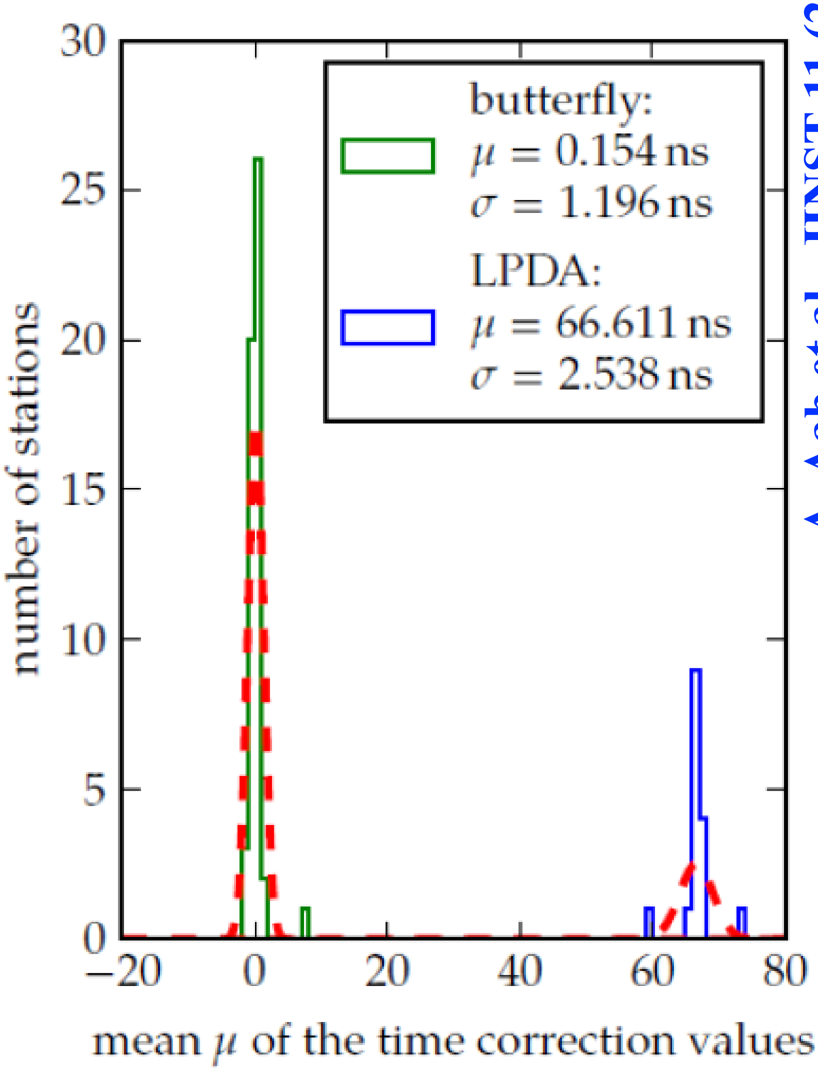

Radiation Processes

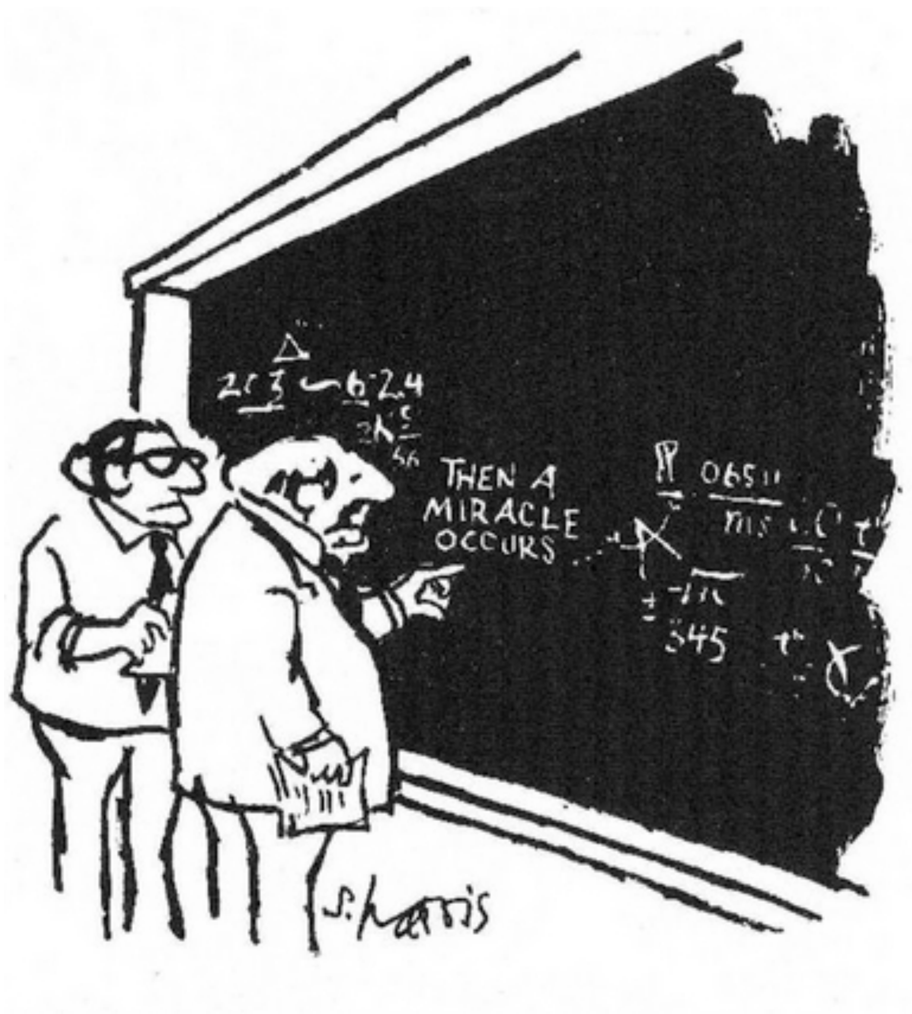

"I think you should be more explicit here in step two."

Radio Emission in Air Showers

Mainly: Charge separation in geomagnetic field

$\vec{E} \propto \vec{v} \times \vec{B}$

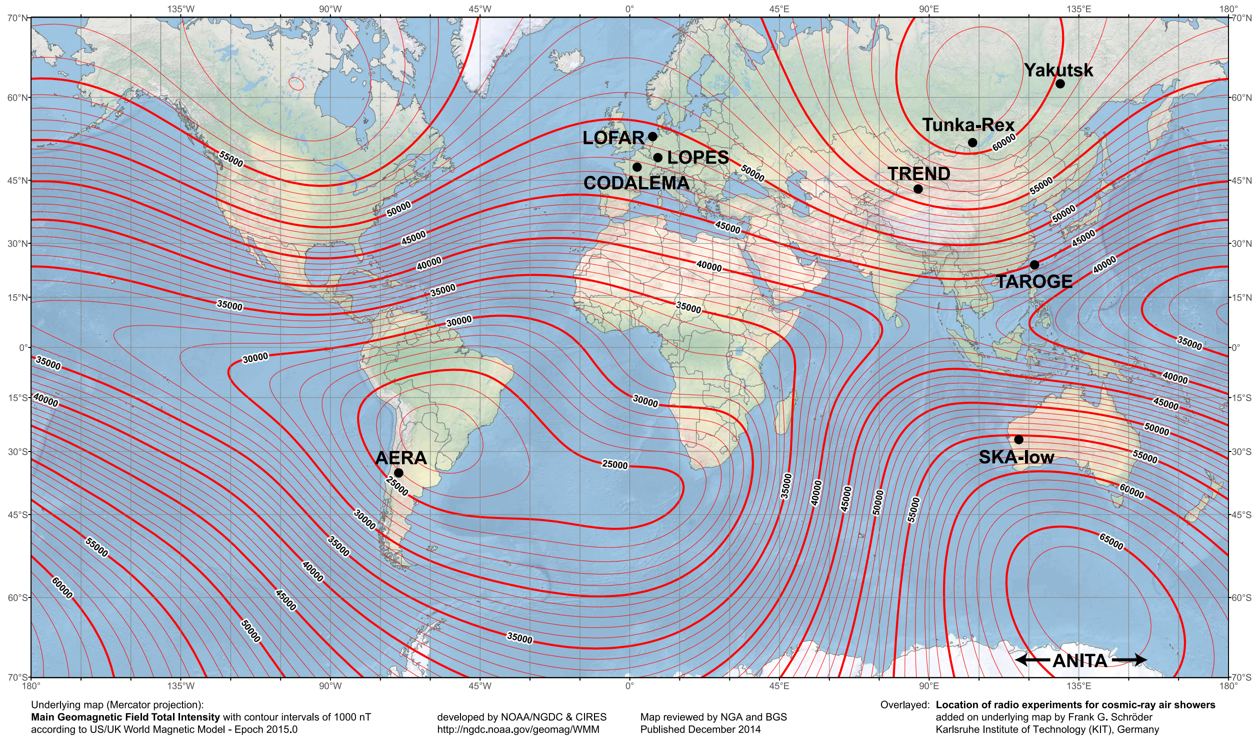

F. Schröder, Prog. Part. Nucl. Phys. 93 (2017) 1

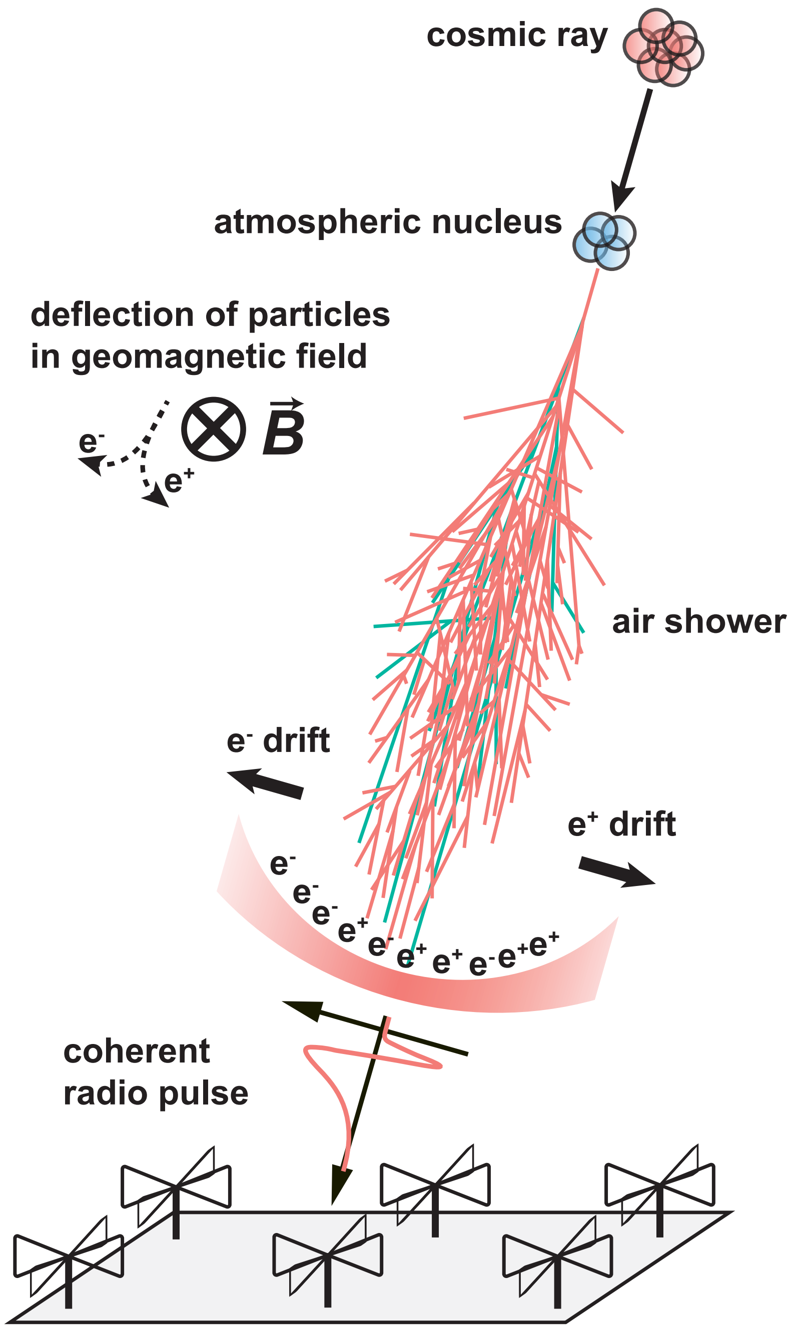

Arrival direction of showers with strong radio signals

north-south asymmetry
v x B effect

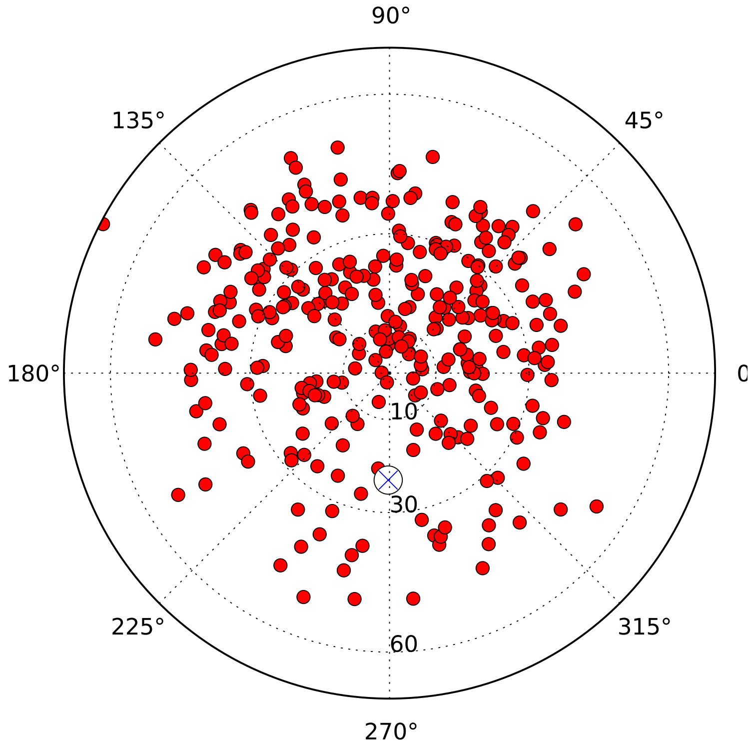

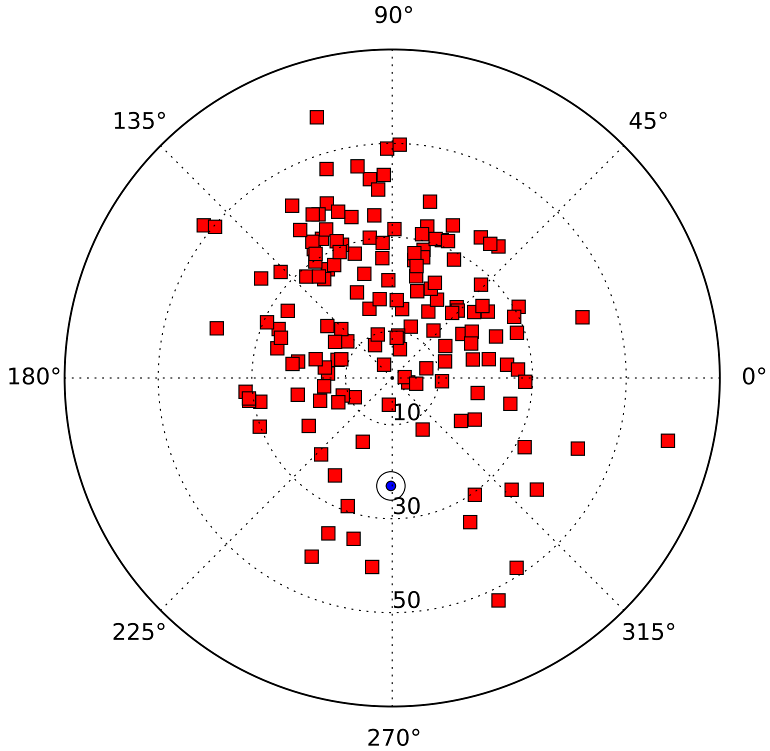

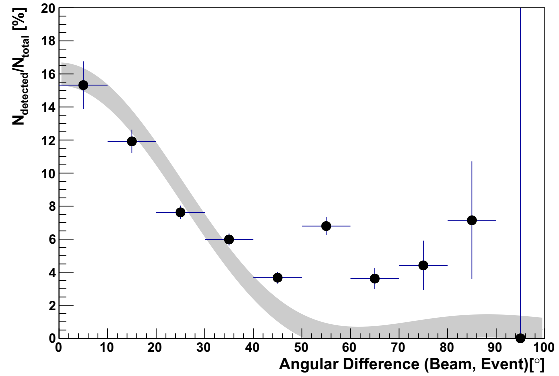

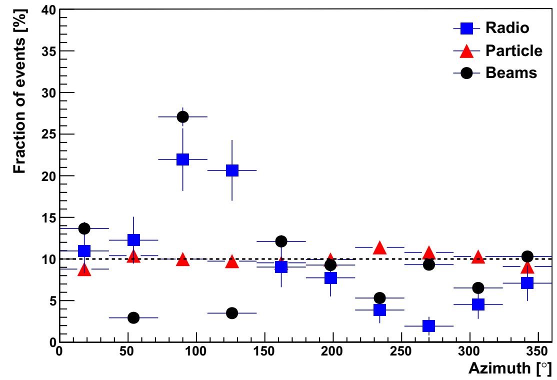

LOFAR

30 - 80 MHz **110 - 190 MHz**

A. Nelles et al., Astroparticle Physics 65 (2015) 11

P. Schellart et al., A&A 560 (2013) A98

Arrival direction of showers with strong radio signals

north-south asymmetry
v x B effect

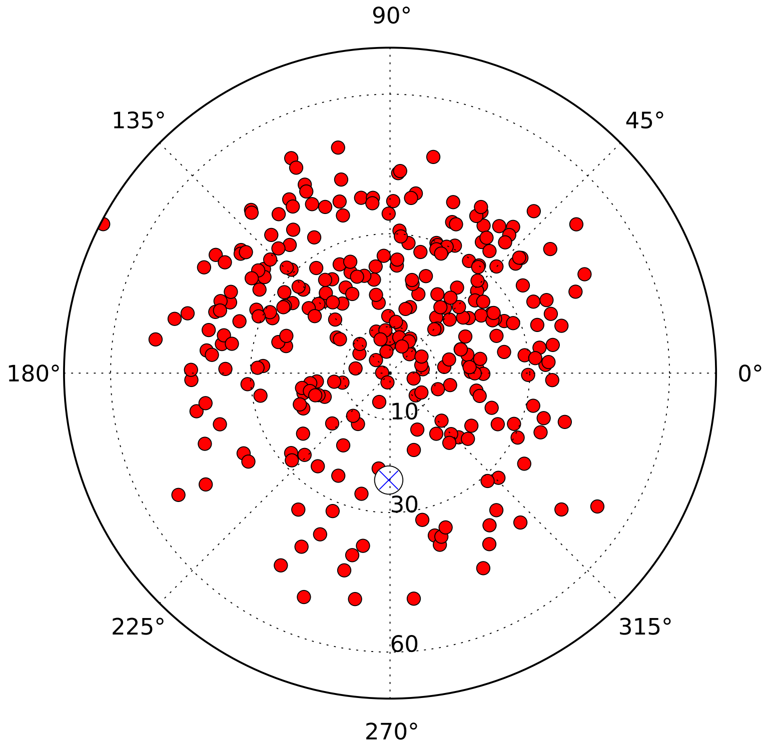

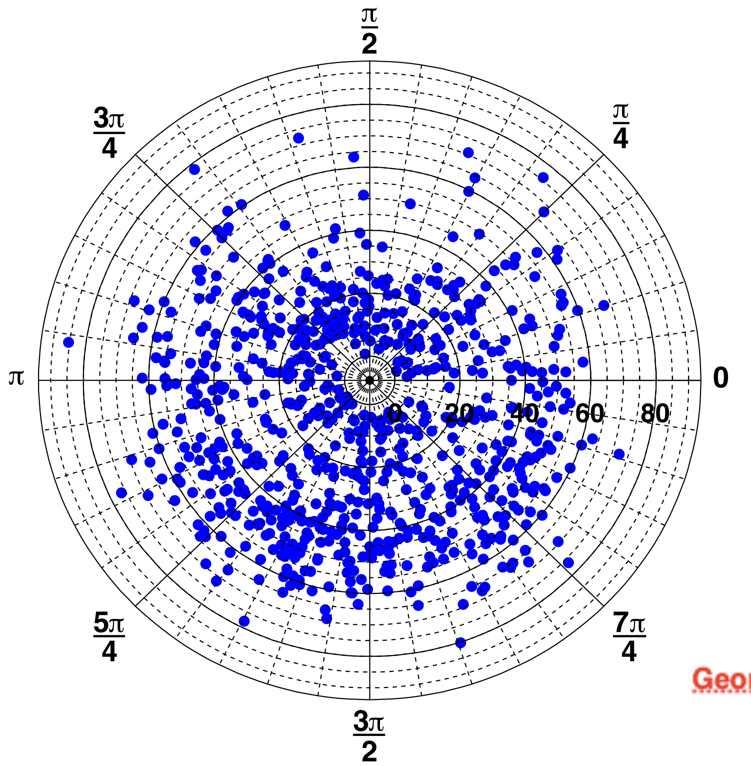

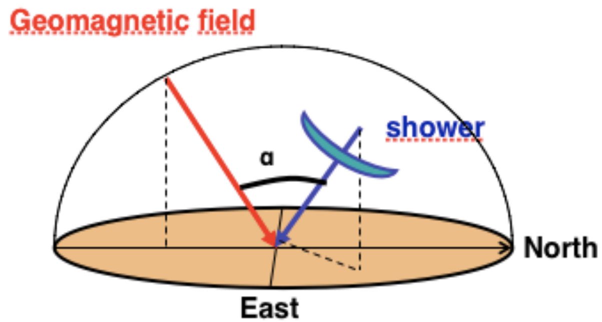

LOFAR

AERA Auger Engineering Radio Array

30 - 80 MHz

P. Schellart et al., A&A 560 (2013) A98

Geomagnetic effect

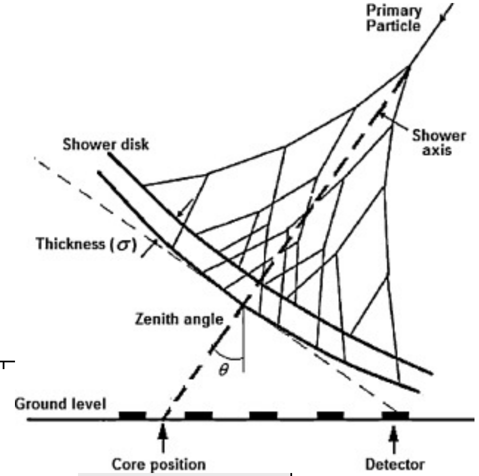

T. Huege / Physics Reports 620 (2016) 1–52

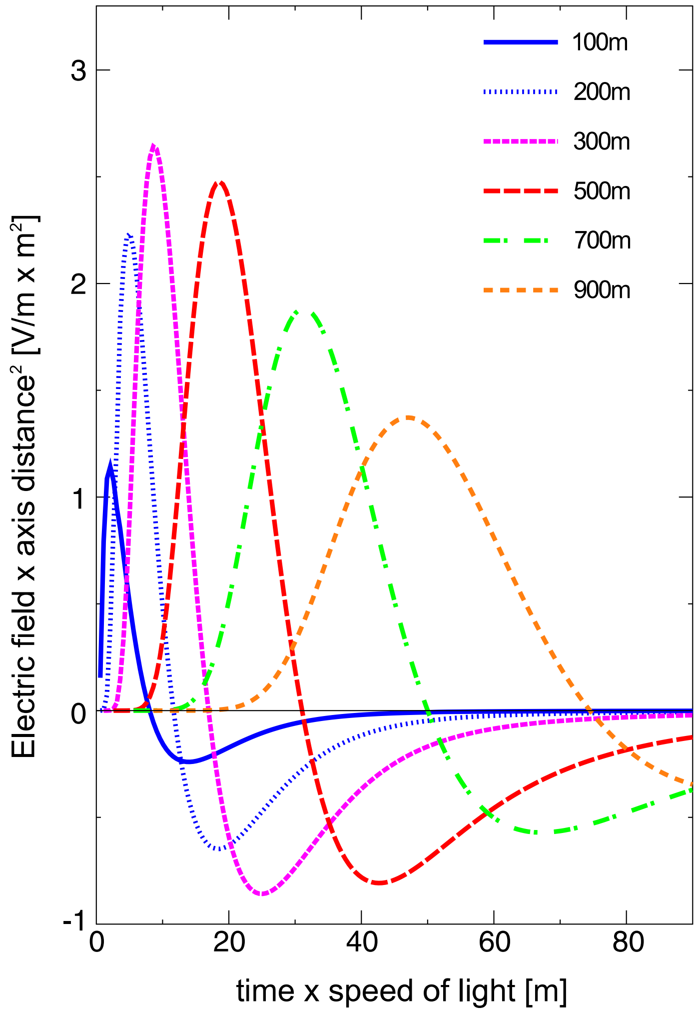

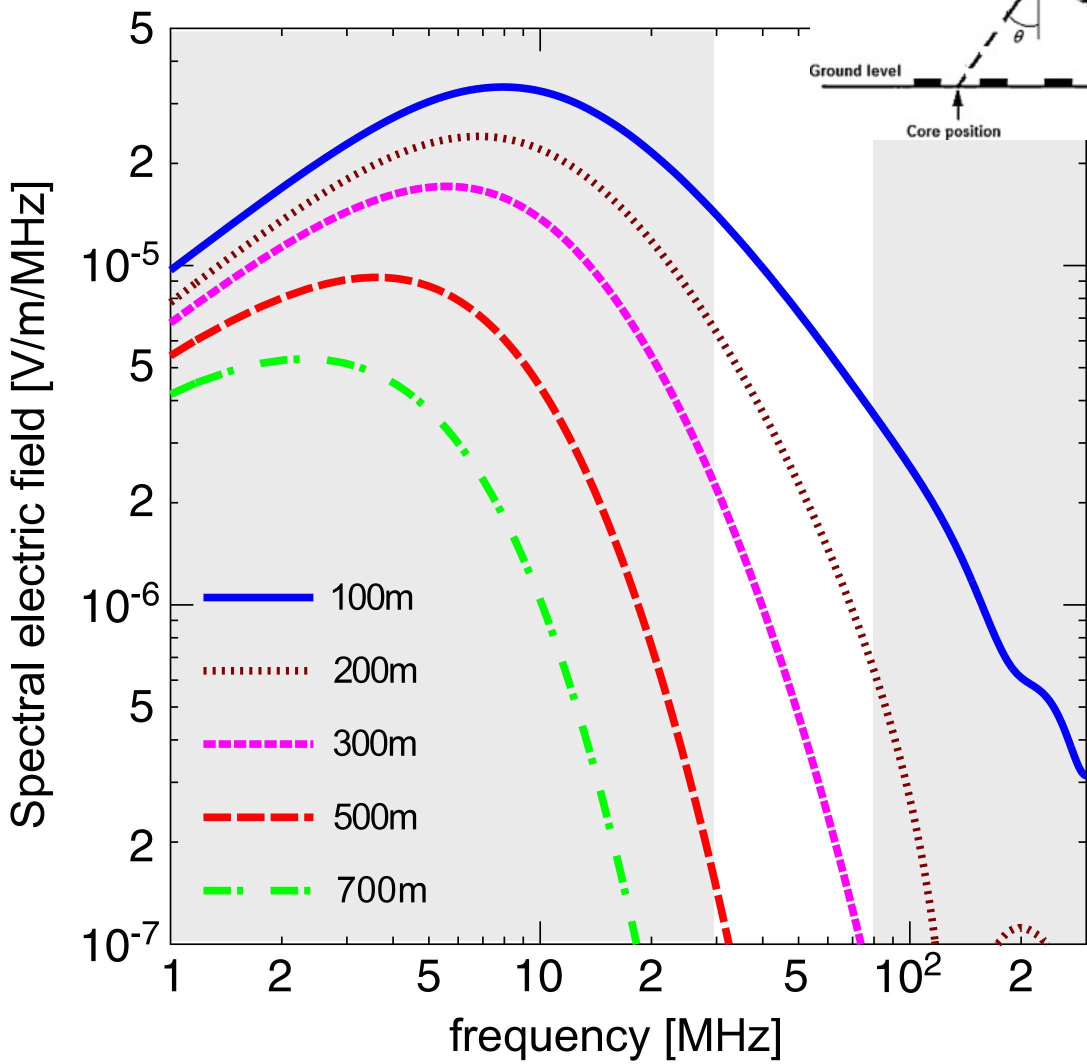

Fig. 4. Radio pulses (top) arising from the time-variation of the geomagnetically induced transverse currents in a 10^{17} eV air shower as observed at various observer distances from the shower axis and their corresponding frequency spectra (bottom). Refractive index effects are not included.
Source: Adapted from [18].

Radio Emission in Air Showers

- Mainly: Charge separation in geomagnetic field
  $\vec{E} \propto \vec{v} \times \vec{B}$

Theory predicts additional mechanisms:

- excess of electrons in shower: charge excess
- superposition of emission due to Cherenkov effects in atmosphere

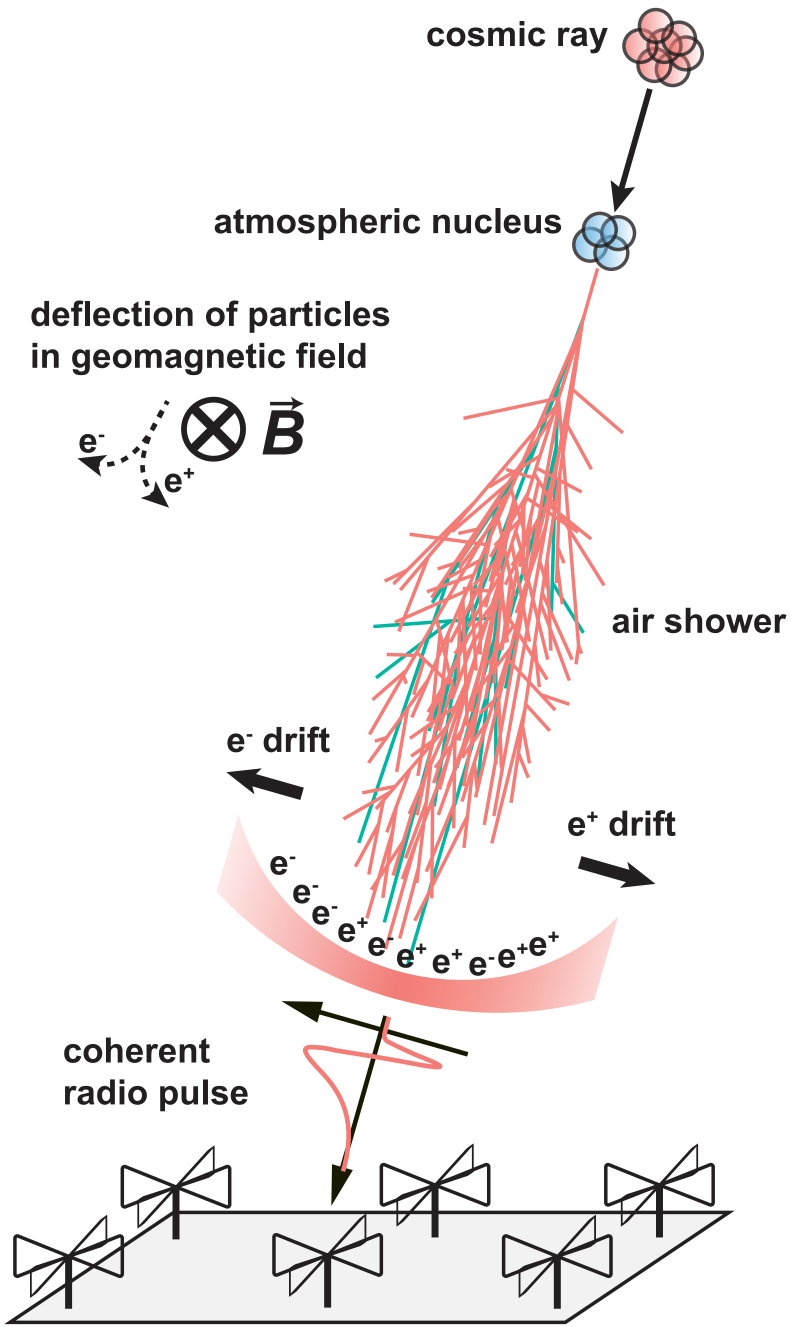

polarization of radio signal

geomagnetic

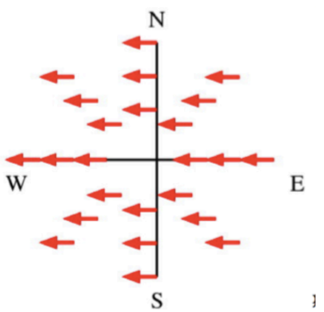

Askaryan

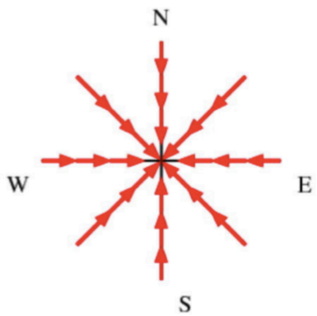

Polarization footprint

of an individual air shower

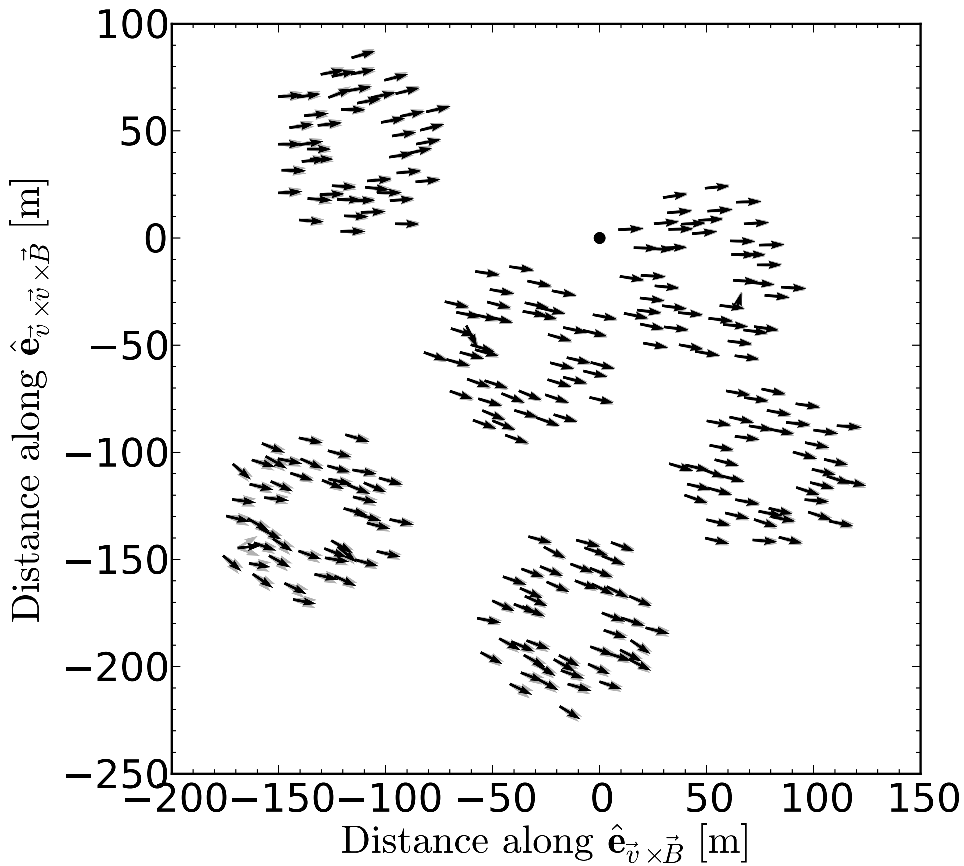

geomagnetic

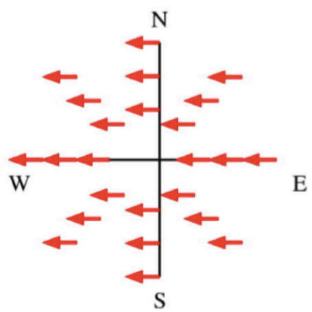

Askaryan

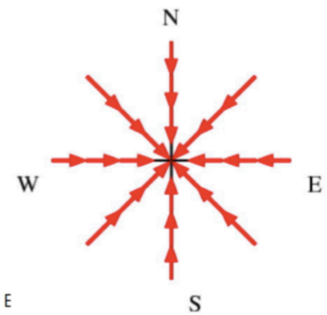

LOFAR

P. Schellart et al., JCAP 10 (2014) 014

Charge excess fraction

$a = \frac{\text{Askaryan}}{\text{geomagnetic}}$

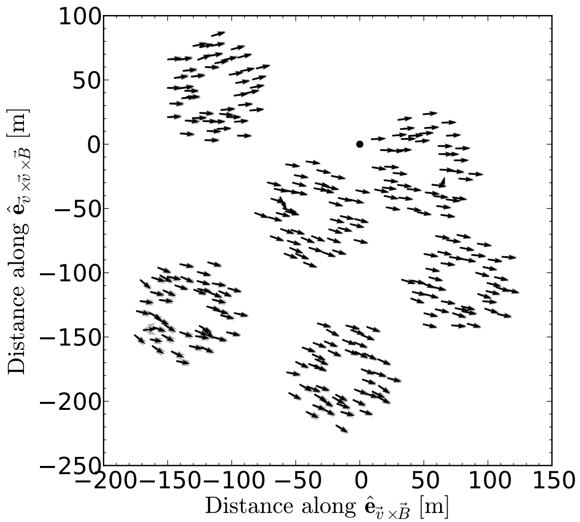

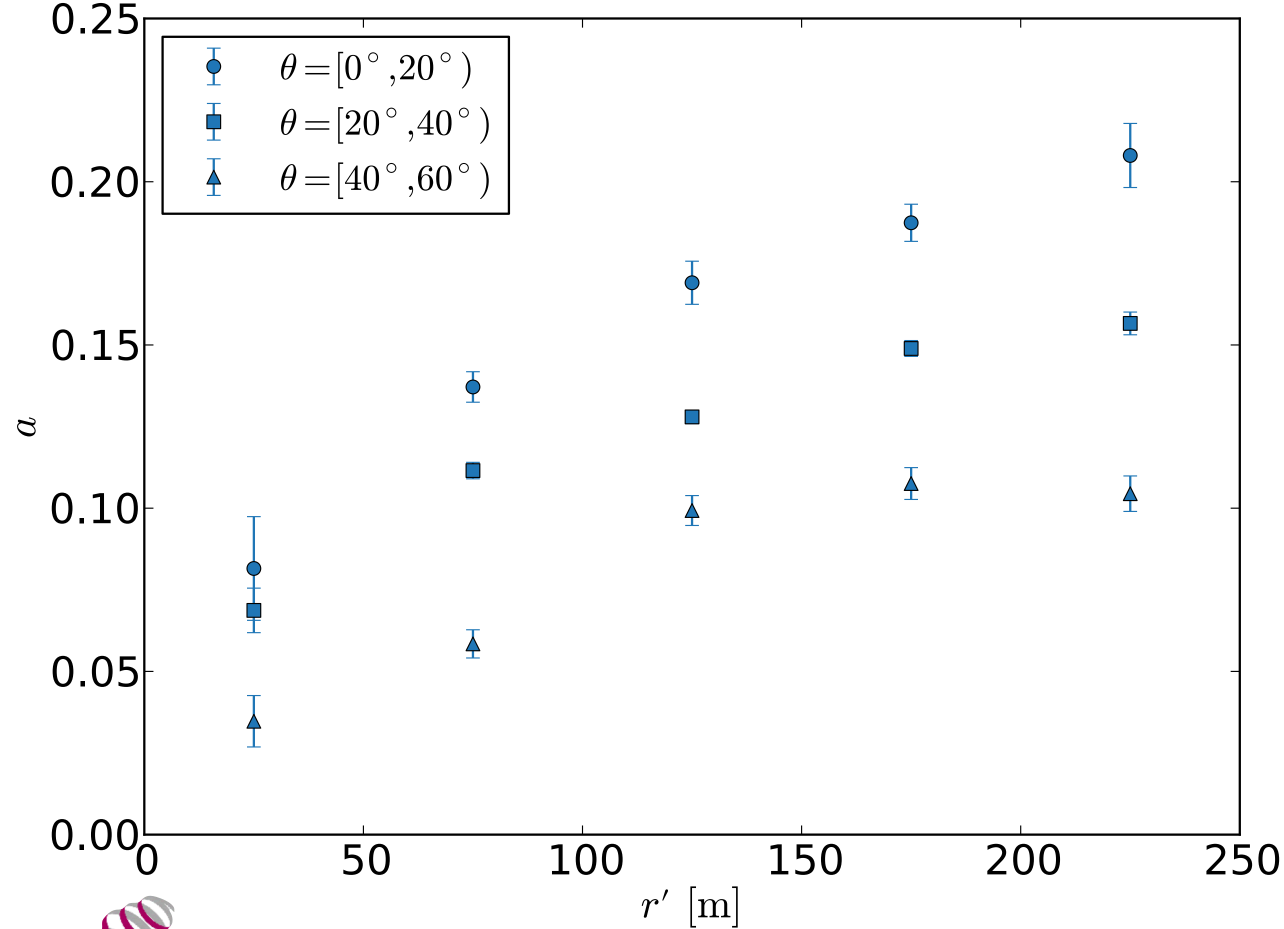

LOFAR

geomagnetic

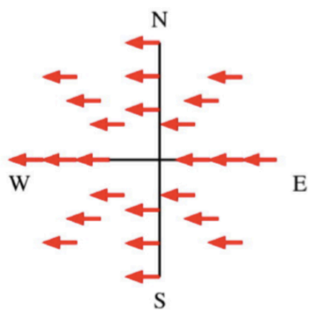

Askaryan

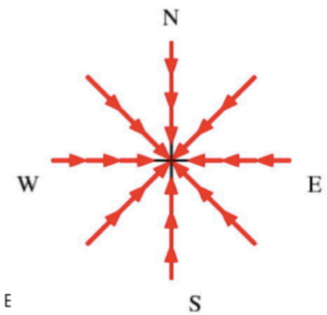

P. Schellart et al., JCAP 10 (2014) 014

Footprint of radio emission on the ground

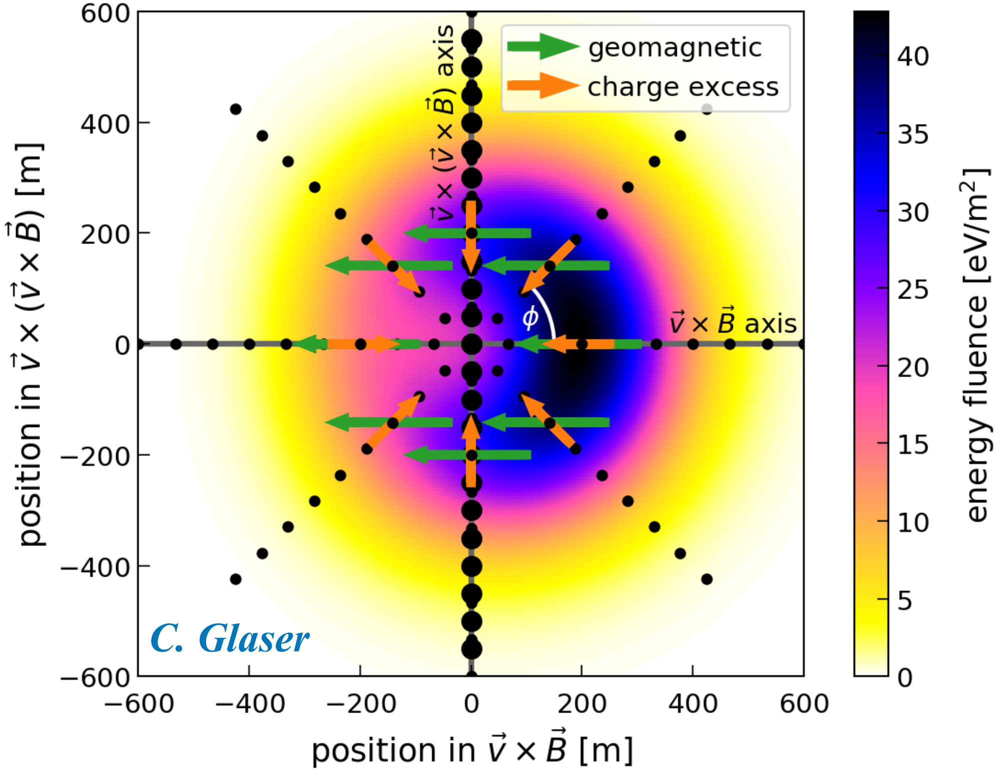

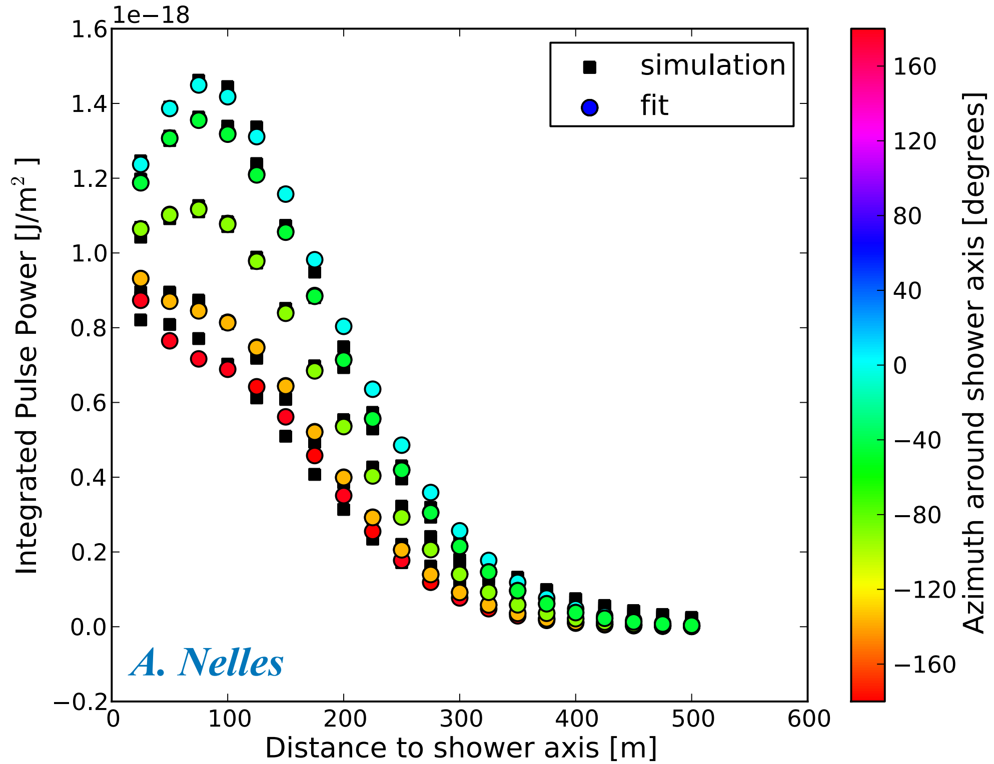

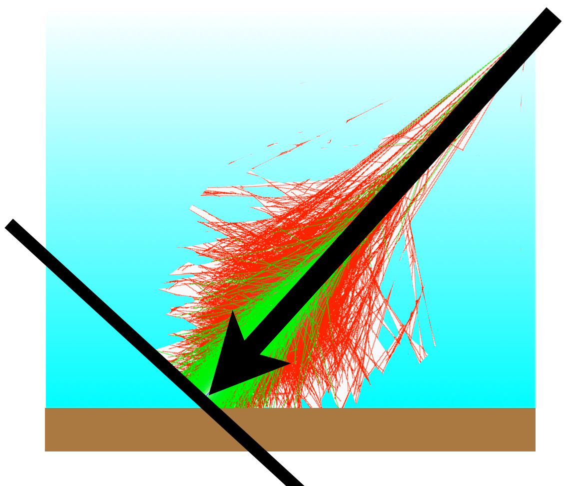

Properties of incoming cosmic ray

- direction
- energy
- type

Direction

Shape of Shower Front

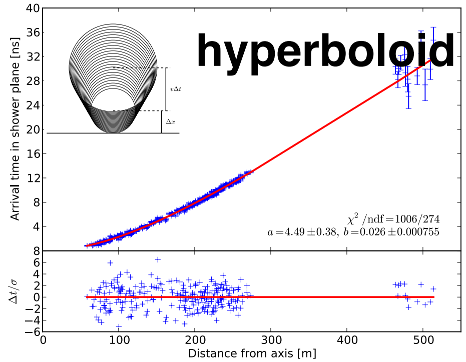

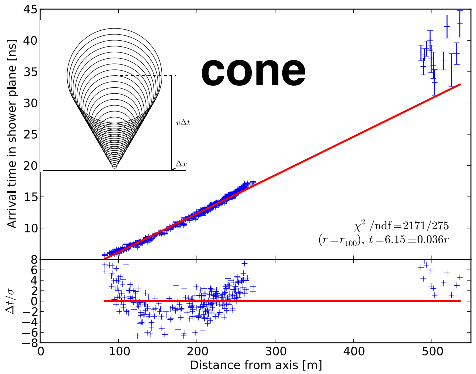

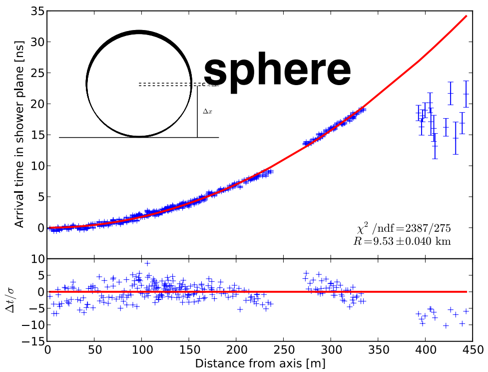

fit quality

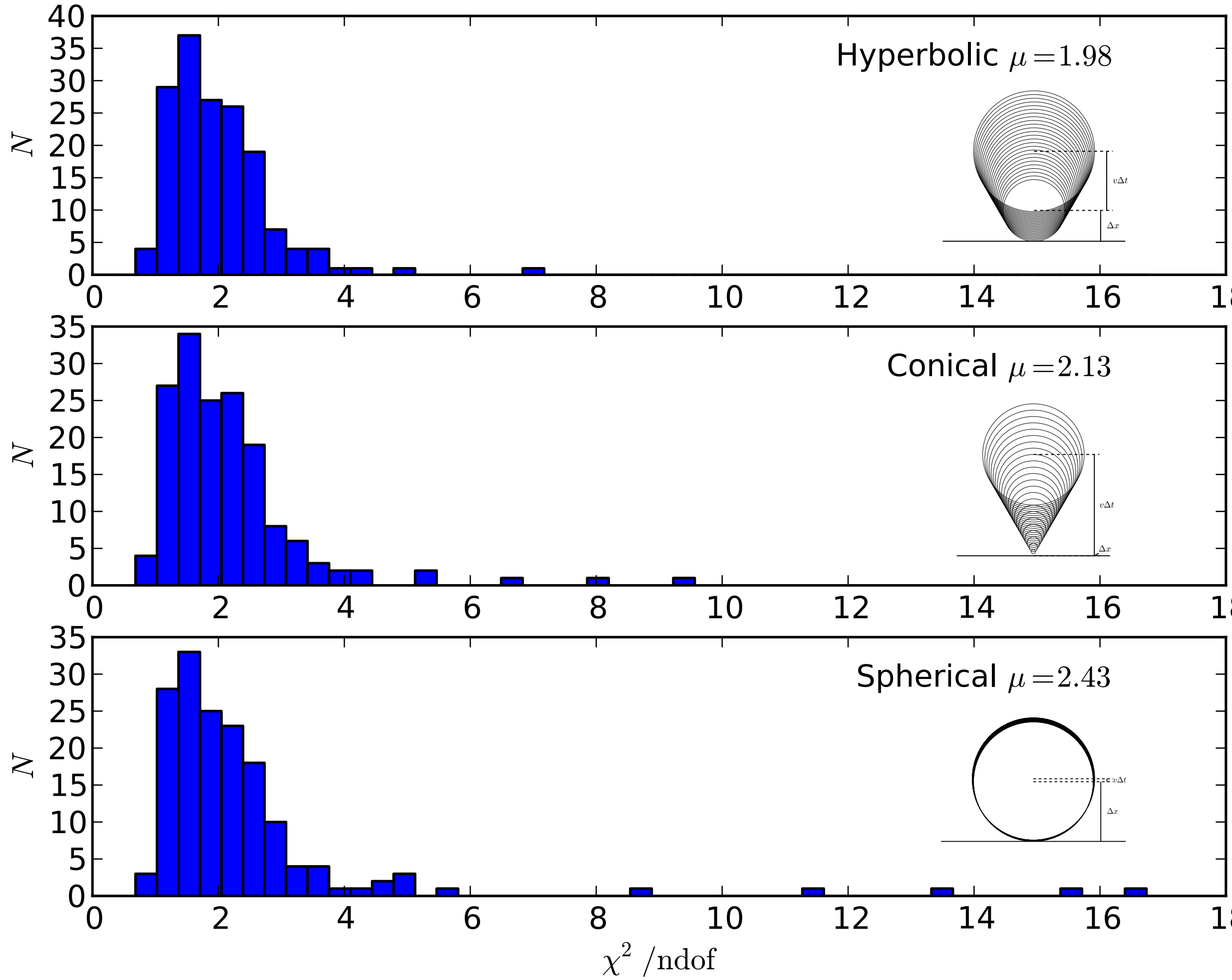

A. Corstanje et al., Astropart. Phys. 61 (2015) 22

Accuracy of Shower Direction

angular difference between..

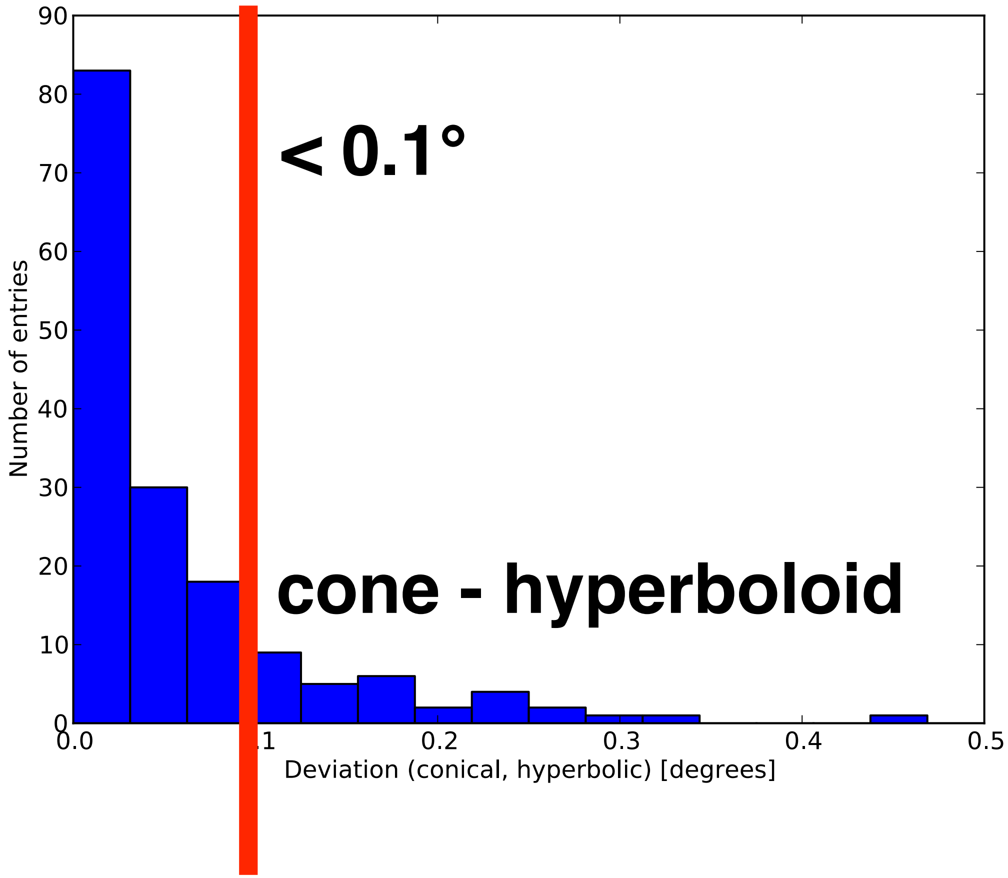

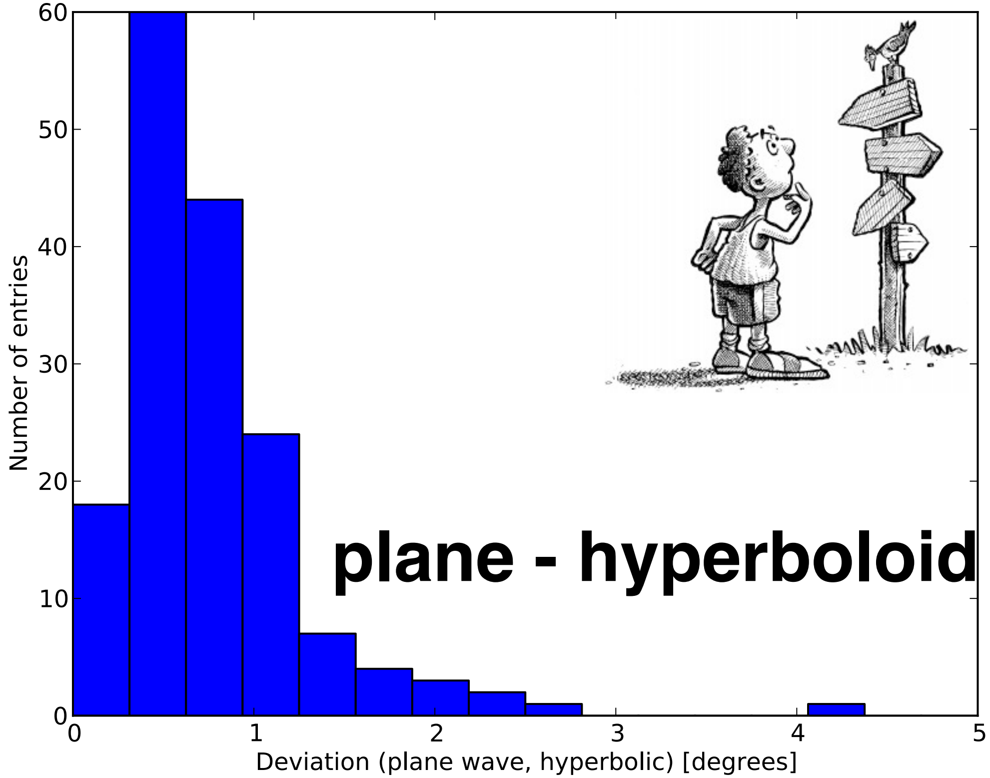

LOFAR

A. Corstanje et al., Astropart. Phys. 61 (2015) 22

Energy

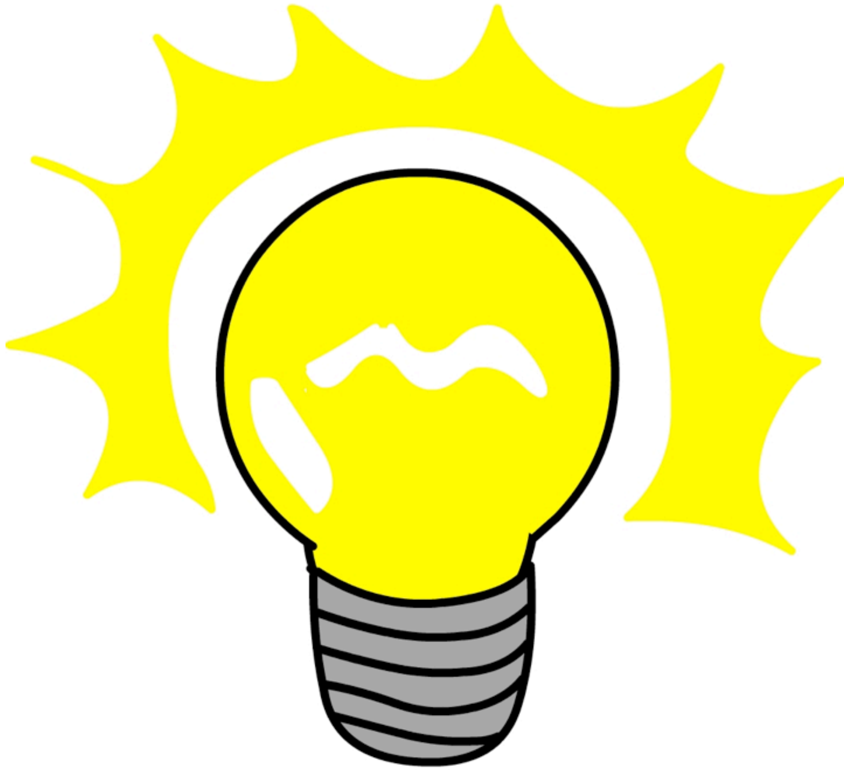

Measurement of the Radiation Energy in the Radio Signal of Extensive Air Showers as a Universal Estimator of Cosmic-Ray Energy

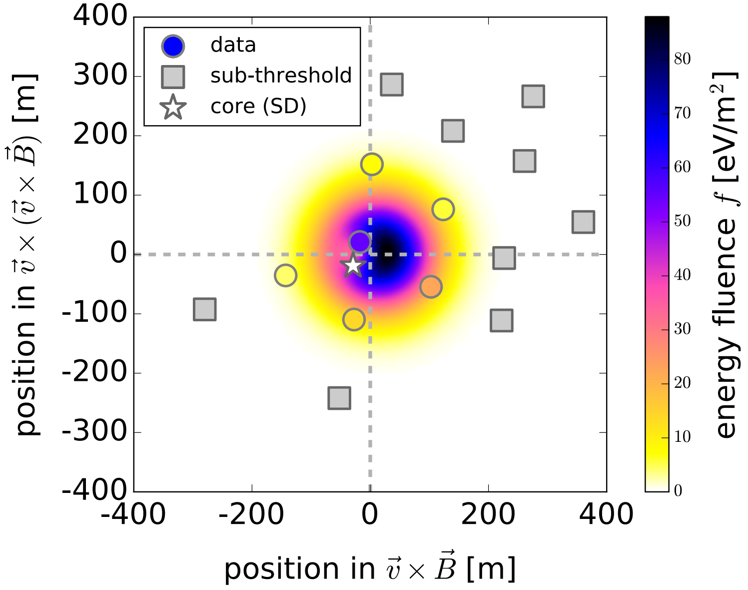

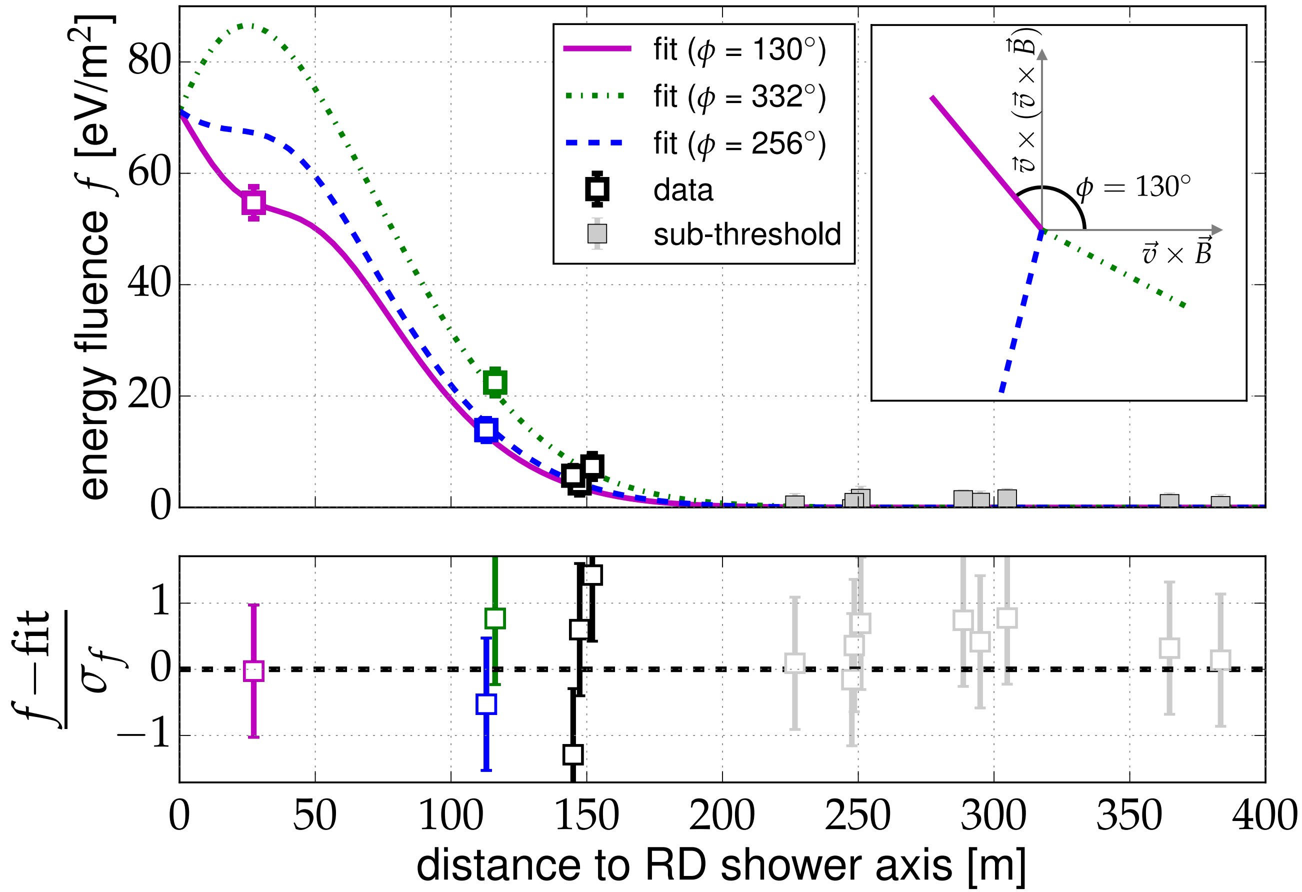

A. Aab et al., PRL 116 (2016) no.24, 241101

Measurement of the Radiation Energy in the Radio Signal of Extensive Air Showers as a Universal Estimator of Cosmic-Ray Energy

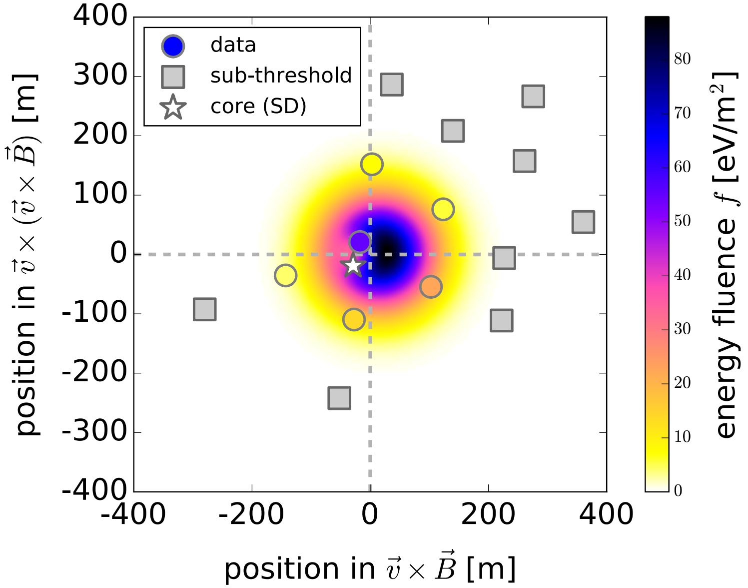

$E_{30\text{-}80}$ MHz = 15.8 MeV @ 10^{18} eV

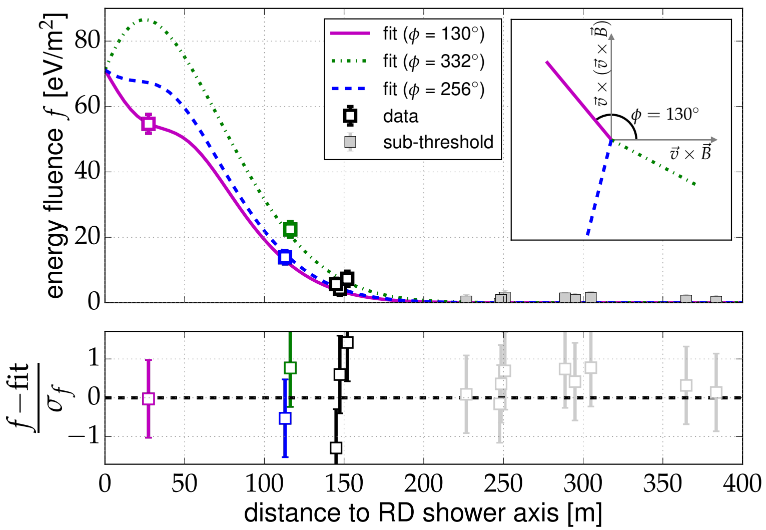

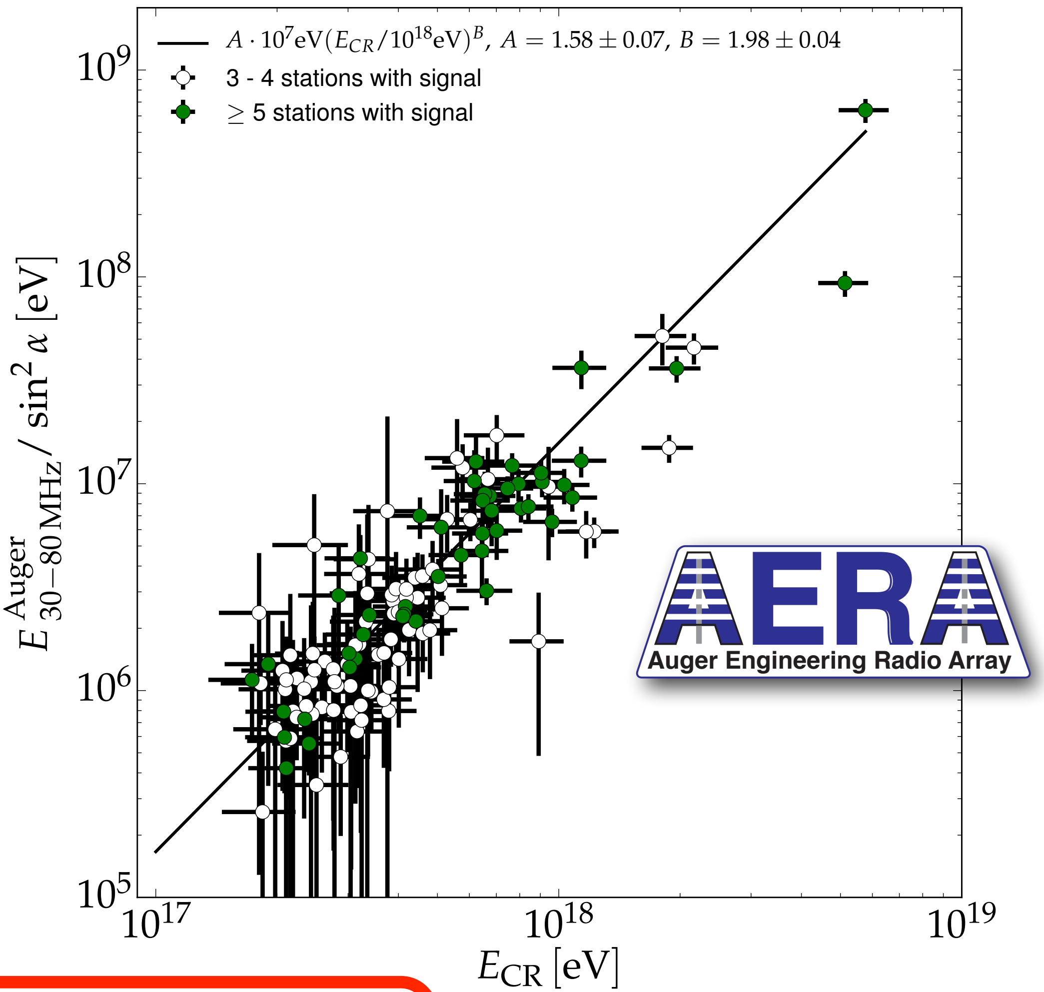

$$E_{30\text{-}80\text{ MHz}} = (15.8 \pm 0.7(\text{stat}) \pm 6.7(\text{syst})\ \text{MeV}) \times \left(\sin\alpha \frac{E_{CR}}{10^{18}\ \text{eV}} \frac{B_{Earth}}{0.24\ \text{G}}\right)^2$$

A. Aab et al., PRL 116 (2016) no.24, 241101

Energy Estimation of Cosmic Rays with the Engineering Radio Array of the Pierre Auger Observatory

$E_{30\text{-}80}$ MHz = 15.8 MeV @ 10^{18} eV

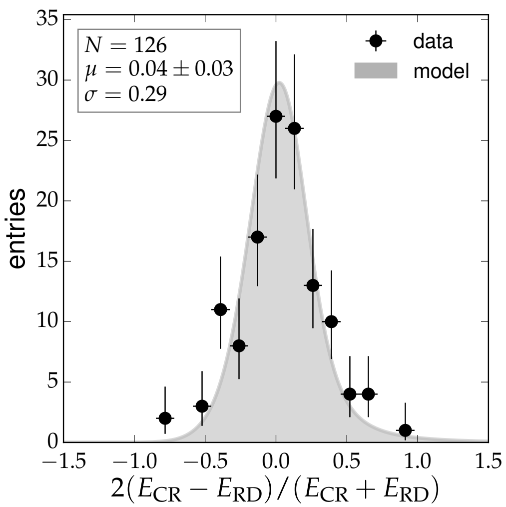

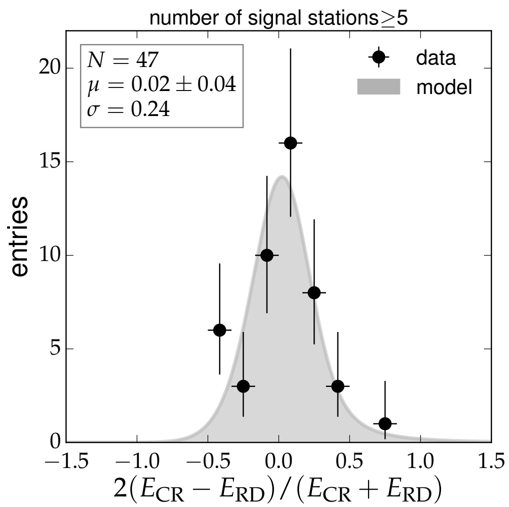

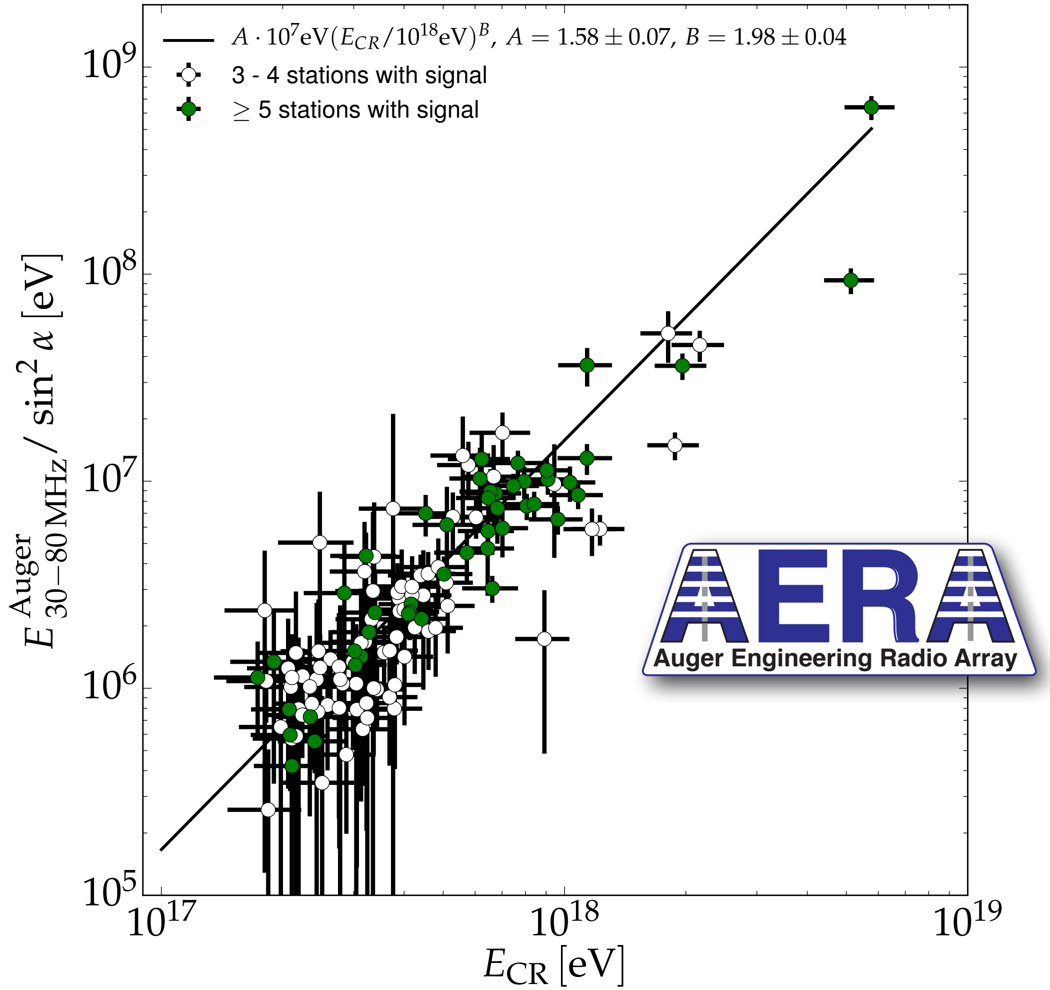

$$\sigma \approx 24\%$$

A. Aab et al., PRD 93 (2016) no.12, 122005
A. Aab et al., PRL 116 (2016) no.24, 241101

Mass

Measurement of particle mass

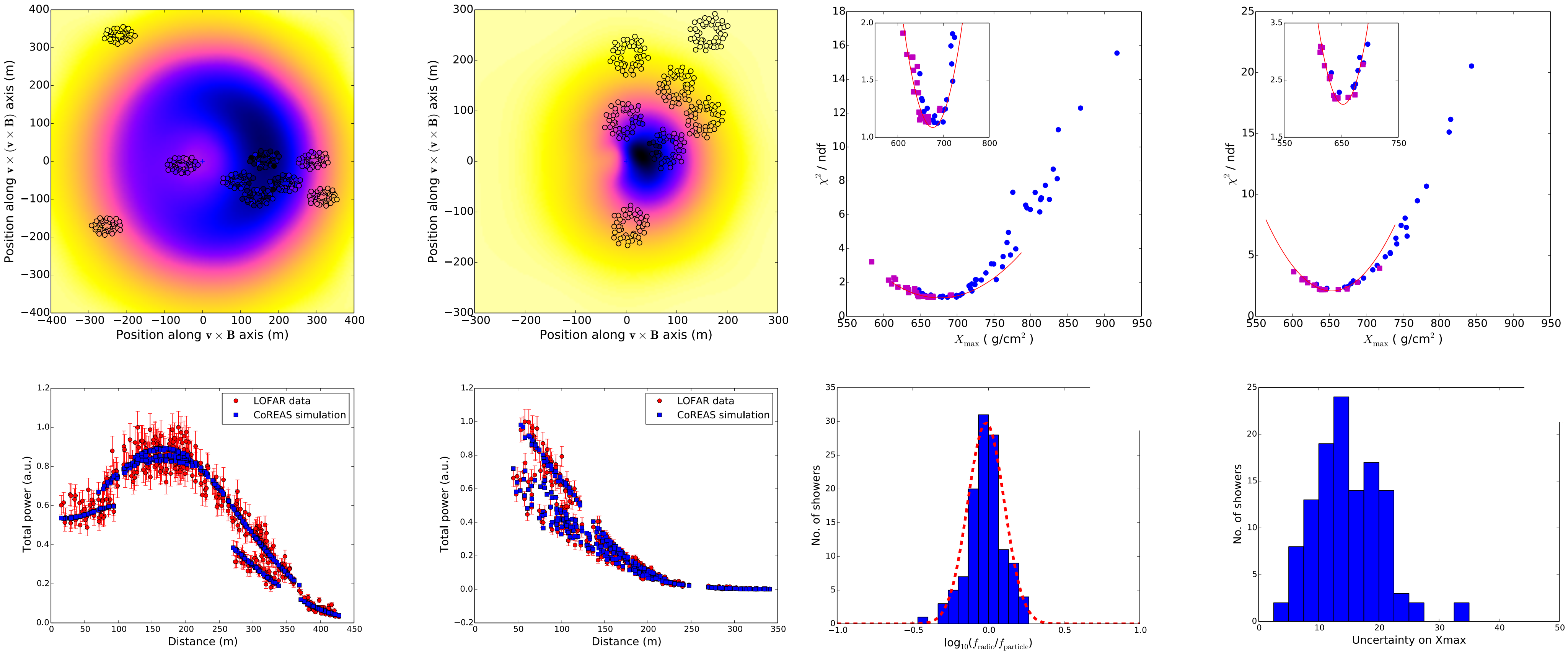

$\sigma_E \approx 32\%$

$\sigma_{X_{max}} \approx 17$ g/cm^2

S. Buitink et al., PRD 90 (2014) 082003

Depth of the shower maximum

LETTER nature
doi:10.1038/nature16976

A large light-mass component of cosmic rays at 10^{17}–$10^{17.5}$ electronvolts from radio observations

S. Buitink[1,2], A. Corstanje[2], H. Falcke[2,3,4,5], J. R. Hörandel[2,4], T. Huege[6], A. Nelles[2,7], J. P. Rachen[2], L. Rossetto[2], P. Schellart[2], O. Scholten[8,9], S. ter Veen[3], S. Thoudam[2], T. N. G. Trinh[8], J. Anderson[10], A. Asgekar[3,11], I. M. Avruch[12,13], M. E. Bell[14], M. J. Bentum[3,15], G. Bernardi[16,17], P. Best[18], A. Bonafede[19], F. Breitling[20], J. W. Broderick[21], W. N. Brouw[3,13], M. Brüggen[19], H. R. Butcher[22], D. Carbone[23], B. Ciardi[24], J. E. Conway[25], F. de Gasperin[19], E. de Geus[3,26], A. Deller[3], R.-J. Dettmar[27], G. van Diepen[3], S. Duscha[3], J. Eislöffel[28], D. Engels[29], J. E. Enriquez[3], R. A. Fallows[3], R. Fender[30], C. Ferrari[31], W. Frieswijk[3], M. A. Garrett[3,32], J. M. Grießmeier[33,34], A. W. Gunst[3], M. P. van Haarlem[3], T. E. Hassall[21], G. Heald[3,13], J. W. T. Hessels[3,23], M. Hoeft[28], A. Horneffer[5], M. Iacobelli[3], H. Intema[32,35], E. Juette[27], A. Karastergiou[30], V. I. Kondratiev[3,36], M. Kramer[5,37], M. Kuniyoshi[38], G. Kuper[3], J. van Leeuwen[3,23], G. M. Loose[3], P. Maat[3], G. Mann[20], S. Markoff[23], R. McFadden[3], D. McKay-Bukowski[39,40], J. P. McKean[3,13], M. Mevius[3,13], D. D. Mulcahy[21], H. Munk[3], M. J. Norden[3], E. Orru[3], H. Paas[41], M. Pandey-Pommier[42], V. N. Pandey[3], M. Pietka[30], R. Pizzo[3], A. G. Polatidis[3], W. Reich[5], H. J. A. Röttgering[32], A. M. M. Scaife[21], D. J. Schwarz[43], M. Serylak[30], J. Sluman[3], O. Smirnov[17,44], B. W. Stappers[37], M. Steinmetz[20], A. Stewart[30], J. Swinbank[23,45], M. Tagger[33], Y. Tang[3], C. Tasse[44,46], M. C. Toribio[3,32], R. Vermeulen[3], C. Vocks[20], C. Vogt[3], R. J. van Weeren[16], R. A. M. J. Wijers[23], S. J. Wijnholds[3], M. W. Wise[3,23], O. Wucknitz[5], S. Yatawatta[3], P. Zarka[47] & J. A. Zensus[5]

Cosmic rays are the highest-energy particles found in nature. Measurements of the mass composition of cosmic rays with energies of 10^{17}–10^{18} electronvolts are essential to understanding whether they have galactic or extragalactic sources. It has also been proposed that the astrophysical neutrino signal[1] comes from accelerators capable of producing cosmic rays of these energies[2]. Cosmic rays initiate air showers—cascades of secondary particles in the atmosphere—and their masses can be inferred from measurements of the atmospheric depth of the shower maximum[3] (X_{max}; the depth of the air shower when it contains the most particles) or of the composition of shower particles reaching the ground[4]. Current measurements[5] have either high uncertainty, or a low duty cycle and a high energy threshold. Radio detection of cosmic rays[6–8] is a rapidly developing technique[9] for determining X_{max} (refs 10, 11) with a duty cycle of, in principle, nearly 100 per cent. The radiation is generated by the separation of relativistic electrons and positrons in the geomagnetic field and a negative charge excess in the shower front[6,12]. Here we report radio measurements of X_{max} with a mean uncertainty of 16 grams per square centimetre for air showers initiated by cosmic rays with energies of 10^{17}–$10^{17.5}$ electronvolts. This high resolution in X_{max} enables us to determine the mass spectrum of the cosmic rays: we find a mixed composition, with a light-mass fraction (protons and helium nuclei) of about 80 per cent. Unless, contrary to current expectations, the extragalactic component of cosmic rays contributes substantially to the total flux below $10^{17.5}$ electronvolts, our measurements indicate the existence of an additional galactic component, to account for the light composition that we measured in the 10^{17}–$10^{17.5}$ electronvolt range.

Observations were made with the Low Frequency Array (LOFAR[13]), a radio telescope consisting of thousands of crossed dipoles with built-in air-shower-detection capability[14]. LOFAR continuously records the radio signals from air showers, while simultaneously running astronomical observations. It comprises a scintillator array (LORA) that triggers the read-out of buffers, storing the full wave-forms received by all antennas.

We selected air showers from the period June 2011 to January 2015 with radio pulses detected in at least 192 antennas. The total uptime was about 150 days, limited by construction and commissioning of the

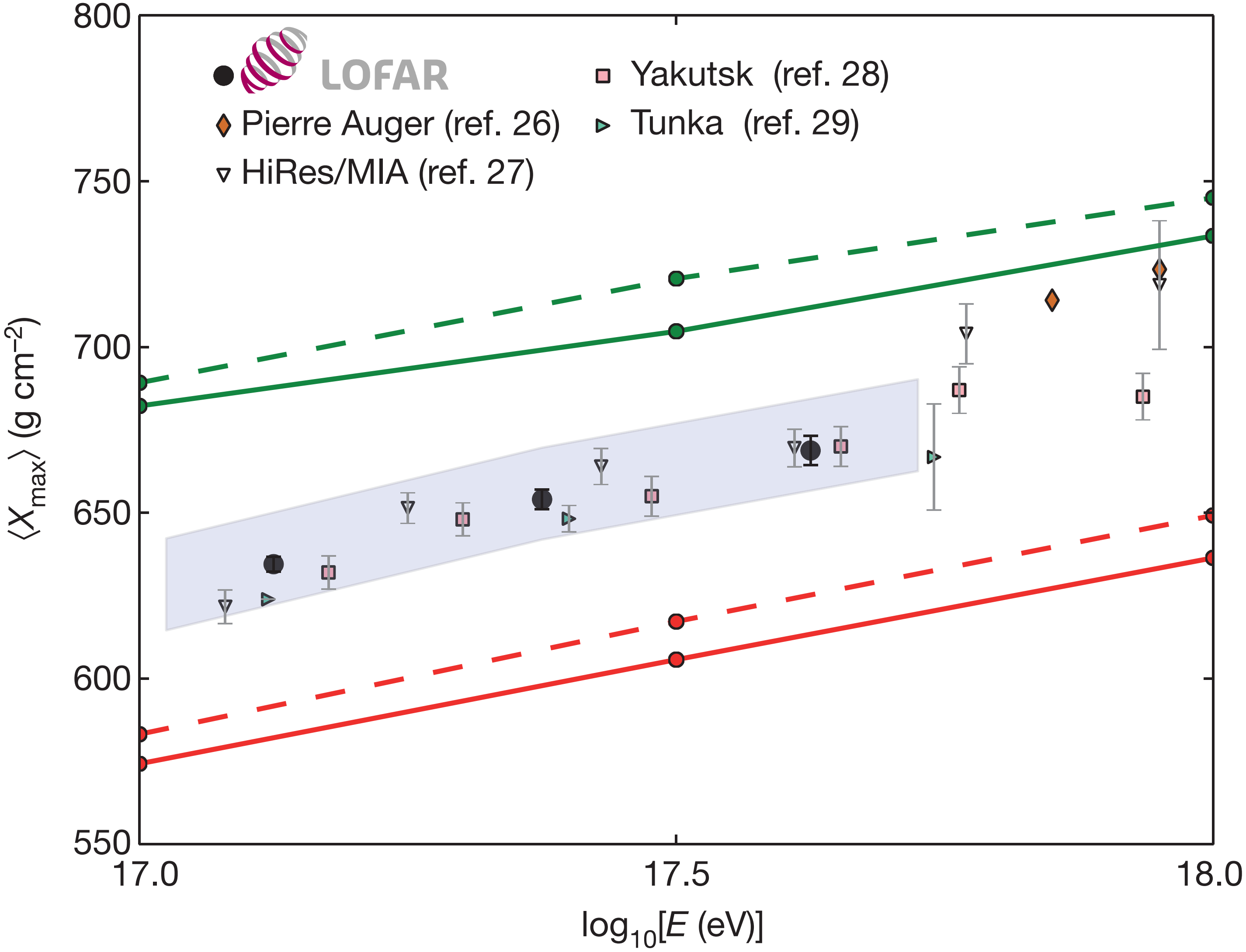

S. Buitink et al., Nature 531 (2016) 70

Results: Resolution of AERA X_{max} method

Radboud University

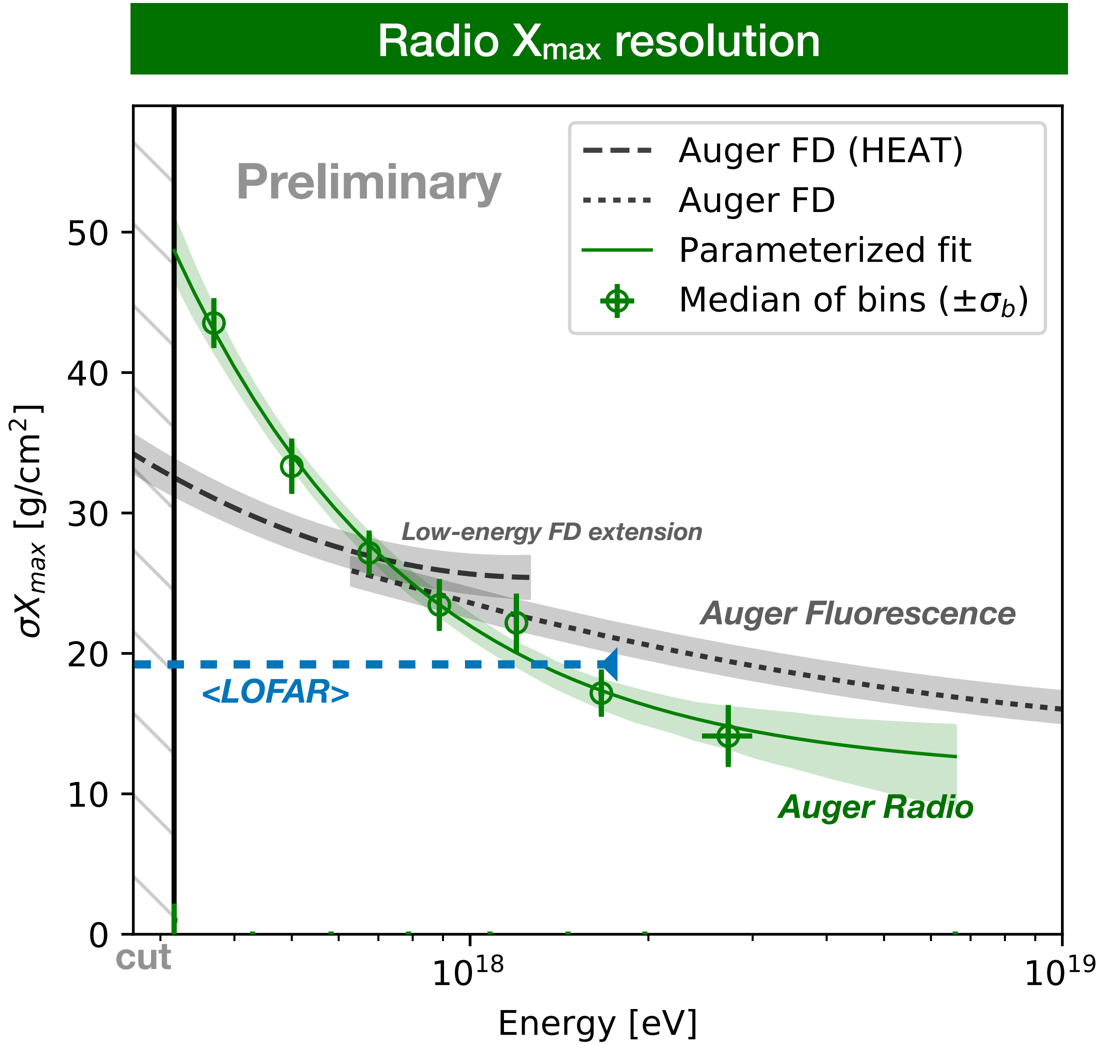

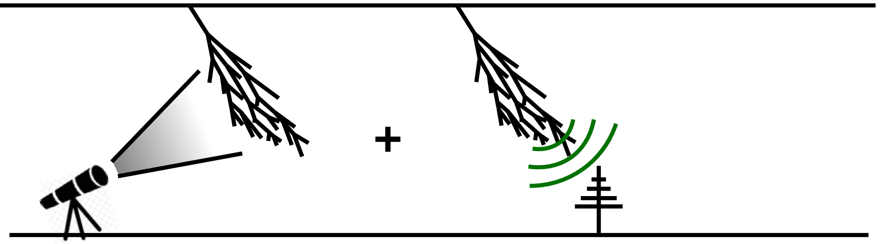

Resolution improves with energy.

- Up to 'better than 15 g/cm² '
- Trend driven by low SNR at low energy.

Resolution competitive with e.g.:

- Auger fluorescence
  [arXiv:1409.4809]
- LOFAR radio (E=$10^{16.8...18.3}$eV)
  [arXiv:2103.12549v2]

Side note:
High resolution is crucial for mass composition studies.

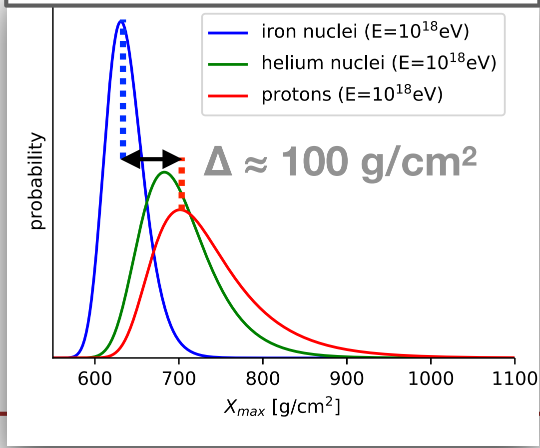

A. Abdul Halim et al., Phys. Rev. D, 109 (2024) 022002
A. Abdul Halim et al., Phys. Rev. Lett., 132 (2024) 021001

Results: AERA vs other (radio) experiments

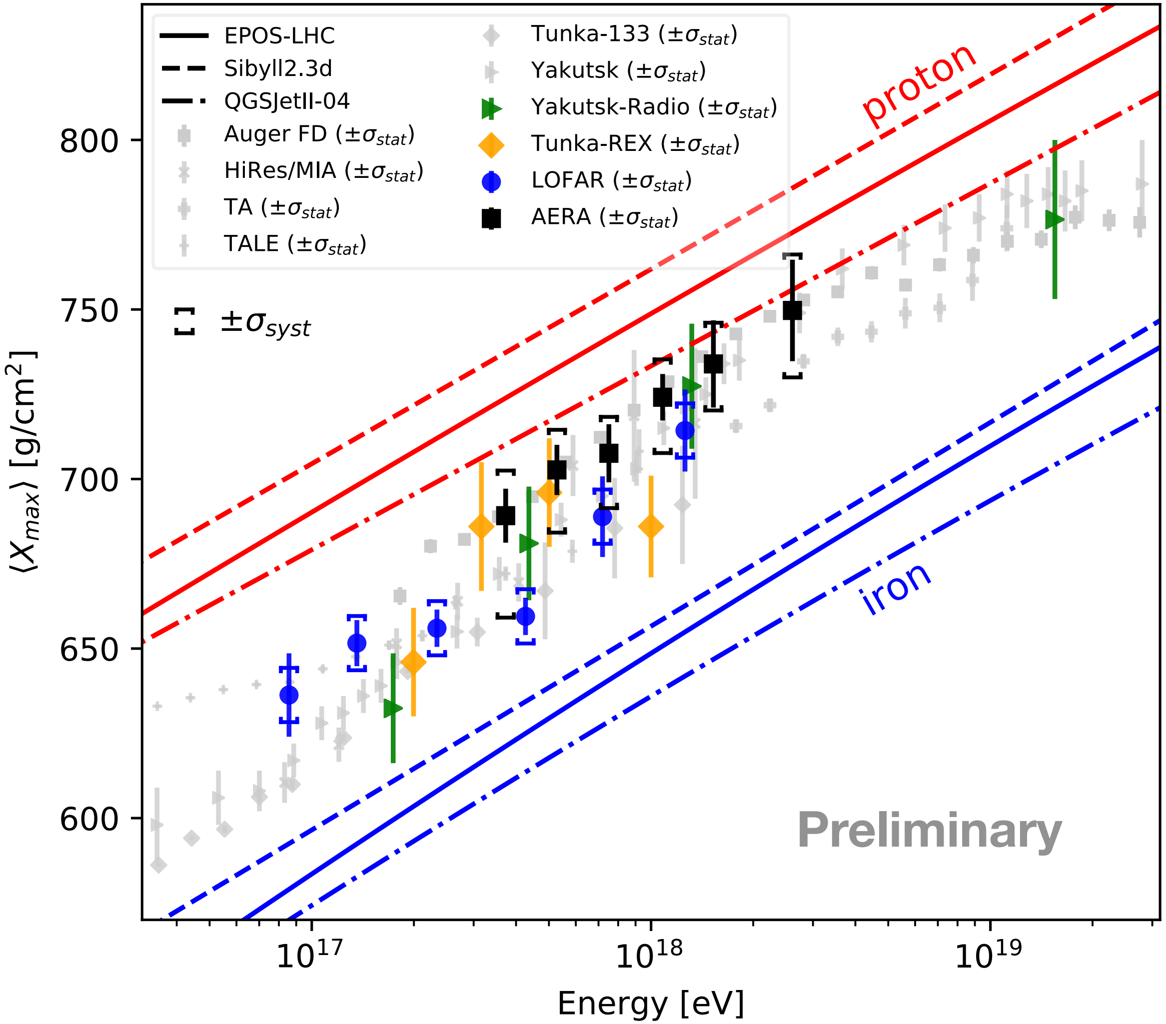

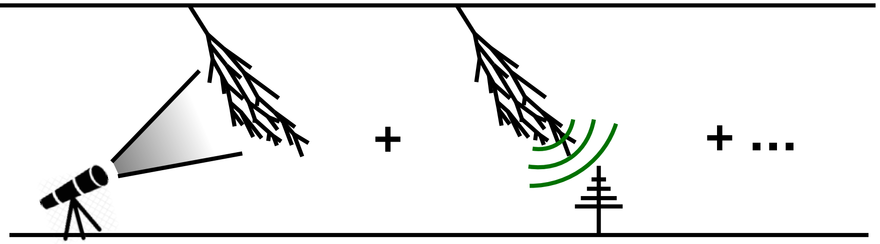

- No general radio-bias w.r.t other techniques (within uncertainties).
- Highlights that systematic uncertainties are key to interpret and compare.
- **LOFAR**-**AERA** differences are being investigated in a working group

—> come talk to us during coffee and lunch!

A. Abdul Halim et al., Phys. Rev. D, 109 (2024) 022002
A. Abdul Halim et al., Phys. Rev. Lett., 132 (2024) 021001

Radbound University

Two independent estimates of systematic uncertainties

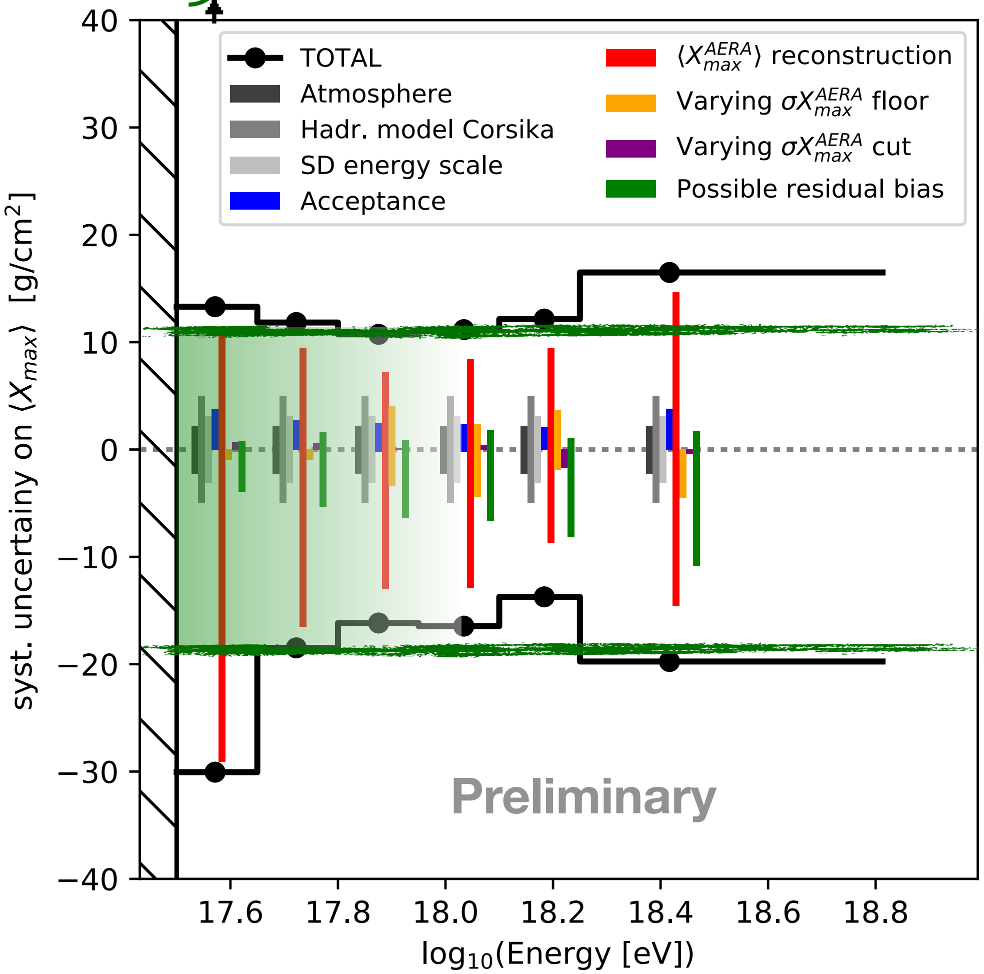

Independent constrained from AERA-FD dataset (most lower E)

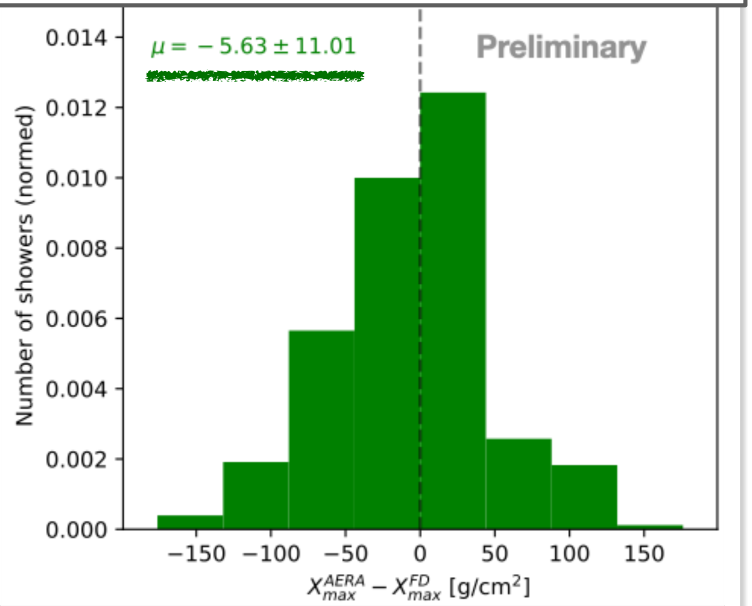

+

FD syst. unc. ~ 10 g/cm²

- **Cross check:** two independent estimates for total systematic uncertainties are in agreement.
  —> suggests systematic uncertainties are well-understood and no significant contribution is missing.

A. Abdul Halim et al., Phys. Rev. D, 109 (2024) 022002
A. Abdul Halim et al., Phys. Rev. Lett., 132 (2024) 021001

Determine the properties of the incoming particle with the radio technique

- direction ~ 0.1° - 0.5°
- energy ~ 15% - 30%
- type (X_{max}) ~ 20 - 30 g/cm^2

(depending on energy, detector spacing, …)

—> radio technique is routinely used to measure properties of cosmic rays


The Future
NEXT EXIT

The Radio Detector of the Pierre Auger Observatory

European Research Council
Established by the European Commission

NWO

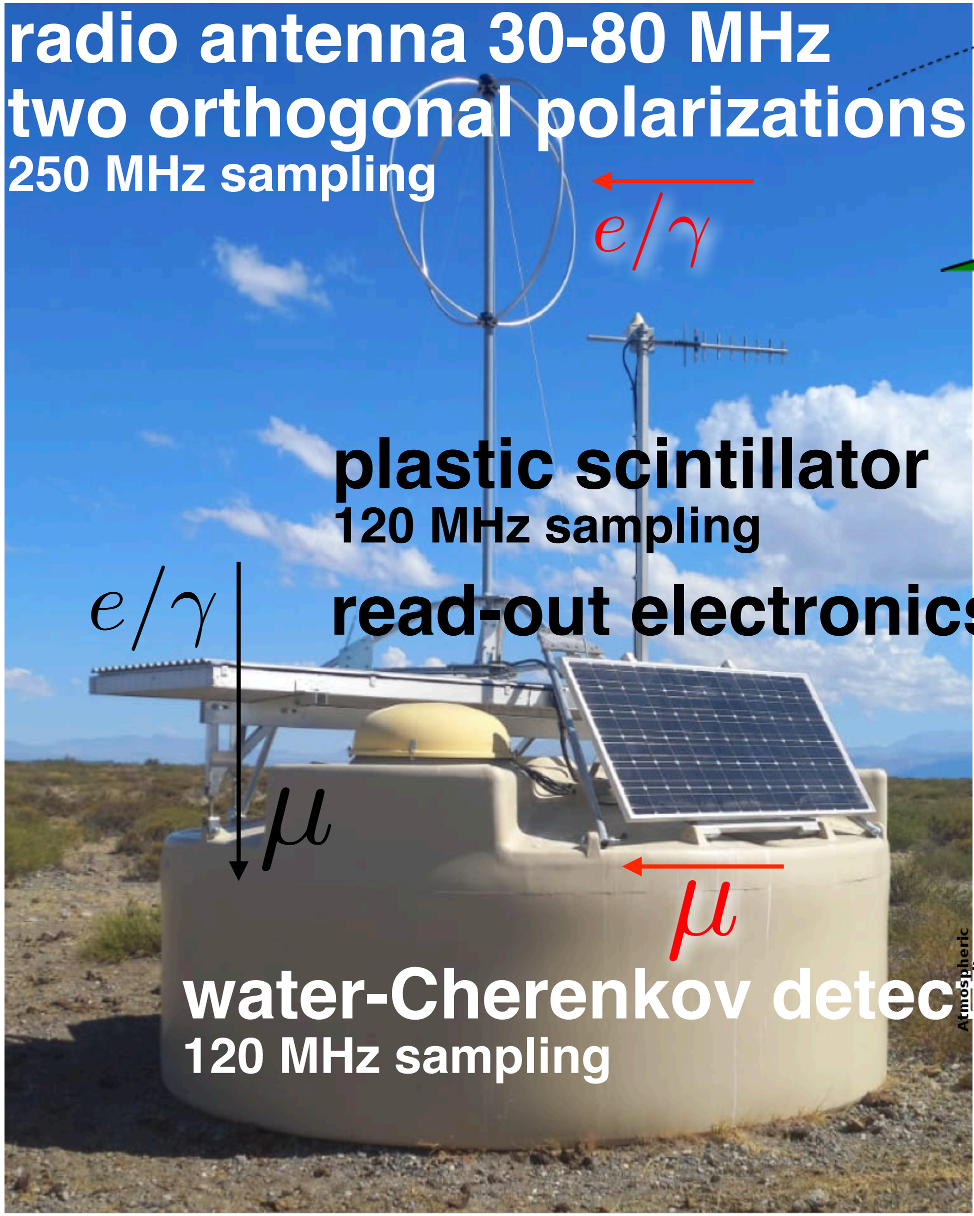

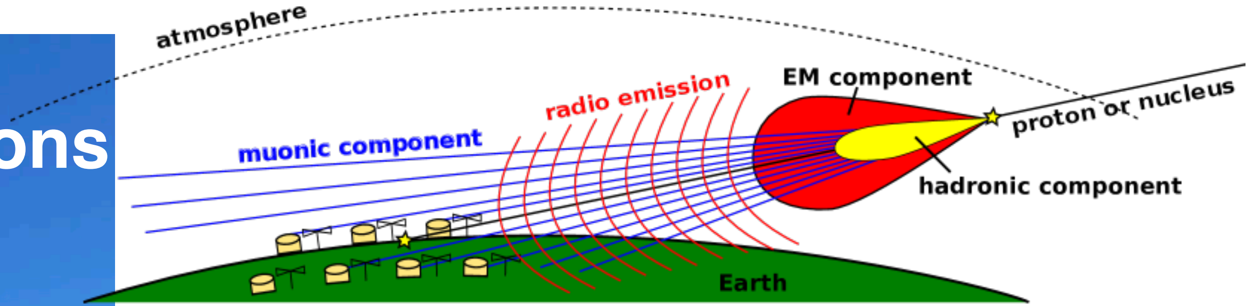

atmosphere of Earth is transparent in 30-80 MHz band

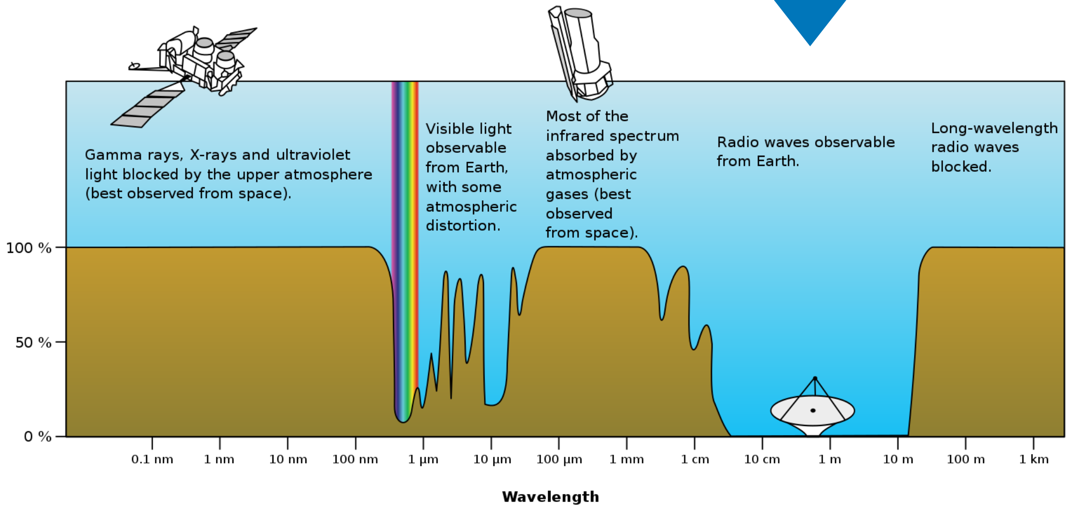

Horizontal air showers have large footprints in radio emission

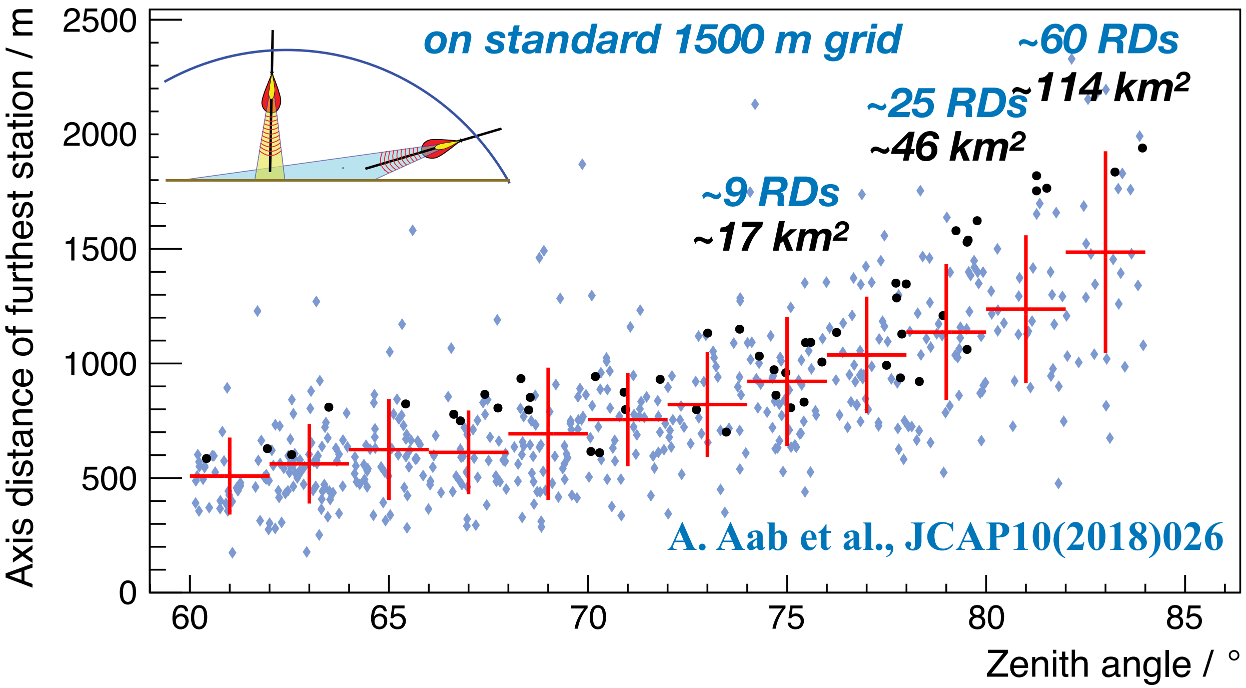

this is MEASURED with the *small* 17km² AERA

Pierre Auger Observatory

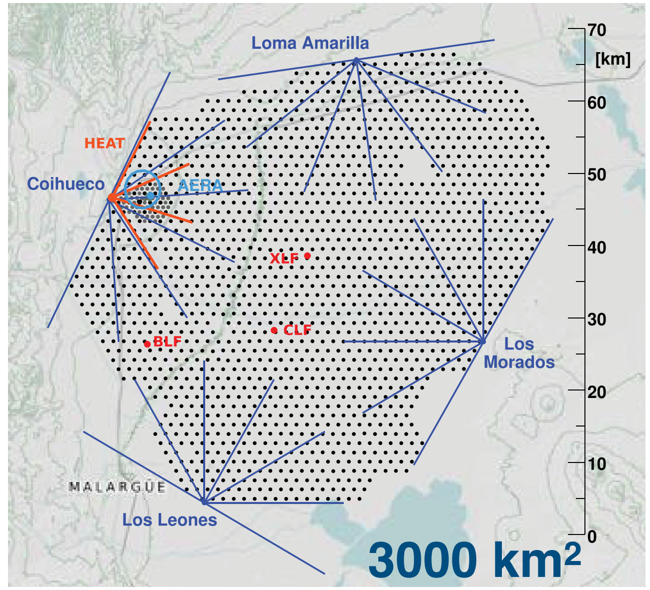

Surface Detector array:
Water Cherenkov Detector,
Surface Scintillator Detector,
Radio Detector
1600 stations on 1500 m grid
61 stations on 750 m grid

extend mass sensitivity to inclined showers $\theta > 60^\circ$

- **increasing measurements of e/m and μ components for inclined showers by an order of magnitude**

- **close to ideal p-Fe separation**

- **increase sky coverage and overlap with TA**

- **RD/WCD has different systematic effects as compared to SSD/WCD**

- **clean measurement of e/m shower component —> independent energy scale**

- **based on 15 years of experience with AERA**

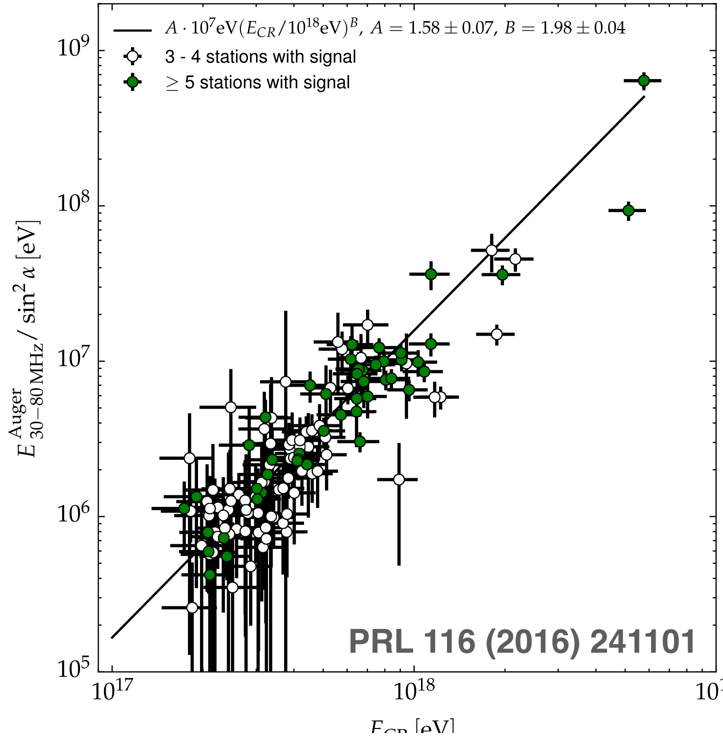

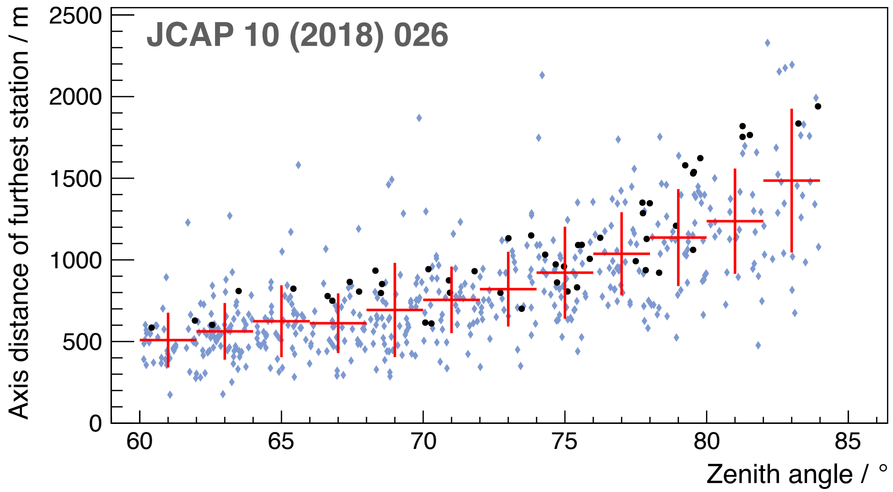

J.R. Hörandel et al, EPJC Web of Conf. 210 (2019) 06005


www.auger.org.ar
AB 183 IH
OBSERVATORIO
PIERRE AUGER


XLF

~500 stations Nov 2023

~1000 stations Mar 2024

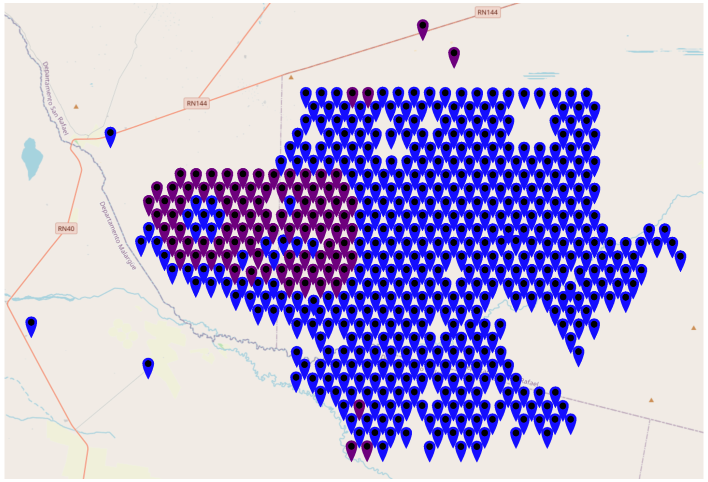

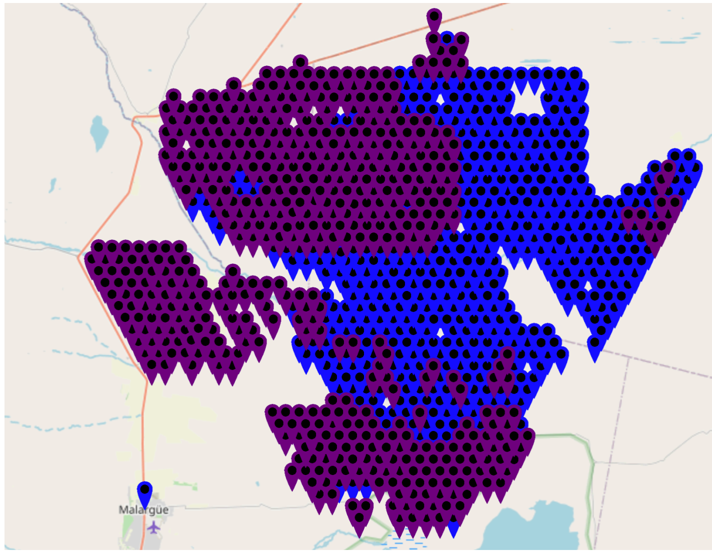

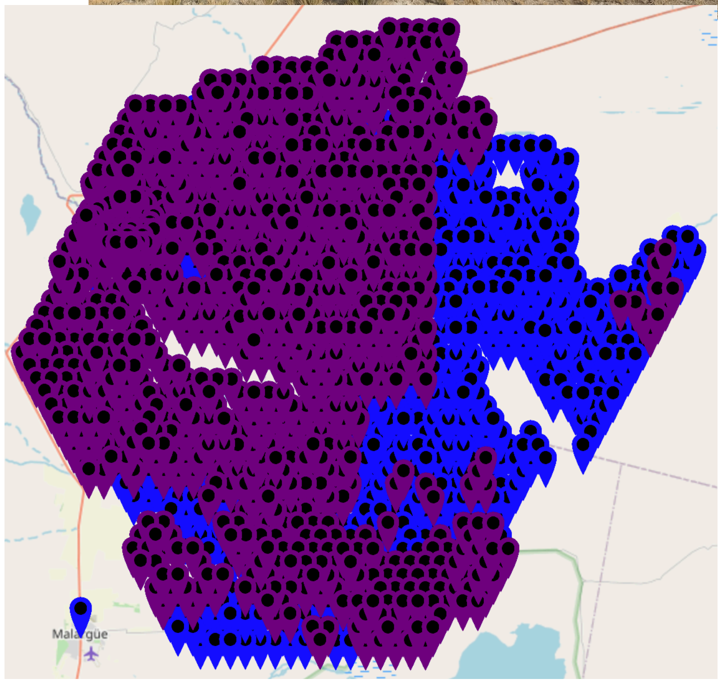

~1360 stations July 2024

PIERRE AUGER OBSERVATORY

installation of digitizers ~7/day
installation of antennas up to ~7/day

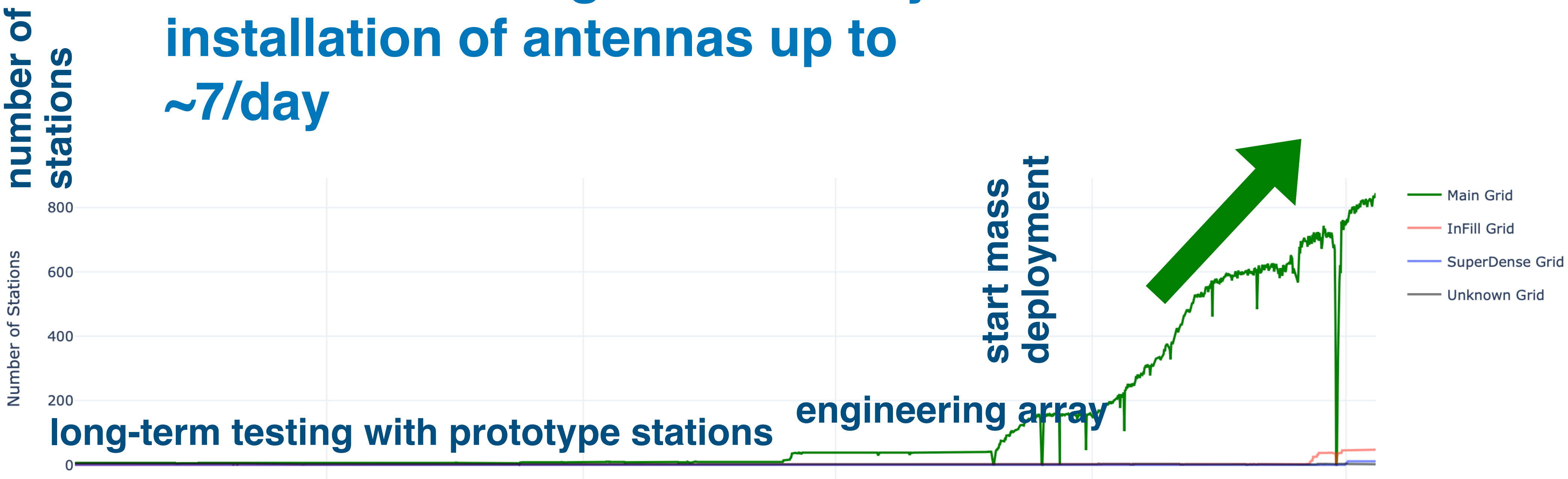

positions in DAQ

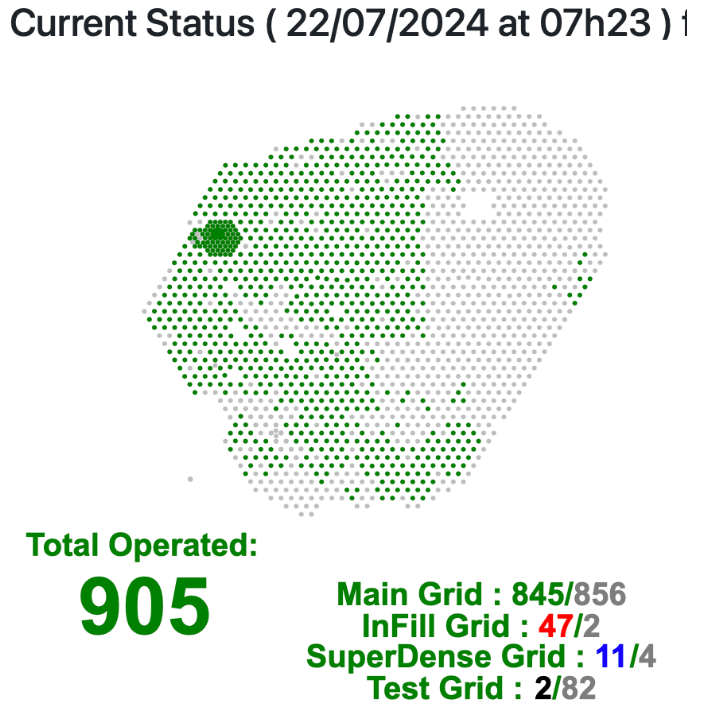

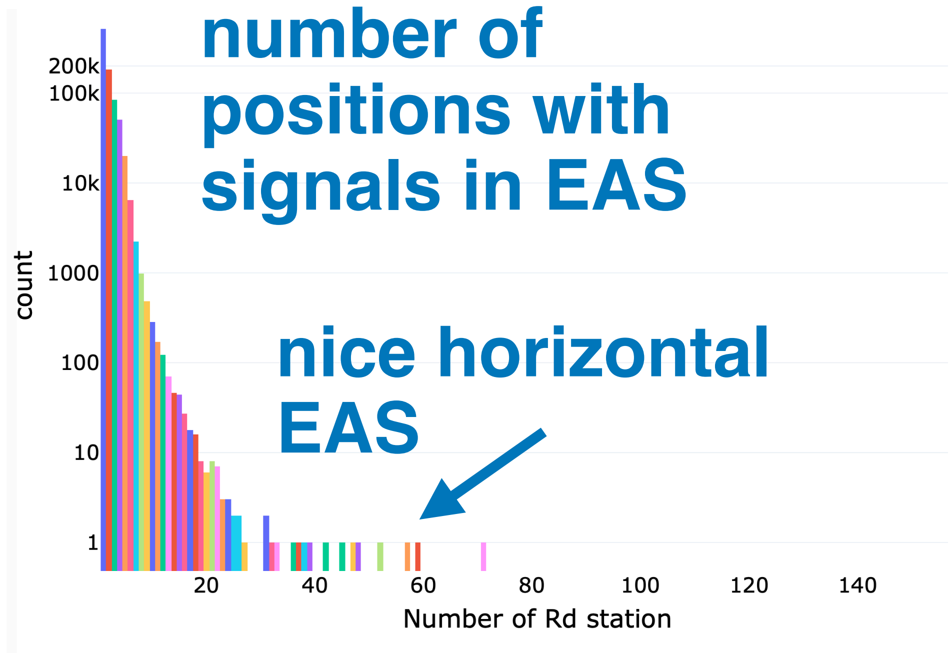

PIERRE AUGER OBSERVATORY

Calibration procedure

thermal cycling (aging) LNA & digitizer → **end-to-end calibration in lab LNA & digitizer** → **simulation of antenna pattern NEC**

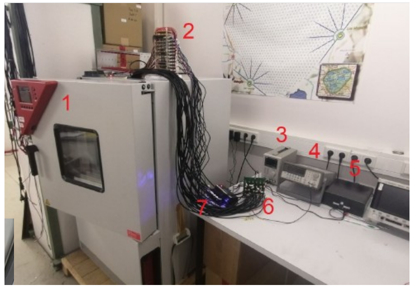

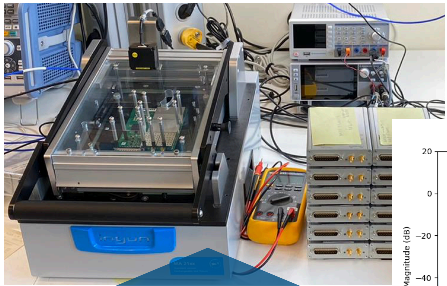

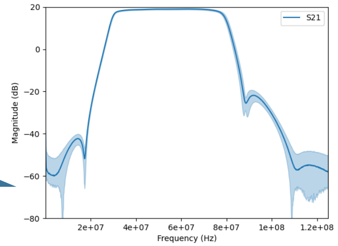

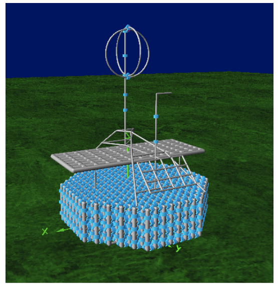

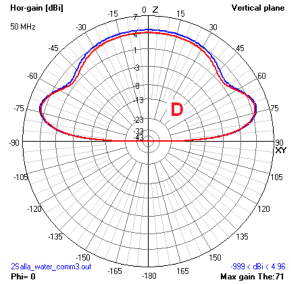

agreement on ~5% level

in-situ calibration with reference antenna → **Galactic emission**

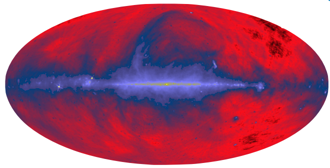

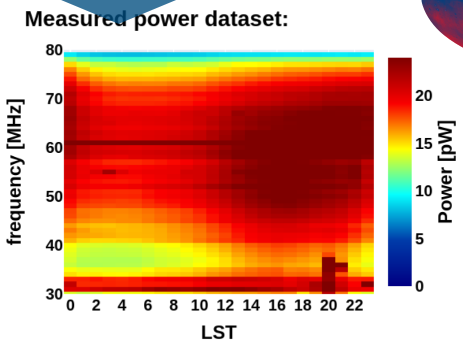

the „muon peak“ for radio

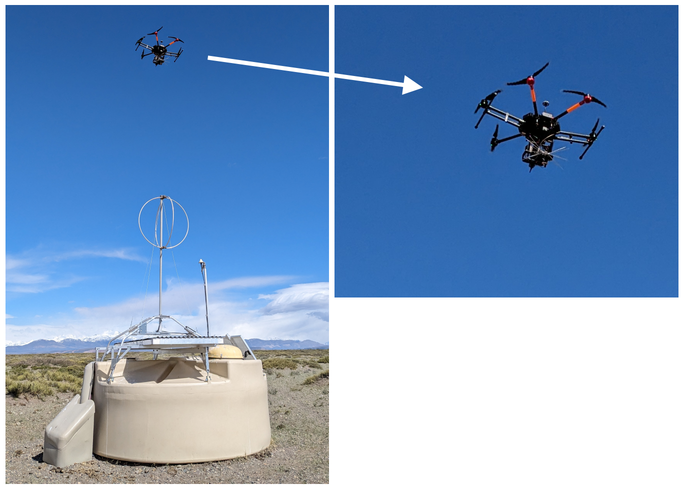

atmospheric electric field

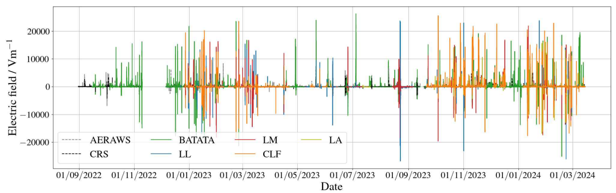

→ **absolutely calibrated signals**

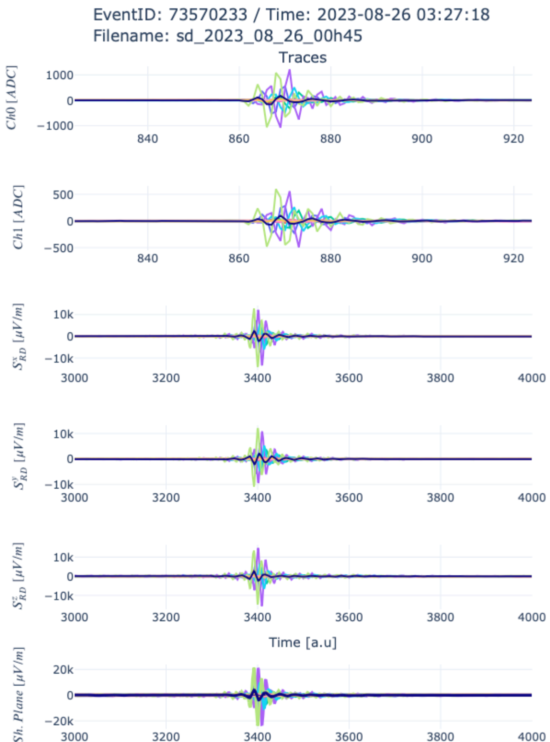

A measured cosmic ray

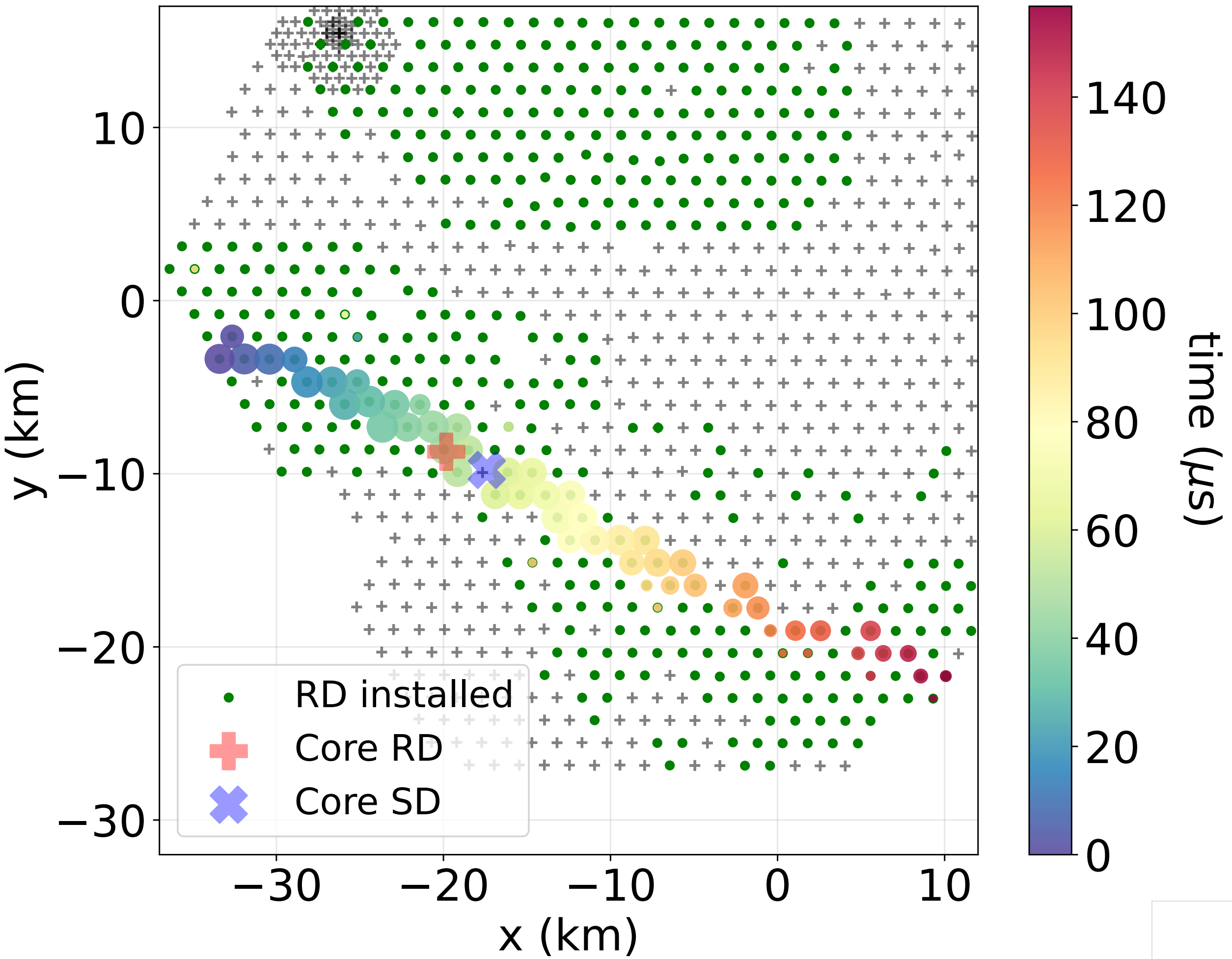

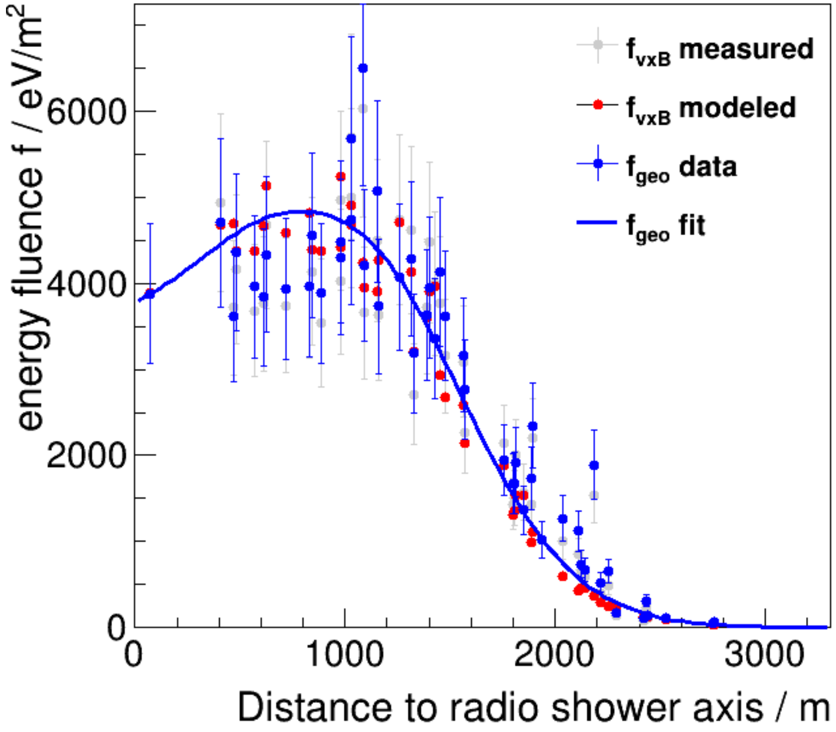

PIERRE AUGER OBSERVATORY

	RD	SD
Azimuth (deg)	156.99±0.01	157±0.1
Zenith (deg)	84.7±0.01	84.7±0.1
Energy (EeV)	36.23 ± 3.34	38.55 ± 2.92
Core X (km)	-19.8	-17.40±0.88
Core Y (km)	-8.73	-9.78±0.45

Eur. Phys. J. C (2020) 80:643
https://doi.org/10.1140/epjc/s10052-020-8216-z
THE EUROPEAN PHYSICAL JOURNAL C
Regular Article - Experimental Physics

Refractive displacement of the radio-emission footprint of inclined air showers simulated with CoREAS

JCAP01(2023)008
Journal of Cosmology and Astroparticle Physics
An IOP and SISSA journal

Signal model and event reconstruction for the radio detection of inclined air showers

F. Schlüter[a,b,*] and T. Huege[a,c]

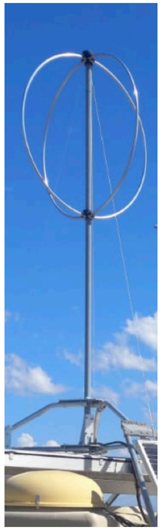

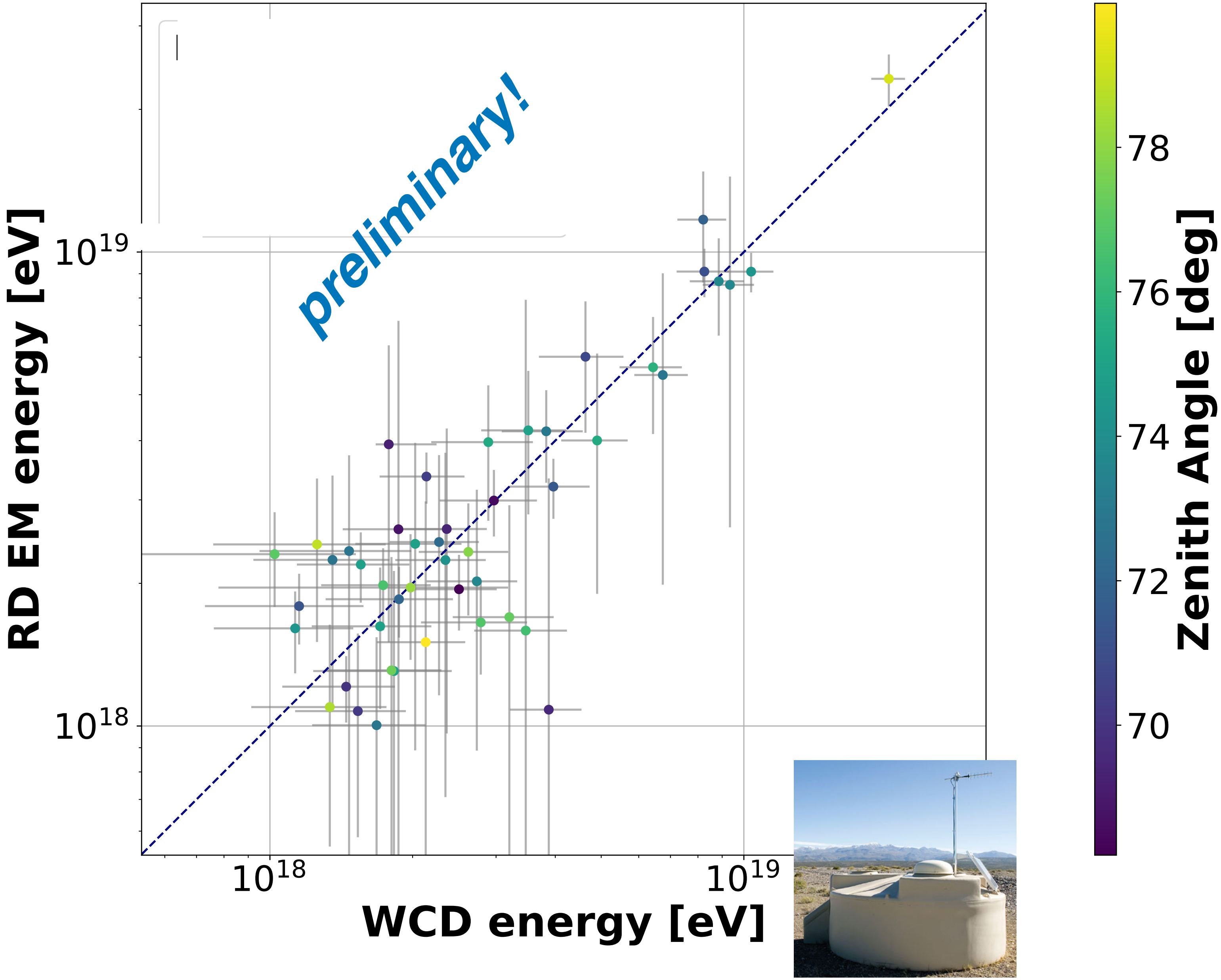

PIERRE AUGER OBSERVATORY

measurement of e/m energy by RD

—> full end-to-end verification of complete chain

Expected number of cosmic rays after 10 years

Using Auger-measured flux

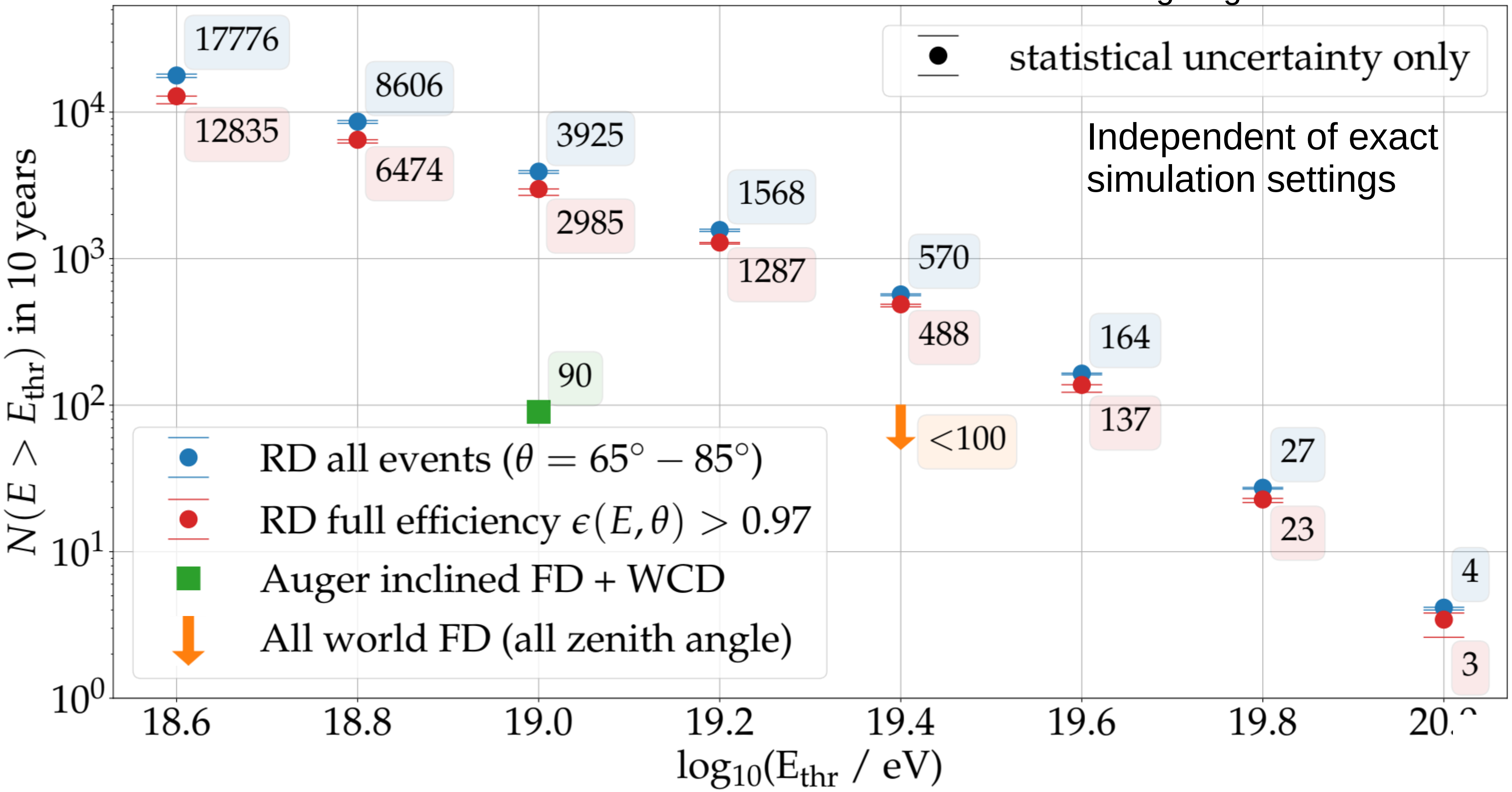

Independent of exact simulation settings

Particle physics in air showers

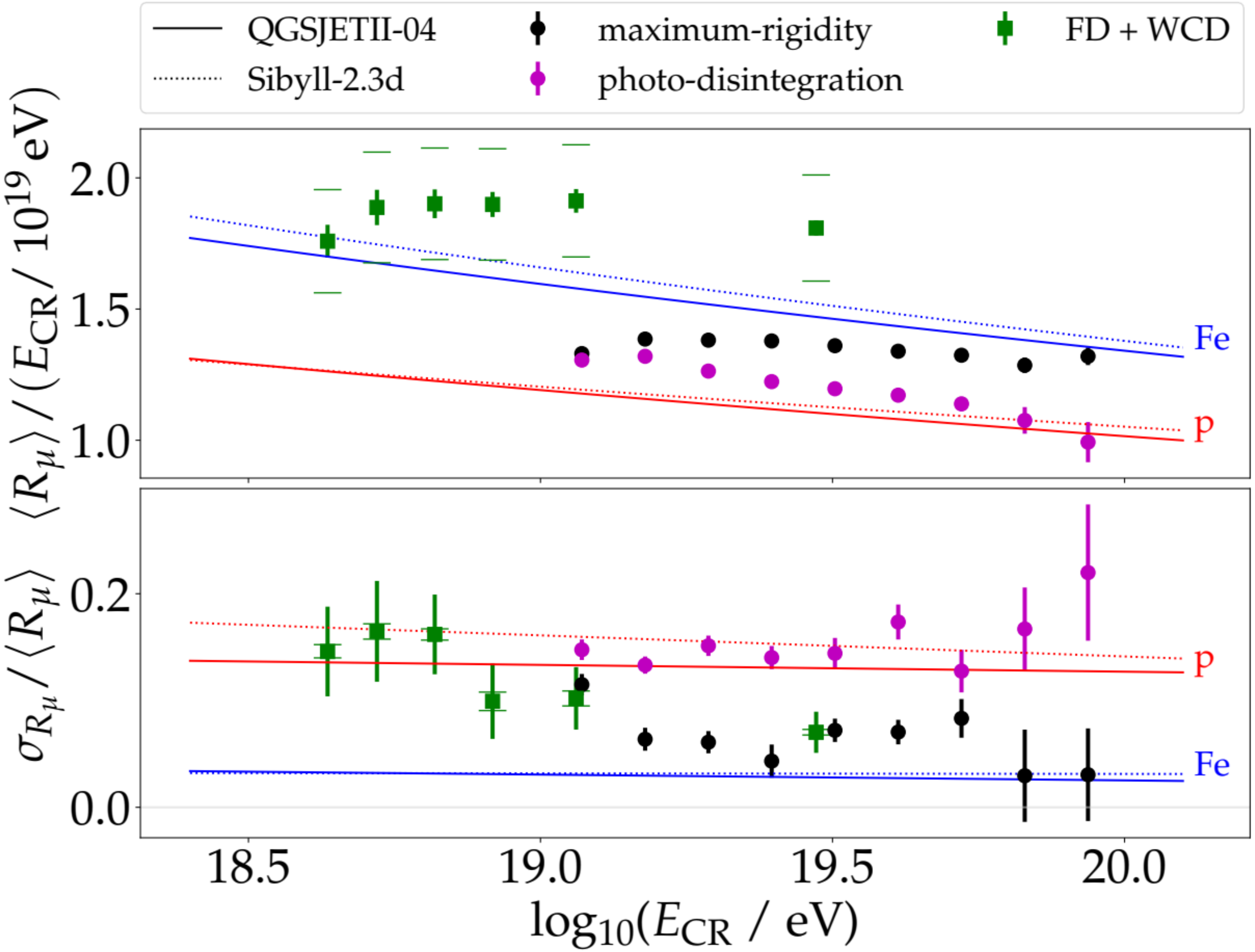

Muons in inclined air showers

—> investigation of muon deficit

Particle type for each cosmic ray

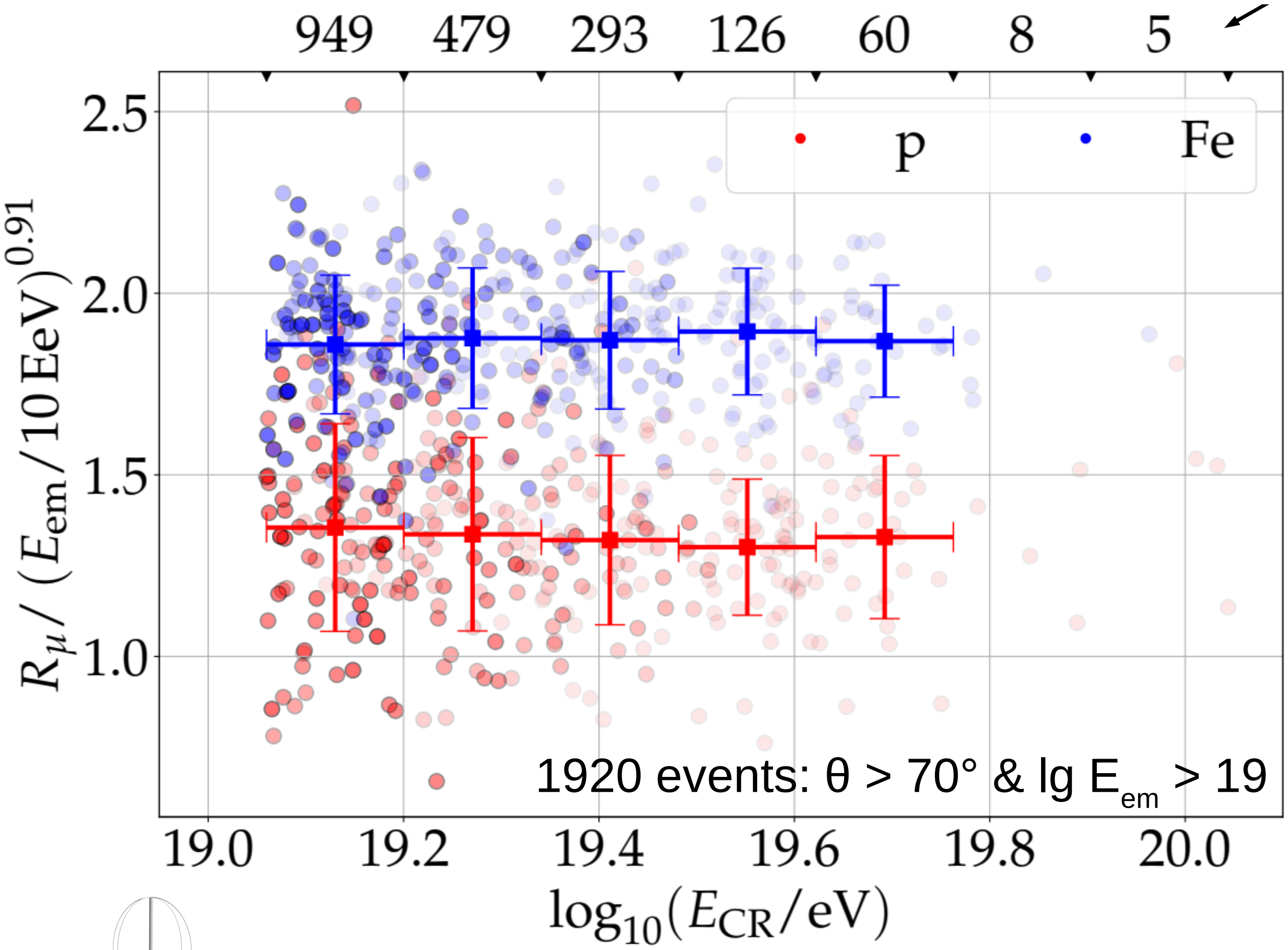

50/50 p-Fe composition with 10 yr RD measurements

figure of Merit:

$$\mathrm{FOM} = \frac{|\langle r_p \rangle - \langle r_{Fe} \rangle|}{\sqrt{\sigma_{r_p}^2 + \sigma_{r_{Fe}}^2}}$$

FOM = 1.61 ± 0.04

equal to X_{max} with perfect resolution

goal for the upgrade: 1.5

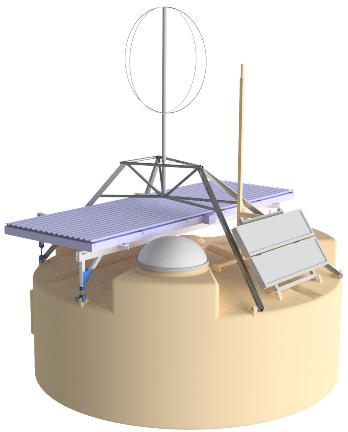

7th International Symposium on Ultra-High-Energy Cosmic Rays

UHECR 2024

Malargüe, Argentina - November 17-21 2024

The symposium is the 7th edition of a series of meetings that bring together the UHECR community. It covers the latest results from UHECR observations, theoretical developments, and future plans in the field. The symposium will focus on the highest energy cosmic rays as well as on cosmic rays with energies above 1 PeV. The agenda includes invited reviews, contributed talks, and reports from inter-collaborative working groups, all in plenary sessions.
Poster contributions are also foreseen.

International Advisory Committee
R. Engel (chair), P. Blasi, A. Castellina, I. De Mitri, T. Ebisuzaki, P. L. Ghia, F. L. Halzen, Y. Itow, K.H. Kampert, P. Klimov, P. Lipari, J. Matthews, S. Ogio, I. H. Park, E. Parizot, E. Resconi, M. Roth, G. Rubtsov, D. Ryu, H. Sagawa, P. Sokolsky, Y. Tsunesada.

Local Organizing Committee
I. Allekotte, B. Andrada, F. Gollán, G. Golup, F. Sánchez.

For more information:
https://indico.ahuekna.org.ar/event/768/
uhecr2024@auger.org.ar